Inaugural dissertation

for

obtaining the doctoral degree

of the

Combined Faculty of Mathematics, Engineering and Natural Sciences

of the

Ruprecht - Karls - University

Heidelberg

Presented by

MSc. Lucia Gordillo Perez

born in: Sevilla, Spain

Oral examination: 24th January 2023

Characterization of BDNF-dependent chromatin responses and adaptations in postmitotic neurons

Referees: Prof. Dr. Ana Martin-Villalba

Dr. Sara Cuylen-Haering

“Como no estás experimentado en las cosas del mundo, todas las cosas que tienen algo de dificultad te parecen imposibles. Confía en el tiempo, que suele dar dulces salidas a muchas amargas dificultades”.

***Don Quijote de la Mancha,* Miguel de Cervantes**

Summary

Brain-derived neurotrophic factor (BDNF) is involved in several neuronal processes such as neuronal growth and differentiation, synapse development, and synaptic plasticity. Alterations in endogenous BDNF levels have been associated with neurological disorders, such as schizophrenia and depression. At the molecular level, stimulating cortical neurons with BDNF activates signalling cascades that culminate in specific transcriptional responses. Although extensive efforts have been made to study BDNF-induced gene regulation of selected loci, little is known about genome-wide chromatin changes triggered by BDNF and how these are regulated. In this PhD thesis, I sought to investigate (1) the molecular response of BDNF stimulation in chromatin regulatory proteins and their cooperation in orchestrating BDNF-dependent transcription and (2) the plasticity of BDNF-induced changes in chromatin upon reiterated stimulation events, in mouse cortical neurons.

To address the first aim, I compared the changes in the subcellular proteomes -in cytosol, nucleoplasm, and chromatin- following stimulation with either BDNF or KCl (which triggers membrane depolarisation). The comparison between responses showed a significantly stronger recruitment of the transcription factor Fos to chromatin upon BDNF treatment. BDNF-affected distal regulatory elements were enriched in Fos binding motifs, often accompanied by other TF motifs. I confirmed that one of these TF families, EGR, regulates the expression of the BDNF-responsive synaptic regulator *Arc* through a novel BDNF-specific enhancer and that this is accomplished through a cooperative effect with Fos.

The chromatin response to BDNF led to a prominent activation of distal regulatory elements, half of which remained accessible for 10 hours post-stimulation. I hypothesised that this sustained accessibility could act as a priming event, influencing the transcriptional outcome in future encounters with BDNF. To investigate this, I sought to identify differences in the transcriptional response of mouse primary neurons primed with BDNF compared to naive cells. The gene expression changes in primed and naive neurons revealed six different clusters, of which four showed marked variations between the first and second encounters with BDNF. Primed neurons presented a strong downregulation of lncRNAs, such as *Meg3, Malat1* and *Ftx*, and lower induction of gene targets of the PI3K pathway. Furthermore, the induction of many BDNF-responsive transcriptional regulators (*Npas4, Nr4a2, Klf6*) was milder in primed neurons, but the expression of neuronal physiology-related genes (*Snca, Cav2, Calca*) was enhanced upon a second BDNF treatment. Chromatin accessibility profiling did not uncover any priming event, but instead, revealed a highly plastic and reversible behaviour in BDNF-regulated regions. However, at the proteome level, I found macroH2A, a transcriptionally repressive histone variant, to accumulate in primed neurons,

pointing out a possible mechanism in conditioning the transcriptional outcome of subsequent stimulations.

In conclusion, the results reported in this thesis enhance our understanding of the BDNF-regulated chromatin responses in neurons and shed light on a novel phenomenon of putative transcriptional adaptation upon priming with BDNF. Taken together, a better understanding of the cellular and molecular consequences of BDNF can pave the road for the design of new therapies for treating BDNF-associated brain disorders.

Zusammenfassung

Der Wachstumsfaktor BDNF (engl. brain derived neurotrophic factor) ist an verschiedenen neuronalen Prozessen wie dem Wachstum und der Differenzierung von Neuronen, der Entwicklung von Synapsen und der synaptischen Plastizität beteiligt. Veränderungen des endogenen BDNF-Spiegels wurden mit neurologischen Störungen wie der Schizophrenie und der Depression in Verbindung gebracht. Auf molekularer Ebene werden durch die Stimulierung kortikaler Neuronen mit BDNF Signalkaskaden aktiviert, die spezifische Genexpressionsreaktionen auslösen. Obwohl umfangreiche Studien unternommen wurden, um die BDNF-induzierte Genregulation ausgewählter Loci zu untersuchen, ist bisweilen wenig über genomweite Chromatinänderungen bekannt, die durch BDNF ausgelöst werden, und darüber, wie diese reguliert werden. Im Rahmen dieser Dissertation untersuchte ich (1) die molekulare Reaktion der BDNF-Stimulation auf Chromatin-regulierende Proteine und ihre Zusammenarbeit bei der Steuerung der BDNF-abhängigen Transkription und (2) die Plastizität der BDNF-induzierten Veränderungen im Chromatin bei wiederholten Stimulationsereignissen in kortikalen Neuronen der Maus.

Um das erste Ziel zu erreichen, verglich ich die Veränderungen in den subzellulären Proteomen - im Zytosol, im Nukleoplasma und im Chromatin - nach einer Stimulation mit BDNF oder mit KCl (wovon das Letztgenannte eine Membrandepolarisation auslöst). Dieser Vergleich zeigte eine signifikant stärkere Rekrutierung des Transkriptionsfaktors Fos an Chromatin nach einer BDNF-Behandlung auf. Die von BDNF beeinflussten distalen regulatorischen DNA-Elemente waren mit Fos-Bindungsmotiven angereichert, die oft von anderen TF-Motiven begleitet wurden. Ich konnte zeigen, dass eine dieser TF-Familien, EGR, die Expression des auf BDNF reagierenden synaptischen Reglers Arc über einen neuartigen BDNF-spezifischen Enhancer reguliert und dass dies durch einen kooperativen Effekt mit Fos erreicht wird.

Die Chromatinantwort auf BDNF führte zu einer ausgeprägten Aktivierung von distalen regulatorischen DNA-Elementen, von denen die Hälfte noch 10 Stunden nach der Stimulation zugänglich war. Ich stellte die Hypothese auf, dass diese anhaltende Zugänglichkeit der DNA als Priming-Ereignis fungieren und das Transkriptionsergebnis bei zukünftigen Begegnungen mit BDNF beeinflussen könnte. Um dies zu untersuchen, verglich ich die transkriptionelle Antwort von primären Neuronen der Maus, die mit BDNF geprimt wurden, zu naiven Neuronen . Die Veränderungen der Genexpression in geprimten und naiven Neuronen ergaben sechs verschiedene Cluster, von denen vier deutliche Unterschiede zwischen der ersten und der zweiten Stimulation mit BDNF aufwiesen. Geprimte Neuronen zeigten eine starke Herunterregulierung von lncRNAs wie Meg3, Malat1 und Ftx und eine geringere Induktion von Zielgenen des PI3K-Signalwegs.

Darüber hinaus war die Induktion vieler auf BDNF reagierender Transkriptionsregulatoren (Npas4, Nr4a2, Klf6) in geprimten Neuronen geringer, wohingegen die Expression von Genen, die mit der neuronalen Physiologie zusammenhängen (Snca, Cav2, Calca) durch eine zweite BDNF-Behandlung verstärkt wurde. Die Untersuchung der Zugänglichkeit des Chromatins ergab zwar kein Priming-Ereignis, aber zeigte stattdessen ein äußerst plastisches und reversibles Verhalten in BDNF-regulierten Regionen. Auf der Proteinebene konnte ich jedoch eine Anreicherung von macroH2A, einer transkriptionell repressiven Histonvariante, in geprimten Neuronen feststellen. Dies wiederum könnte auf einen möglichen Mechanismus zur Konditionierung der transkriptionellen Antwort auf nachfolgende Stimulationen hinweisen.

Abschließend ermöglichen die in dieser Arbeit berichteten Ergebnisse unser Verständnis der BDNF-regulierten Chromatin-Reaktionen in Neuronen zu erweitern. Ferner, stellt sieeinen neuartigen Mechanismus vor, der potenziell die transkriptionelle Anpassung Priming mit BDNF darstellt. Schließlich kann ein verbessertes Verständnis der zellulären und molekularen Folgen von BDNF den Weg für die Entwicklung neuer Therapien zur Behandlung von BDNF-assoziierten Gehirnerkrankungen ebnen.

.

Contents

Acknowledgements

I would like to thank my supervisor, Min Noh, for giving me this opportunity and supporting my career. But above that, thank you for teaching me that perseverance and speaking out can take you very far. I would also like to thank Paola Grandi, without whom I would not have made it this far and for being a motivational example. Great appreciation to my TAC members, Prof. Ana Martin, Sara Cuylen and Mikhail Savitski for their stimulating discussions and guidance in this project. Many thanks to Annarita Patrizi for being part of my thesis defence committee.

I had the pleasure to work with amazing colleagues, who have been very inspiring and supportive throughout this journey. Many thanks to Inyoung, Lotta, Daria and Mikael, who were already gone by the time I had to write this thesis, and yet their help and nice discussions made a difference. For all the guidance, encouraging feedback and for sharing real neuroscience, special thanks to Jenny, you are always inspiring. I feel extremely thankful for having shared this journey with the best labmate and my friend, Matteo Your eternal smile makes any problem look smaller, thank you for being so caring and supportive. For making the lab feel like home, I will thank Nadine, Sara, Maria and Victor - especially the AssEMBL team, I couldn't have found a greater treasure along the way. All my gratitude goes to Umut, who was always there to help and with something smart to say, and to Thomas and Vibha, for the nice feedback.

During my stay at EMBL, I was lucky enough to interact with very talented scientists who thaught me a great deal. I will be forever thankful to Tim Pollex, Vikram Ratnu, Nacho Ibarra and Henrik Hammarén for this. As well, thanks to the fantastic people at GeneCore for all the technical support, especially to Vladimir, Laura, Mireia, Nayara and Ferris.

The moments I would regret getting myself on this journey, they were reason enough to continue: my predoc fellows from 2018. Special appreciation goes to my partner in crime, Anna, and to Karolina, Agata, Alberto, Jesus, Gil, Ana and Andrea. I love you guys. I'd also like to thank Maja and Ahmad, who always had kind words (with singing involved) for me and were a great support. As well, I won't forget my biggest discovery, Wolfi, I cannot believe how lucky I got to find you on my way.

A foothold that grants you a different perspective and helps you keep your sanity. Those are my friends from Spain. Thank you, Petit Comité. Especially to my Andrea, the best friend one can have. To Rocio and Ara, I wish I would see you more often. Last but not least, thank you, Lo, I will be forever thankful to have found you again.

My warmest thank you goes to my family, my parents Mariló and Paco, and my siblings Pablo and Clara, for blindly believing in me and for encouraging me to continue growing, even though it may mean to be away from each other.

And to Luca, without your unconditional support I would have often felt lost. Thank you for always being there for me, with a smile and probably good food.

…Marina, you left us too soon. This is for you.

Abbreviations

BDNF	Brain-derived neurotrophic factor
ATAC-seq	Assay for transposase-accessible chromatin followed by sequencing
ChIP	Chromatin Immunoprecipitation
DAP	Differentially abundant protein
DAR	Differentially accessible region
DEG	Differentially expressed gene
DIV	Days in vitro
E15.5	Embryonic day 15 and a half
FDR	False discovery rate
GO	Gene Ontology
IEG	Immediate early gene
IF	Immunofluorescence
KCl	Potassium Chloride
KO	Knock-out
LRG	Late response gene
LTD	Long-term depression
LTP	Long-term potentiation
MEF	Mouse Embryonic Fibroblast
mESC	mouse Embryonic Stem Cell
mRNA-seq	messenger RNA sequencing
MS	Mass Spectrometry
NPC	Neuronal precursor cell
PTM	Post-translational modification
qPCR	quantitative polymerase chain reaction
TF	Transcription factor
TFBS	Transcription factor binding site
TrkB	Tropomyosin-related receptor tyrosine kinase 2
TSS	Transcription start site

List of Figures

List of Tables

CHAPTER 1:

INTRODUCTION

Cells are dynamic entities that can display different characteristics and perform several functions depending on the developmental and physiological status of the organism they form. How cells change their phenotype and adapt to environmental cues generally requires gene expression changes starting from a common genomic sequence in a finely regulated and complex process.

The external cues may provoke a fast, reversible and transient cellular response or, in addition, stable and permanent changes in the cell. In the first case, the cell requires mechanisms capable of inducing a response and, at the same time, of enabling a setback to the state prior to stimulation to be able to respond again in later encounters. Alternatively, the signal may need to be integrated and translated into permanent physiological changes, requiring long-lasting modifications. In both cases, the response to stimuli is orchestrated at the level of gene expression. The transcriptional regulation of stimulus-responsive genes is achieved through transcription factors (TFs), regulatory proteins that bind to specific DNA sequences, the TF binding sites (TFBS), to induce or repress transcription. During dynamic processes such as development or upon external stimulation, the genomic DNA sequence stays unchanged, hence a different layer of regulation must step into the game to confer cell type-, time- and stimulus-specificity in the transcriptional response. To induce as well as maintain a certain transcriptional pattern in response to extracellular stimuli, epigenetic modifications are established on chromatin, a structure composed of DNA and proteins where the genetic material of the eukaryotic cells is stored. The term *epigenetics* was first coined by Conrad Waddington[1] to explain the interactions between the environment and the genome of an organism during development to induce phenotypic changes. Epigenetic modifications of the chromatin can be introduced in a rapid manner, which makes them an ideal mechanism to integrate information in response to stimulation[2]. They can also be reversible to enable a transient response, and yet they can also last for long periods of time, for they can also be permanent and even be heritable[3]. In this case, the transcriptional changes introduced by epigenetic modifications in response to stimulation can be preserved, ultimately leading to an acquired stimulus-dependent phenotype.

1.1. Transcriptional regulation in response to stimuli by inducible transcription factors

Each organism has a genetic sequence common to all the cells composing it, yet at each developmental stage, tissue or physiological state the cellular phenotype differs. This is achieved by differential gene expression patterns arising from the genome through varying regulatory mechanisms that fine-tune the expression to fit the context of the cell. The genetic information of the cell is stored in chromatin, which is highly dynamic and serves as the substrate for transcription. Modifications of the chromatin environments, such as the introduction of epigenetic modifications, lead to the reorganization of the chromatin accessibility landscape, influencing the transcriptional outcome.

Different chromatin elements can act as players in the regulation of gene expression, in particular in response to stimuli (**Fig.1**). *Cis*-regulatory elements are DNA sequences that possess the ability to regulate gene expression generally because of the affinity of TFs to bind them. These elements are often classified as promoters, enhancers, silencers and insulators[4]. Conversely, *trans*-acting factors are proteins directly recruited by DNA or other elements of chromatin, where they perform a catalytic function (epigenetic regulators and remodelers) or serve as a docking platform for other factors (transcription factors and co-activators). Promoters are regions around the transcription start site (TSS) of a gene composed of several binding sites for regulatory proteins able to recruit the RNA polymerase II complex to initiate transcription. In mammals, initiation of transcription by the RNA polymerase II requires the assembly of the preinitiation complex (PIC), a set of general transcription factors (GTF) bound to the core promoter to grant accessibility to the polymerase machinery[5]. Further phosphorylations of the C-terminal domain of the RNA polymerase II will translate into transcriptional initiation, elongation or termination[6]. Apart from the GTF binding sites to most promoters, they may also display alternative sequences that can bind stimulus-responsive factors[7]. For example, the promoter of the alpha-globin genes presents TFBS, such as the one for NF-E1, that mediate tissue-specific activation of these genes[8].

Similarly, enhancers also contain multiple TFBS and are particularly interesting due to their ability to regulate specific genes from a far away distance. Although there are many *cis*-regulatory elements containing TFBS that could be bound by TFs, often the concerted action of multiple binding events is necessary to allow the proper association of these factors on chromatin. And more importantly, these TFBS may not be accessible in some cellular states and be sequestered in heterochromatinic regions, i.e., highly compacted chromatin deprived of transcriptional events[9]. Generally, the decompaction of chromatin at *cis*-regulatory elements is driven by pioneer TF-mediated recruitment of chromatin remodelers

and modifying enzymes (see **Section 1.1.2**). Pioneer TFs are able to recognise and bind their TFBS on the surface of nucleosomes even on compacted chromatin[10]. Once an enhancer has been made accessible, bound TFs also interact with co-activators such as the mediator complex[11]. The communication between enhancer-bound elements and the RNA polymerase II complex in the promoter is achieved through chromatin looping, which enables the proximal contact of these distal regulatory elements. Several proteins mediate chromatin looping, such as CCCTC-binding factor (CTCF) and cohesin[12]. Finally, silencers are DNA sequences bound by repressor TFs to prevent the induction of the transcriptional machinery at promoters and enhancers[13], and insulators manage to concentrate positive (from enhancers) or negative signals (from silencers) and prevent their spreading to non-targeted regions[14].

Regulation of gene expression in response to environmental cues often requires not only the presence of specific TFBS but also the ability of the TF to bind them. TF specificity for the DNA can be altered by the collaboration with other TFs or transcriptional co-regulators, which influences their ability to induce or repress transcription[15]. In a general view, the abundance of a TF is directly correlated with the transcription of its target genes. This is the case of the Nuclear Factor-κB (NFκB), where the increase in its abundance in response to inflammation and the immune response activation leads to a progressive increment in target gene expression[16]. However, for certain cases, a non-linear relation between TF abundance and target expression may be a consequence of the cooperative binding of TFs. Only after the binding of a first TF, a second TF with an adjacent TFBS may be able to bind in a cooperative manner[17]. This is established through (DNA-mediated[18]) protein-protein interactions. This behaviour leads to an “on/off” binary response, often seen in the case of developmentally regulated genes[19]. Furthermore, post-translational modifications (PTMs) of TFs[20,21] can change their affinity to bind DNA or other TFs[22], as well as their subcellular localization[23] and stability[24], changing their ability to induce gene expression.

All these events, TF binding, differential enhancer and promoter accessibility, co-factor recruitment, looping and contact with promoter elements to activate the RNA polymerase II machinery can be orchestrated in response to external cues by a plethora of mechanisms. Although TFs and cis-regulatory elements permit the stimulus-regulated induction or repression, they lack the capacity to maintain or store this information and adapt to it. In this regard, epigenetic regulatory mechanisms provide the missing piece to the system's full functionality, allowing the response as well as the adaptation to stimuli.

1.2. Integration of information on chromatin through epigenetic mechanisms

The hypothesis that chromatin could be a platform for storing information in response to environmental cues through signal transduction was postulated over 20 years ago[25]. Once the external signal has been transduced to the nucleus of the cell, changes in the transcriptional program will lead to the consequent physiological response. To orchestrate these changes, transcription factors and epigenetic regulators need to be activated according to the signalling cues. Apart from the regulatory mechanisms described in **Section 1.1,** epigenetic mechanisms also emerge as a system able to induce gene expression changes in response to stimulation. Some of these mechanisms are histone PTMs, DNA methylation, nucleosome remodelling, incorporation of histone variants and activity of non-coding RNAs. In the following, a brief introduction to each phenomenon concerning their ability to sense extracellular changes is given and can be seen in **Fig.1**.

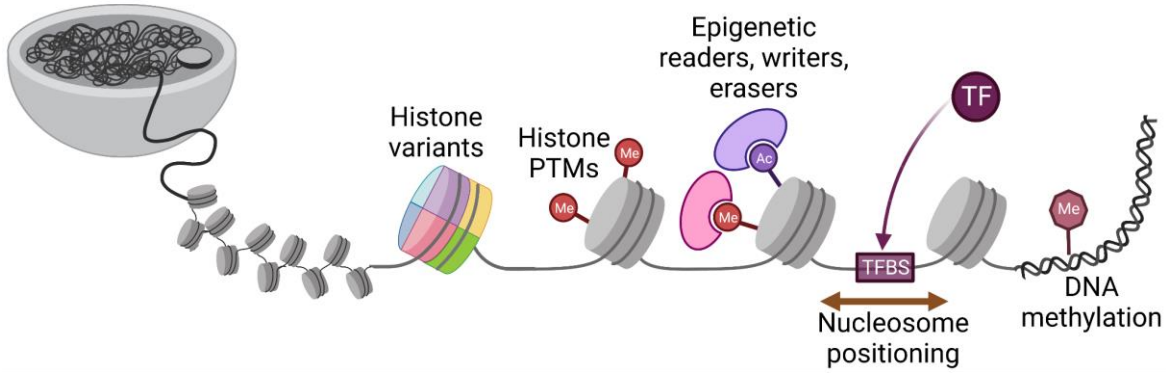

Figure 1. Stimulus-responsive (epigenetic) mechanisms regulating gene expression.
The genetic material of eukaryotic cells is stored in the nucleus in the form of chromatin, a mixture of DNA and proteins. The nucleosome is the basic unit of chromatin, formed of DNA wrapped around histone proteins. Relevant transcriptional regulatory mechanisms, focused on chromatin-related events, are depicted here: incorporation of histone variants to nucleosomes, the addition of PTMs to histones by epigenetic writers or their removal by erasers, binding to histone PTM by readers, differential positioning of nucleosomes to allow different TFs to access their TFBS and methylation of DNA. ncRNAs are not shown since they are not structural components of chromatin as the rest of the mechanisms. PTM: post-translational modifications, TF: transcription factor, TFBS: transcription factor binding site, Ac: acetyl group, Me: methyl group. Created with BioRender.com.

1.2.1. Histone post-translational modifications

Several kinds of modifications on the tails of histone, basic proteins composing the nucleosomes, have been described to be associated with the regulation of gene expression in a time-, tissue- or stimulus-specific manner. The best-known

modifications are acetylation and methylation of lysine residues, although phosphorylation of serine, threonine and tyrosine also play a relevant role in signal-induced transcriptional activation, such as the regulation of the DNA damage response[26]. The enzymes performing the deposition and removal of these histone marks are the histone *writers* and *erasers*, respectively. Most of these proteins are able to sense the physiological state of the cell since their substrates or cofactors are metabolites present in the cell[27,28,29]. As an outcome of signal transduction to the nucleus, external cues induce modifications on these enzymes to induce or repress their activity via PTMs. This can enhance their interactions with binding partners or their substrate, or relocate them to and from the nuclear compartment.

To date, it is not fully understood if the modifications of histone tails, where most of the PTMs happen, are a cause or a consequence of other regulatory mechanisms inducing or repressing transcription[30–32], but they can be associated with transcriptional states. Dynamic induction of gene transcription by cellular processes, such as memory formation in the brain, is often associated with the acetylation of lysine 27 residue in histone H3 (H3K27ac) by the lysine acetyltransferases (KATs) CREB-binding protein (CBP) and p300[33]. This mark is often found at active enhancers and promoters, which may be pre-marked monomethylated H3K4 (H3K4me1) and trimethylated H3K4 (H3K4me3), respectively[31]. Methylation of H3K4 is performed by Myeloid/lymphoid or mixed-lineage leukaemia 3 and 4 (MLL3, MLL4)[34]. The combination of pre-existing and newly added histone marks adds a layer of combinations to induce specific transcriptional patterns. For instance, in terminally differentiated cells such as macrophages, *latent* enhancers are delineated after stimulation by the deposition of H3K4me1 and restimulation enhances their target gene expression by the additional deposition of H3K27ac by CBP or p300[35]. To inactivate enhancers, histone deacetylases (HDACs) can remove this mark[36]**.**

Furthermore, the polycomb repressive complex (PRC) is able to regulate the temporal transcriptional dynamics by repressing transcription through the tri-methylation of H3K27 (H3K27me3). The regulation of PRC function can be regulated by external stimuli[37] and developmental cues affecting the subunit composition of the complex[38], to form facultative heterochromatin. Conversely, constitutive heterochromatin is marked by the deposition of H3K9me2 and H3K9me3, which confer a tightly-packed repressive environment to silence the expression of repetitive sequences or transposable elements[39].

Besides *writers* and *erasers* of histone marks*, readers* can sense and bind these modifications. This helps transmit the signal that induced the deposition of the mark by recruitment of additional protein complexes necessary for transcription induction or repression. This is the case of the bromodomain and extra-terminal domain (BET) protein family, which binds acetylated histone tails and musters up the positive transcription elongation factor b (p-TEFb) to chromatin allowing

phosphorylation of RNA polymerase II to induce elongation of stimulus-responsive genes[40]. The chromodomain moiety, present in PRC and chromodomain helicase DNA-binding proteins (CHDs), presents affinity for methylated lysines - e.g., H3K4me1/2/3, H3K27me3[41]. Depending on the additional catalytic activity of the *reader*, recognition of methylated histones can lead to further methylation or demethylation as well as chromatin remodelling, as is the case of CHD8[42].

1.2.2. DNA methylation

The addition of a methyl group to the fifth carbon of cytosines in DNA, forming 5-methylcytosines, induces the recruitment of transcriptional repressors or inhibits the binding of transcription factors, regulating transcription. Three DNA methyltransferases (DNMTs) catalyse this reaction: DNMT1, DNMT3A and DNMT3B. While DNMT1 is in charge of maintaining the methylation pattern in dividing cells, DNMT3A and B perform *de novo* methylation in response to extracellular stimuli[43]. Methylation of cytosines in mammals happens on CpG dinucleotides[44], and it is considered a repressive mark[45]. Therefore, CpG islands, genomic regions with a high CpG content associated with *cis*-regulatory elements, are commonly hypomethylated[46]. Methylation of these regulatory sequences, such as insulators, can prevent the binding of *trans*-acting factors such as CTCF[47], and active demethylation of these elements is often required to allow the binding of TFs or other factors[48]. Apart from contributing to the hindrance of *trans*-acting factor binding, the transcriptional repression mechanism by methylated CpGs lies on the recognition by methyl-CpG binding proteins (MBPs), such as the methyl-CpG binding protein 2 (MeCP2), which upon binding methylated cytosines initiates the recruitment of *trans*-acting repressing factors as HDAC-containing complexes[49]**.** To reverse the DNA methylation status, ten-eleven translocation (TET) enzymes TET1, TET2 and TET3 oxidize 5-methylcytosines to 5-hydroxymethylcytosines (5hmC)[50], which is also an epigenetic mark predominantly found in the brain[51] and that may be associated with gene expression regulation[52,53]. Oxydation of methylated CpG and DNA demethylation can be induced by developmental cues, metabolic changes or immune activation[54].

1.2.3. Nucleosome remodelling and histone variants

Chromatin remodelling complexes depend on adenosine triphosphate (ATP) to position nucleosomes, enabling the underlying DNA cis-regulatory elements to become accessible or inaccessible for transcription factors and the transcriptional machinery. The main mammalian families of chromatin remodelers are SWI/SNF (switch/sucrose non-fermentable), ISWI (imitation SWI), CHDs and INO80 (SWI2/SNF2 related). All of them form large protein complexes composed of different subunits that can confer substrate specificity as well as the ability to respond in a tissue-, time- or stimulus-dependent manner[55]. Additionally, nucleosome remodelling allows for histone turnover and the incorporation of

histone variants into chromatin. Histone variants change the physical properties of the chromatin structure, enhancing or hindering transcription. For instance, H3.3, a variant of the canonical histone H3, is associated with active genes, whilst macroH2A, a variant of H2A, is deposited across large repressed regions such as the inactive X chromosome[56]. In recent years, macroH2A has also been described to allow induction of gene expression in response to stimuli[57,58].

1.2.4. Non-coding RNAs

The vast majority of the genome is transcribed in non-coding transcripts (ncRNA). The recent finding that these ncRNAs perform a regulatory function on gene expression opened a window to explore their implications in developmental and tissue-specific processes and cellular response to stress. The best-known species of ncRNAs that present a regulatory function are enhancer RNAs (eRNA), long non-coding RNAs (lncRNAs) and microRNAs (miRNAs). Although promoter elements initiate transcription, enhancers regulate transcription in a tissue-specific manner and in response to the physiological states of the cell. Upon activation, eRNAs are transcribed from the enhancer sequence and help maintain the accessibility status of the enhancer to allow transcription factor binding, for instance, during macrophage activation[59]. Likewise, lncRNAs display a wide range of regulatory mechanisms of transcription in a localization- and time-specific manner, depending on their interactions with other coding transcripts and proteins[60]. One of the best-known lncRNAs is the X-linked X-inactive-specific transcript (*Xist*), which initiates the inactivation of the X chromosome in mammalian females by recruiting several *trans*-acting repressors in a timely manner during development[61]. Another example is the lncRNA UMLILO recruits WD repeat-containing protein 5 (WDR5)-Kmt2a complex to the promoters of chemokine genes to enhance their priming for the immune response by H3K4me3 marking[62]. On the contrary, the lncRNA *Bdnf* antisense transcript (*BDNF-AS*) downregulates the expression of *Bdnf* by maintaining the PRC mark H3K27me3[63]. While lncRNA are classified by a greater length than 200 bp, miRNAs do not exceed 25 nucleotides and generally inhibit the translation of target genes in a post-transcriptional manner. In neurons, for example, miRNA biogenesis components are localised at the dendrites to allow localization-specific degradation of transcripts induced by neuronal activity[64].

1.3. Chromatin function and regulation in the stimulation of post-mitotic neurons

Post-mitotic neurons present the formidable capacity to respond to environmental changes in a dynamic and adaptable manner while reliably maintaining acquired information, such as the long-term memories of an organism[65,66]. Neurons store information both at the genomic and synaptic level[67], and are able to react and incorporate new cues encountered throughout their impressively long lifetime. Different forms of synaptic plasticity, where the strength of a synapse is adjusted after activation to adapt to new cues[68], illustrate how the synapse can store information[69] in the time range of milliseconds to hours[70], and even longer periods of time[71]. Nevertheless, in order to incorporate durable changes another relevant hub to store information is the nucleus of the cell. Following the same transcriptional regulatory mechanisms as the ones described in **Section 1.1**, the neuron is able to fulfil this purpose in response not only to synaptic activation via neurotransmitters but also to other stimuli such as growth factors.

The chromatin landscape is crucial for correct brain development. Neurodevelopmental disorders including autism, schizophrenia, bipolar disorder or intellectual disabilities are early-onset diseases affecting primarily neuronal cells. The causality of these disorders has been linked to genetic mutations affecting genes encoding epigenetic regulators. For example, the Rubinstein-Taybi syndrome affects the transcriptional coactivator CBP and the Rett syndrome is caused by mutations in the methylated CpG reader MeCP2, causing mental retardation in females[72]. Likewise, various mental disorders convey mutations in several subunits of the chromatin remodeler complex BAF (mammalian SWI/SNF), as in Coffin-Siris[73], Nicolaides-Baraitser[74] or Kleefstra's syndromes[75].

Additionally, with such a long lifetime, neurons can experience a progressive accumulation of physiological defects that may lead to the dysregulation of transcriptional patterns. In fact, alterations in the chromatin environment have been associated with neurodegenerative diseases[76]. Some of the neuronal processes affected in neurodegeneration, such as cognition and memory recall, rely on the correct signalling to transcriptional regulators to couple external cues to gene expression[77]. For instance, ageing mice display a reduced ability to acetylate H4K12, which seems to be responsible for the induction of gene transcription programs associated with memory consolidation[78]. Additionally, PRC2 deficiency in adult neurons leads to a progressive neurodegeneration phenotype, supposedly caused by the concomitant derepression of non-neuronal and death-promoting genes[79].

The role of epigenetics in neurological disorders indicates the vital relevance of epigenetic regulation of gene expression in neuronal function and heightens the need for a deeper understanding of how these processes are regulated.

1.3.1. Regulation of activity-induced transcription

Neurons can be activated by another neuron at the synapse[80]. Neuronal activation occurs as a consequence of the neuronal response to environmental stimulation such as sensory experience, development, injury and drugs. In this process, the release of neurotransmitters from the presynaptic cell activates receptors in the postsynaptic cell that induce a flow of cations towards and from inside the cell. The changes in the cation gradient lead to the depolarization of the cell, changing the membrane voltage or potential, and ultimately to the generation of an action potential[81]. The generated action potential can be propagated throughout the cell and the axon until it reaches a target cell to induce depolarization at the synapse[82]. Neuronal activity can be inhibited by the neurotoxin tetrodotoxin (TTX), which inhibits sodium channels, affecting the cation gradient needed for depolarization[83].

The formation[84]and the strength of synapses are highly plastic phenomena conditioned by neuronal activity that influence neuronal connectivity[85]. Activity-dependent synaptic plasticity refers to the modulation in the efficiency of a synapse after synaptic activation to adapt to the input signal[86]. Long-lasting forms of synaptic plasticity are long-term potentiation (LTP) and long-term depression (LTD), and they have long been regarded as the basis of memory and learning processes[87–89]. These processes have been found to be dependent on intracellular calcium (Ca^{2+}) increase[90] and, importantly, on transcriptional changes [91,92]. Without induction of gene expression and the subsequent protein production, long-term memories cannot be formed [93].

The transcriptional response induced by neuronal activity has been shown to be induced by a wide variety of stimuli[94]. There are several common factors in the stimulus-responsive transcription triggered by different signals, yet it maintains a certain level of specificity to guarantee an adequate response to the extracellular cue. The transcriptional response is often described as biphasic, composed of an initial fast and transient activation of a subset of genes, the immediate early genes (IEG), whose products generally are regulatory factors that will orchestrate the second and slower wave of transcription, comprised of the late response genes (LRG), which are thought to display more specific functions to the response[95] (**Fig.2**).

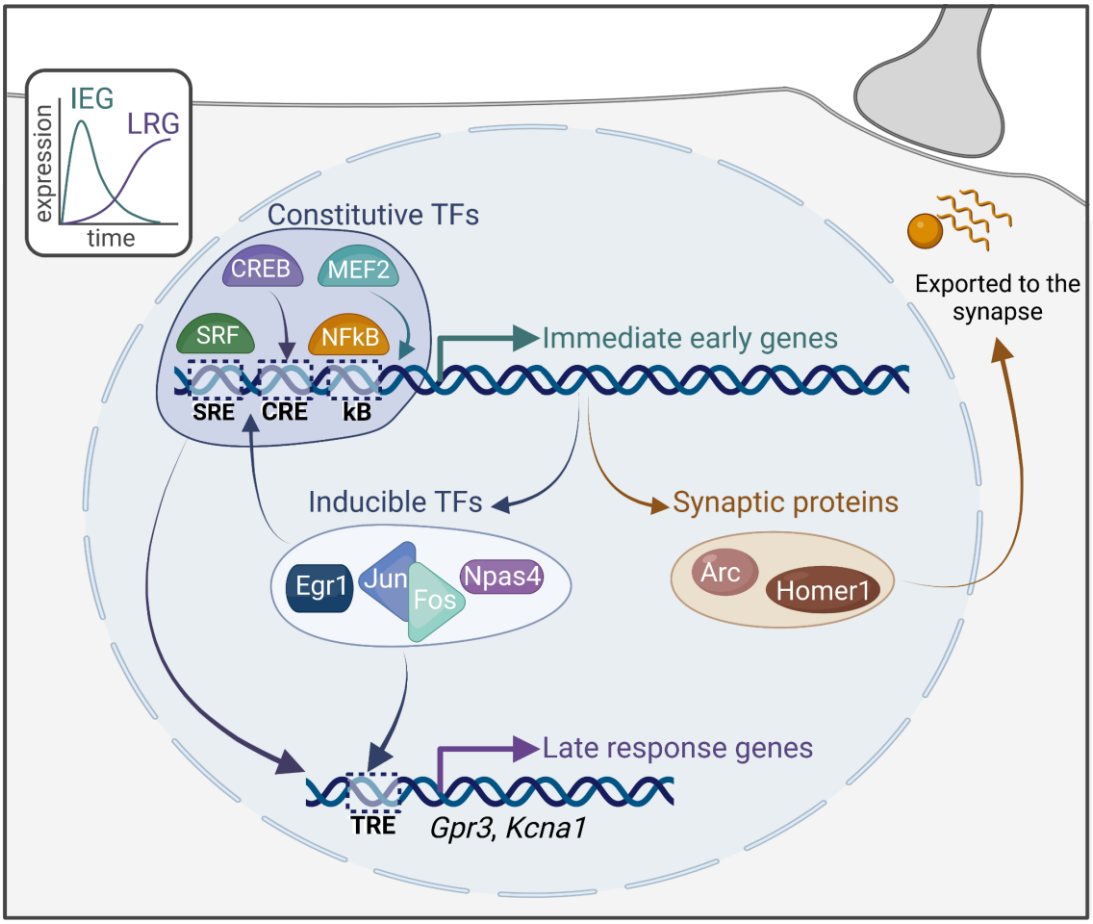

Figure 2. Transcriptional regulation in response to neuronal activity.
Dynamics of the activity-dependent transcription show a biphasic response, with the initial transcription of the IEG and the later response of the LRGs. Constitutive, stimulus-inducible TFs such as SRF, CREB, MEF2 and NFkB are recruited to the promoter of the IEGs to induce their transcription independently of de novo protein synthesis. IEGs comprise a group of inducible TFs (Egr1, Fos, Jun, Npas4) and synaptic effector proteins (Arc, Homer1a). The latter can be exported to the synapse, where they can be found at both the transcript and protein levels. Ultimately, IEGs regulate the transcription of the LRGs (Grp3, Kcna1), which is protein-synthesis dependent. IEG: Immediate Early Gene, LRG: Late Response Gene, CREB: CRE Binding protein, SRF: Serum Response Factor, MEF2: Myocyte Enhancer Factor-2, SRE: Serum-Response Element, CRE: cAMP-response element, TRE: TPA-response element, Gpr3: G-protein coupled receptor 3, Kcna1: Potassium Voltage-Gated Channel Subfamily A Member 1. Created with *BioRender.com.*

1.3.1.1. Immediate early genes

Already in the late 1980s, it was seen that neuronal activity [96] and other stimuli[97,98] strongly induced a set of genes, later called immediate-early genes (IEG) [99]. These genes encode regulatory proteins, such as kinase/phosphatases and transcription factors, but also synaptic effector molecules directly involved in the reorganization of neuronal connectivity required for memory formation. IEGs can be classified as rapid and delayed IEGs. Rapid IEGs, such as *Fos, Egr1* and *Arc*, display binding of stalled RNA polymerase II at their TSS for fast transcriptional induction[100]. *Jun, Dusp1, Klf4, Btg2* and *Bdnf* are examples of delayed IEGs which, on the other hand, show a slower response and unbound promoters by

RNA polymerase[101]. The two groups of genes are induced upon specific activity patterns: while brief and transient activity is enough to induce the rapid IEGs, delayed IEGs require a longer, sustained depolarization to be transcribed[102]. The differences in the induction of rapid and delayed IEGs seem to be correlated with eRNAs, where eRNAs arising from enhancers close by the promoter of rapid IEGs are sensitive to brief depolarization. The enhancers with rapid eRNA generation show higher accessibility and greater binding of activity-regulated TFs than enhancers associated with delayed IEGs. However, they do not include RNA polymerase II stalling as the rapid IEGs promoters[102]. Upon neuronal depolarization, the induction mitogen-activated protein kinase (MAPK) pathway is necessary for the transcription of rapid but not delayed IEGs. Another activity-induced pathway, Ca^{2+}/calmodulin-dependent protein kinase IV (CaMKIV), does not seem to regulate either rapid or delayed IEGs transcription[102], emphasising the specific complex communication between activity-induced cellular and transcriptional processes.

Recently, an additional epigenetic feature of the IEGs in developing neurons and stem cells was described[103]. IEGs present a bipartite signature, with H3K27ac at their promoter together -regarded as an active enhancer and promoter mark- with the repressive mark H3K27me3 on gene bodies, which prevents transcriptional elongation. Upon strong activation, the removal of the polycomb mark allows successful transcription, preventing incorrect random activation and assuring specific induction of IEGs. Furthermore, the duration of the IEG activation is brief and tightly regulated both at the transcriptional and post-transcriptional levels. Several miRNAs target IEG transcripts to maintain low levels in the absence of stimuli. Upon neuronal activation, the levels of these miRNAs are reduced, allowing transcription of the IEGs[104]. Additionally, IEG protein products are often unstable and subjected to degradation by the proteasome in a ubiquitination-independent manner[105].

Transcription of IEGs happens independently of *de novo* protein synthesis[99,106] very rapidly (already within minutes for rapid IEGs), indicating that the transcriptional regulators required for their induction are already present in the cell. Most of the promoters and enhancers of the IEGs present stimulus-responsive TFBSs, such as cAMP responsive element (CRE), serum-response element (SRE), or κB, bound by CREB, SRF and NFκB, respectively[107] and myocyte-specific enhancer factor-2 (MEF2) binding sites (**Fig.2**). This suggests a rather redundant activation mechanism common to most of the IEGs, even in different contexts of induction. Given that IEGs are triggered not only in response to neuronal activation but also to inflammation and differentiation[108,109], their specific induction relies on the TFBS at promoter and enhancers, and their differential usage[110,111]. For example, the five known enhancers regulating *Fos* expression are activated differentially in response to different stimuli, supposedly due to the different TFBS they display (**Fig.3**), which also may cause these

enhancers to establish contacts with the *Fos* promoter in a stimulus-specific manner.

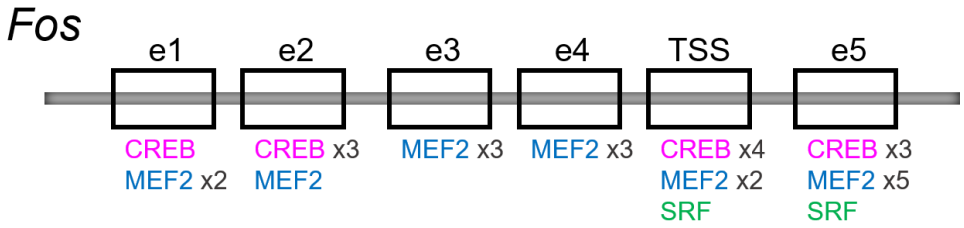

Figure 3. Schematic representation of Fos enhancers with identified TFBS.
Adapted from Joo *et al*. [111].

Among the IEGs, two of the best characterized are *Fos*, a transcription factor part of the activator protein 1 (AP-1) complex, and *Arc*, the activity-regulated cytoskeleton-associated protein involved in neuronal plasticity processes. *Fos* is not only induced in neurons or just by neuronal activity but also in response to growth factors[112], serum[113] and stress[106], and it plays central roles in regulating cell proliferation, differentiation and survival in several cell types[114]. The AP-1 complex is composed of Fos-Jun heterodimers, both containing a basic leucine zipper domain (bZIP) for dimerization and DNA binding, and binds the TPA responsive element (TRE)[107]. Formation of the AP-1 complex is strictly necessary for Fos activity[107]. While Fos is often used as a marker of neuronal activity, *Arc* is essential for the maintenance of long-term forms of plasticity and memory consolidation. *Arc* does not encode for a TF but for a structural protein involved in endocytosis that plays highly relevant roles in LTP, LTD and homeostatic plasticity[115]. In mice, the synaptic activity-responsive elements (SARE), a 100 bp element upstream *Arc* TSS composed of CREB, MEF2 and SRF binding sites, is sufficient to induce *Arc* expression triggered by synaptic activity[116]. Once transcribed, *Arc* mRNA is transported to the synapse and accumulates at the site of local synaptic activation, where it is translated[117]. *Arc* mRNA is subjected to nonsense-mediated RNA decay (NMD) to regulate spatial and temporal control of Arc synthesis.

1.3.1.2. Late-response genes: regulators of synaptic plasticity

Neuronal response to a wide variety of activity patterns and stimuli initiates a highly conserved pattern of IEG expression. However, the expression of the LRG, or secondary response genes (SRG), is tailored to the signal and generates a defined phenotypic response. The transcription of LRGs, in contrast to the IEGs, is dependent on new protein synthesis to regulate their expression, which starts later than the IEGs (**Fig.2**). A large fraction of the LRGs are proteins that regulate synaptic function and connectivity, such as Candidate plasticity gene 15 (Cpg15), which enhances dendritic outgrowth and synapse maturation. Cpg15 is a

glycosylphosphatidylinositol-anchored membrane protein, implying that most likely its role in neuronal physiology is through intercellular interactions[118]. Additional examples of LRGs with structural functions are G-protein coupled receptor 3 (Gpr3) and Potassium Voltage-Gated Channel Subfamily A Member 1 (Kcna1)[102]. LRGs with regulatory functions include the serum-inducible kinase (SNK), which enhances neurotrophin-mediated dendritic arborization[119] and mediates the phosphorylation of a postsynaptic protein (SPAR) to induce its degradation, destabilizing synapses[118]. But one of the most interesting examples of LRGs is the brain-derived neurotrophic factor (BDNF) since it is induced upon neuronal activity and regulates several neurologically relevant processes, such as memory formation. In the upcoming section, a deeper description of BDNF functionality and the regulation of associated processes is provided in detail, given the essential role of BDNF in the present thesis.

1.3.2. Neuronal response to BDNF and its regulation

1.3.2.1. BDNF: a member of the neurotrophin family

The BDNF is a member of the neurotrophin family, essential regulators of mammalian neurodevelopment and brain function, composed as well of the nerve growth factor (NGF), neurotrophin-3 (NT-3) and neurotrophin-4 (NT-4)[120]. Neurotrophins are small (~12 kDa), secreted proteins that form non-covalent dimers to bind two different cell surface receptors; the p75 neurotrophin receptor ($p75^{NTR}$), a member of the tumour necrosis factor receptor superfamily, and the tropomyosin-related (Trk) receptor tyrosine kinase. Although all neurotrophins bind $p75^{NTR}$, each neurotrophin has specificity for a different Trk receptor; NGF for TrkA, BDNF and NT-4 for TrkB, and NT-3 for TrkC[121]. Not only neurons produce and secrete BDNF but also microglial cells[122]. BDNF is the most abundant neurotrophin in the brain and it is particularly interesting because its expression, secretion and functional properties are dependent on neuronal activity, as are other relevant biological processes such as cognition and memory formation, where BDNF also plays a role[123].

1.3.2.2. BDNF functions in the brain

BDNF presents different roles in the brain depending on the developmental stage of the neurons. During development, BDNF is necessary for the differentiation of progenitor cells into neurons (neurogenesis)[124]. Yet, in adult neurons, it is responsible for inducing morphological and functional changes that shape neuronal connectivity[125]. BDNF is one of the most studied neurotrophins because of its role as a mediator of LTP in mature neurons. LTP, a form of synaptic plasticity, has been described to be a phenomenon common to different areas of the brain, including the cerebral cortex and amygdala, but the adult hippocampus is the best-known system undergoing LTP. Different studies have linked LTP with learning, memory formation and consolidation[126], making it a highly relevant

process in neurobiology. BDNF acts on both the pre- and post-synaptic cell to modulate synaptic efficiency, by enhancing neurotransmitter release and the sensitivity to it in the post-synaptic neuron[127,128].

BDNF also mediates the balance between neuronal apoptosis and survival[129,130], predominantly in the peripheral nervous system[131]. In the central nervous system, its role shifts towards the regulation of morphological changes in mature neurons like dendritic outgrowth[132,133] and spine maturation[134]. These structural changes come accompanied by the adjustment of neuronal connectivity through synapse formation, stabilization and removal, an outcome also triggered by the neurotrophin[135]. BDNF can lead to the formation of both excitatory and inhibitory synapses in hippocampal neurons[136]. The effect of BDNF on synaptogenesis and maturation relies on the ability of BDNF to trigger transcriptional changes. Many of the BDNF-regulated processes are transcription-dependent, such as LTP. LTP can be explained in three sequential phases -short-term potentiation, early LTP and late LTP- and while the first two are independent of transcription, BDNF-mediated late LTP is transcription- and translation-dependent[137], indicating that BDNF regulation of transcription is crucial for the correct function of the brain.

In highly polarized cells such as neurons, for an external stimulus binding the cellular surface to induce gene transcription, a series of signal transduction pathways are required to convey the information to the nucleus. This is also the case for BDNF. However, apart from relying on signalling pathways to induce long-lasting consequences, BDNF also exerts fast effects on the target cell by inducing local changes when binding to its receptor. These can include rearrangements at the synapse mediated by PTMs of already existing synaptic components, such as receptors. For instance, BDNF binding to TrkB and the following activation of the receptor leads to the phosphorylation of NMDA receptors in the plasma membrane, in particular of the GluN1 and GluN2B subunits[138,139], which increases the probability of receptor opening and postsynaptic response to glutamate release[140]. Additionally, BDNF induces local protein translation from dendritic mRNAs[141], conferring the neurotrophin the ability to modulate neuronal function in a location- and time-specific manner. Following the previous example, it was recently described that the application of BDNF to hippocampal neurons led to the synaptic synthesis of PYK2 (non-receptor tyrosine kinase 2), a kinase that promotes the integration of GluN2B at the synapse, and that this is required to mediate LTP[142].

1.3.2.3. Regulation of BDNF expression

In mammals, BDNF starts being expressed during early postnatal brain development and can be found in all brain regions, with higher concentrations in the hippocampus and neocortex[143]. The transcription of the *Bdnf* gene is dependent on neuronal activity and, ultimately, on intracellular Ca^{2+} increase. Upon neuronal activation, membrane depolarization leads to a Ca^{2+} influx through

voltage-gated Ca^{2+} channels (VGCCs)[144] and Ca^{2+}-permeable glutamate receptors, especially NMDA receptors[145,146]. Through different signal transduction cascades[147], this leads to the phosphorylation of the cAMP-response element binding protein (CREB) [148] and the calcium-response factor (CaRF)[149] and binding to the BDNF promoter. BDNF has 9 promoters in humans and 8 in rodents[150], each one being activated in response to different cues[151]. The usage of a specific BDNF promoter in response to activation is specific to the physiological state and cell type, but also to the differences in the pattern, duration and source of intracellular Ca^{2+} increase[152]. Alternative promoter usage could lead to alternative splicing of the BDNF transcript[153], which influences the subcellular localisation and stability of BDNF, and allows the spatiotemporal fine-tuning of BDNF functions[150,154,155].

Epigenetic mechanisms also govern the regulation of BDNF transcription in an activity-dependent manner. The *Bdnf* promoter is methylated before activation and is bound by methyl-CpG binding protein 2 (MeCP2)[156], a repressive transcription factor that exerts its function through the recruitment of the histone deacetylase complex (histone deacetylase 1 (HDAC1) and SIN3 transcription regulator family member A (SIN3A))[157]. Neuronal activity would induce MeCP2 phosphorylation and its release from the promoter together with the HDAC complex, enabling *Bdnf* transcription. Demethylation of the *Bdnf* promoter also occurs during neuronal activation in adult hippocampal neurons via the product of the IEG *Gadd45b* and ultimately allows adult neurogenesis[158]. Furthermore, a long non-coding RNA (lncRNA) associated with the *Bdnf* locus, *Bdnf-antisense* (*Bdnf-as*), represses BDNF expression by changing the chromatin conformation at the *bdnf* locus[159]. However, this antisense transcript has not been found in mouse and rat[160]. The *Bdnf-as* plays a role in neurological disorders such as Alzheimer's and Parkison's disease and autism spectrum disorders, but also in several cancers, giving it a role as a prognosis marker for the tumour malignancy[161].

Finally, BDNF binding to its receptor TrkB prompts a positive feedback loop by inducing BDNF expression from promoters I, III and IV through MAPK activation of AP-1 transcription factors[162].

1.3.2.4. Secretion of BDNF

Once transcribed, BDNF is initially synthesized as pre-pro-BDNF in the endoplasmic reticulum. After the removal of a signalling peptide, the pro-BDNF precursor is later cleaved to mature BDNF intra-[163] and extracellularly, this last one dependent on plasmin[164] and metalloproteases 2 and 9 (MMP2, 9)[165,166]. Secretion of mature BDNF happens through a constitutive pathway via small secretory vesicles (50-100 nm diameter), which are released in the cell periphery independently of any stimulus[167]. On the contrary, a regulated pathway induces pro-BDNF packaging into large dense core vesicles or large secretory granules containing prohormone convertases[168] in a Ca^{2+}-dependent manner in response

to neuronal activity and stimuli, such as membrane depolarisation, high-frequency stimulation, theta burst stimulation or the neurotrophin itself[169,170].

A single-nucleotide polymorphism (SNP) in the *Bdnf* gene leads to the Val66Met mutation in the pro-domain of the immature BDNF. Mutated pro-BDNF displays defects in the sorting of BDNF into secretory granules[171]. Despite having normal BDNF production, the failure in BDNF localization to the synapse and its release to the extracellular matrix leads to low levels of extracellular BDNF. In humans, carriers of this mutation display smaller hippocampal volume and variation in cortical morphology, which are associated with reduced memory function[172].

1.3.2.5. Downstream effects of neurotrophin receptor binding

At physiological conditions, neurotrophins are basic molecules, a rare property for secreted proteins that allows them to stick to cell surfaces and the extracellular matrix and limits their range of action to proximity to their secretion site[173]. The binding of the neurotrophins to their receptors elicits receptor dimerisation and activation of different signalling kinases, depending on the receptor concentration and the localization at the membrane[121,174]. Additionally, the kinetics of BDNF release from the producer cell and its local concentration will also influence the configuration of the responsive pathways, leading to a whole range of diverse outcomes upon BDNF-receptor binding[175,176].

Pro-BDNF and mature BDNF bind $p75^{NTR}$ and TrkB receptors, both in the secreting and target cell. Pro-BDNF presents a higher affinity for $p75^{NTR}$ than mature BDNF[177,178]. The balance between the activation of $p75^{NTR}$ or TrkB is extremely important in regulating BDNF-dependent neuronal survival. While activation of the BDNF canonical receptor, TrkB, elicits most of the survival and growth properties of the neurotrophin through the mitogen-activated protein kinase (MAPK), phosphatidylinositol 3-kinase (PI3K) and phospholipase C_γ (PLC_γ) pathways[173] (Table 1), binding to $p75^{NTR}$ can activate a pro-apoptotic response through the Jun kinase (JNK) pathway or may, on the contrary, induce a pro-survival response through Nuclear Factor κB (NFκB)[179] (Table 1). A summary of the main activated pathways by TrkB and $p75^{NTR}$ together with the principal functional outcomes can be seen in Table 1. $p75^{NTR}$-induced JNK pro-apoptotic cues are repressed by TrkB activation of pro-survival signalling, to ensure a consistent biological response. Likewise, $p75^{NTR}$-dependent NFκB pathway activation contributes to the survival effects of TrkB activation[180]. Of note, $p75^{NTR}$ binding by pro-BDNF regulates long-term depression (LTD) in the hippocampus [181] and amygdala[182], whereas the mature ligand is a mediator of LTP when binding TrkB.

Table 1. Main signalling pathways induced by BDNF receptors TrkB and p75NTR and their principal outcomes.

Receptor	Induced pathway	Outcome
$p75^{NTR}$	NFκB	Neuronal survival
$p75^{NTR}$	JNK	Apoptosis
TrkB	MAPK/MEK	Neuronal differentiation / maturation
TrkB	PI3K/Akt/mTOR	Neuronal survival / Dendritic mRNA translation
TrkB	PLC_γ	Ca^{2+} increase, synaptic plasticity (LTP)

Fig.4 shows a summary of the main known pathways responsive to the neurotrophin when binding the canonical receptor TrkB, with a special focus on their convergence in the nucleus. Naturally, once BDNF binds TrkB, the receptor undergoes autophosphorylation at Tyr515 and serves as a docking point for the Src homology and Collagen (Shc) adaptor protein[183]. Activated Shc induces both the PI3K and MAPK (also named MEK) pathways. Both kinases start a series of signal transduction events that overlap to a certain degree, yet can induce different outcomes. PI3K phosphorylates protein kinase B (PKB, also known as Akt) and ultimately leads to the BDNF-controlled protein translation directly at the dendrites induced by the mammalian target of rapamycin (mTOR)-signalling[184–186]. Furthermore, Akt mediates the phosphorylation of chromatin-modifying enzymes, conveying the signal to the nucleus and regulating transcription. Akt phosphorylates EZH2, a PRC subunit responsible for H3K27me3 deposition, preventing its binding to H3 leading to transcriptional derepression[37]. The acetyltransferase p300, which mediates acetylation of many lysine residues in the histone tails and other proteins, is also a target of Akt phosphorylation, leading to p300 associated gene expression[187].

The activation of Shc through TrkB phosphorylation at Tyr515 also triggers the MAPK signalling pathway by activating Ras, and the phosphorylations of Raf, MEK1/2 and extracellular signal-regulated kinase (ERK1/2)[188]. This pathway can stay active for sustained periods via the small GTPase Rap1[189]. In addition to MEK1/2, Ras also triggers MEK5, which ultimately leads to ERK5-dependent activation of the myocyte enhancer factor 2 (MEF2), a transcriptional regulator that conveys this signal to the nucleus[190].

The docking protein Shc gets additionally activated by binding to phosphorylated Tyr816 in TrkB and recruits PLC_γ, which catalyzes the conversion of phosphatidylinositides to diacylglycerol (DAG) and inositol 1,4,5 triphosphate (IP_3). IP_3 induces the release of Ca^{2+} from intracellular stores. The increase in intracellular Ca^{2+} levels activates calcium-dependent kinases belonging to the CaMK pathway. In parallel, DAG is able to regulate protein kinase C (PKC), which establishes a cross-talk with the ERK signalling pathway to regulate neurite

outgrowth[191]. DAG may also act as a second messenger[192] to induce PLC-dependent activation of transient receptor potential canonical 3 (TRPC3) channel, which triggers cation (Na^+, Ca^{2+}) influx into the neuron[193].

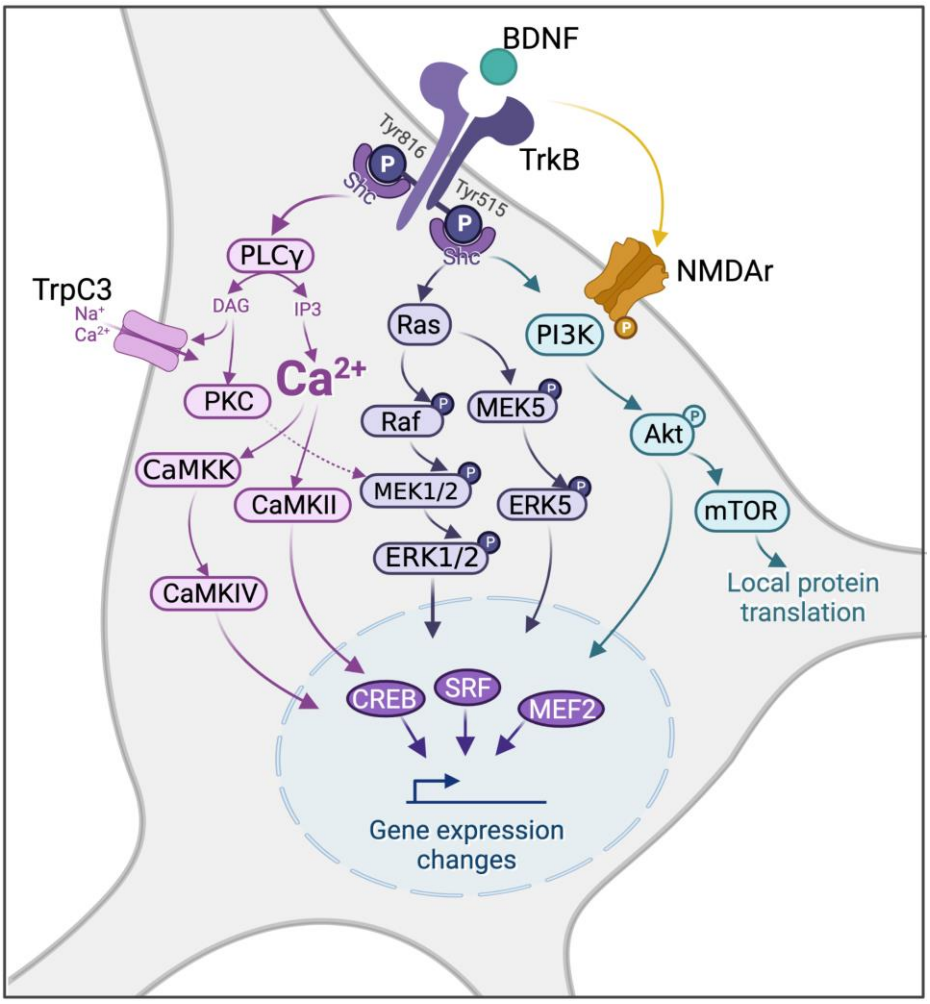

Figure 4. BDNF-induced signalling pathways.
The three main pathways induced by BDNF-TrkB binding are PI3K (phosphatidyl-inositol 3 kinase), MEK/MAPK (mitogen-activated protein kinase) and PLCγ (phospholipase C_γ). All of these pathways transduce the extracellular signal to the nucleus of the cell, where activity-dependent transcription factors (CREB, SRF, MEF2 and others) reorganize to induce transcription. Activation of TrkB receptors also triggers the activation of NMDA and TrpC3 receptors. Image created with BioRender.com

Transmission of the BDNF signal can happen by sequential phosphorylation of signal transduction proteins, i.e., Ras/MAPK pathway, but the BDNF-TrkB complex can in addition get internalized by endocytosis, forming a biochemically active signalling endosome, directly transmitting the signal by itself. The endosome undergoes a microtubule-dependent retrograde (axon-to-soma) or anterograde (dendrite-to-soma) transport that is necessary for the phosphorylation of CREB and induction of *Fos* and *Arc* expression[194,195]. Dendrite-to-nucleus anterograde signalling is Ca^{2+} and MEK1/2-dependent, whereas retrograde signalling is MEK5/MEF2-dependent[195,196], illustrating the complexity in the BDNF mode of action tightly associated with its diverse functions.

Ultimately, the convergence of these signalling cascades in the nucleus induces the BDNF-responsive transcription. Initially, BDNF stimulation orchestrates activity-dependent transcription factors such as CREB[197], MEF2[195,196] or SRF[198] (**Fig.4**) which bind the promoter elements of the IEG. Some of the BDNF-responsive IEG are *Arc*, *Nr4a1* and *Egr1*[199], related to synaptic plasticity. However, comprehension of BDNF-induced transcriptional response, its regulation and dependency on signalling pathways is still to be fully addressed.

1.3.2.6. BDNF in human disease

BDNF fulfils highly relevant purposes in the brain. The dysregulation of BDNF production leading to lower availability of BDNF, as already mentioned in **section 1.3.2.4**, can affect the normal physiology of the brain. In Alzheimer's disease, levels of BDNF transcript are three- to four-fold lower than in healthy individuals[200]. Similarly, in patients with Schizophrenia levels of both BDNF transcript and protein are reduced[201,202]. Likewise, the pathophysiology of depression has strongly been correlated with lower levels of the neurotrophin, and treatment with antidepressants such as ketamine rescues the normal levels of BDNF[203].

Although increasing the levels of BDNF is thought to have therapeutic potential against neurodegeneration and depression, this is limited since BDNF cannot cross the blood-brain barrier. An ongoing phase I clinical trial (*NCT05040217, ClinicalTrials.gov*) is testing the preliminary efficacy of adenoviral delivery of *bdnf* with gene therapy to treat patients with Alzheimer's disease and mild cognitive impairment. Alternatively, several epigenetic drugs have been approved by the FDA primarily for the treatment of cancer malignancies since they regulate gene expression without affecting the genetic sequence. In mouse models, epigenetic drugs already show promising results in cardiovascular[204] and neurodegenerative diseases[205]. Understanding the functional consequences of BDNF in the cell not only at the synapse but also at the level of transcriptional regulation can offer insights into alternative therapies for neurotrophin-related brain disorders by epigenetic drugs.

1.4. Aims and motivation of this project

Neuronal stimulation-induced transcription is the ultimate downstream effect of activated signalling cascades and one of the proposed mechanisms to store the external information to trigger long-lasting changes in the cell. Providing a comprehensive view of the transcriptional changes upon different conditions of neuronal stimulation will aid in understanding stimulus-induced phenotypic changes. This can shed light on new therapeutic approaches to target neurological disorders where these regulatory mechanisms are dysregulated.

The main objective of my PhD study is to gain a better understanding of the chromatin response to stimulation that orchestrates the transcription of inducible genes in postmitotic neurons. Many studies have addressed the neuronal response to different stimuli[198,206,111] in a gene-specific manner. Therefore, I aimed to define the changes in the chromatin landscape at a genome-wide level using genomic and proteomic approaches. In particular, detecting proteins related to transcriptional regulation is challenging[207–209] as it requires the development of more sensitive proteomic methods. To address this, I applied a subcellular-proteome enrichment, with a special focus on chromatin-bound and nuclear-soluble proteins, to study the proteome dynamics in response to stimulation.

The integration of multi-omic datasets can often reveal regulatory mechanisms at the chromatin level that affect gene expression and, ultimately, phenotypic characteristics, that may not have been identified when independently studying each omics dataset. A joint study in the labs of Noh and Zaugg, led by Dr. Ignacio Ibarra, Dr. Vikram Ratnu and me, attempted to integrate gene expression and chromatin accessibility changes in response to BDNF and KCl to identify the role of BDNF in chromatin regulation[210]**.** I contributed to generating a stimulation-specific subcellular proteomics dataset to characterize the behaviour of transcriptional regulatory proteins. Furthermore, I assessed the effect of transcription factor cooperativity in controlling BDNF-specific gene expression in an enhancer-dependent manner.

In light of the strong and lasting effect of BDNF on chromatin accessibility, I reasoned that these changes in the chromatin landscape could condition the transcriptional response in future encounters with BDNF. In this hypothesis, I wondered if the durability of the chromatin response could act as a bookmarking event that would lead to an enhanced or desensitized response to the same stimulus. To address this, I aimed at studying the differences at the transcriptional level between neurons stimulated once or twice with BDNF, to identify genes with enhanced or desensitized transcription. Secondly, I aimed to profile the chromatin accessibility to associate it with the changes in gene expression, in an attempt to identify chromatin regulatory elements that could condition the adaptions in the transcriptional response. To shed further light on possible mechanisms of

transcriptional bookmarking, my goal was to characterize the epigenetic landscape by assessing the differential deposition of histone marks, which is currently ongoing. The overarching goal was first to assess if there was a phenomenon of transcriptional adaptation to BDNF in postmitotic neurons and, if so, identify possible mechanisms regulating this adaptation.

CHAPTER 2:

MATERIALS & METHODS

2.1. Cell culture and treatments

Mouse primary cortical neurons. CD1 mouse embryos at embryonic day 15 and a half (E15.5) were used for obtaining primary cortical neurons. Pregnant females were sacrificed by cervical dislocation, and embryos were taken out from the embryonic sac and sacrificed by decapitation. Cortical tissue was dissected under a dissection microscope after removing the meninges and transferred to a 1.5 ml tube containing cold neurobasal medium. For dissociation, the cortical tissue was placed on ice and chopped using a scalpel, followed by treatment with 3 ml of Accutase (Thermofisher) for 10 minutes at 37°C. During digestion, the tissue was treated with 250 units of Benzonase (Millipore) to digest released genomic DNA from dead cells in order to prevent it from promoting cell clumping. After quenching with serum, tissue was gently homogenized by pipetting and passed through a 70 µm strainer before plating.
Nunc^{TM} culture plates (Thermofisher) were coated with 0.1 mg/ml of poly-D-lysine (Sigma) and 2.5 µg/mL of laminin (Sigma) beforehand. Cells were plated at a density of $1x10^7$ cells/mm^2 in Neurobasal medium (Gibco) containing 1% penicillin/streptomycin, 2% B27 supplement and N-2 supplement (Thermofisher). Media was fully replaced 2 hours after plating, and half the volume was replaced with fresh media twice a week. Neurons were used for experiments after 6 days *in vitro* (DIV) and maintained up to 11 DIV.
All dissections and primary neuronal cultures were conducted by me.

Stimulation with BDNF and KCl, and T-5224 treatment. Before stimulation, cultures were silenced with 100 µM D-(-)-2-Amino-5-phosphonopentanoic acid (AP-5; Tocris), an NMDAr antagonist, and 1 µM tetrodotoxin (TTX; Tocris), a sodium channel blocker, for 1h by directly adding them to the culture medium. BDNF (R&D Biosystems) was added to the culture at a concentration of 10 ng/ml. Membrane depolarization was triggered by adding 55 mM KCl to the medium by diluting 3 times a depolarization buffer composed of 170 mM KCl, 2 mM $CaCl_2$, 1mM $MgCl_2$ and 10 mM 4-(2-hydroxyethyl)- 1-piperazineethanesulfonic acid (HEPES), described in Kim *et al*.[211] For the comparison between BDNF and KCl stimulations, cells were treated or left untreated (with TTX and AP-5 in the medium) at DIV7 for 1h before collection.
For the double stimulation system with BDNF, cells on DIV9 were blocked with TTX and AP-5 for 1h. One set of cultures was treated with 10 ng/ml BDNF for another hour whilst another set was left untreated (with TTX and AP-5) for the same time. After that, media from all cultures were exchanged by conditioned

media and left to rest for 48h. On DIV11, all cultures were silenced again for 1h and cultures were either treated with BDNF for 1h or left untreated for the same amount of time prior to collection.
To study Fos effect on *Arc* transcription, I applied the small molecule inhibitor T-5224 [212] for 1h prior to BDNF stimulation, simultaneously with the addition of AP-5 and TTX. T-5224 was added directly to the medium from a 1000-fold concentrated stock in DMSO to the desired final concentration.
All treatments and stimulations were conducted by me. KCl stimulation was adapted from protocols from Michael Greenberg's lab (Harvard Medical School) and the BDNF double stimulation system was conceived by me.

Mouse Embryonic Stem Cell (mESC) maintenance and differentiation to glutamatergic neurons. mESC were obtained from male 129-B13 agouti mice and cultured in ES-medium based on Knock-Out Dulbecco's Modified Eagle Medium (DMEM; Gibco) containing 15% EmbryoMax fetal bovine serum (FBS; Millipore), 1% penicillin/streptomycin (Gibco), 1% non-essential amino acids (Gibco), 1% GlutaMax (Gibco), 0.1% β-mercaptoethanol (Sigma) and 20 ng/ml leukaemia inhibitory factor (LIF; produced by the EMBL Protein Expression and Purification Core Facility) in a humidified incubator at 37°C and 5% CO_2. Culture flasks were coated with 0.1% gelatin prior to seeding the cells. When seeding cryopreserved cells or after Fluorescence-activated Cell Sorting (FACS), immortalised primary mouse embryonic fibroblasts (MEF) were used as a feeder layer. Media were changed daily and cells were passaged every other day by trypsinizing (TrypLE^{TM}, Gibco) cells for 5 minutes at 37°C.
Differentiation of mESC to glutamatergic neurons was performed based on the protocol by Bibel *et al.* [213]. Briefly, I removed the LIF from mESC culture and 4 million cells were grown in suspension using 10 cm non-adherent plates to promote the formation of cellular aggregates (CA) or embryoid bodies for 8 days. Cells were cultured in CA medium, composed of DMEM high glucose (Gibco), 10% FBS, 1% penicillin-streptomycin, 1% non-essential amino acids, 1% Na-pyruvate (Gibco), 1% GlutaMax and 0.1% β -mercaptoethanol, which was changed on days 2, 4 and 6. On day 6, CA medium was supplemented with 5 µM retinoic acid (Roche) to promote the differentiation towards the neuronal lineage. On day 8, neuronal precursor cells (NPCs) were dissociated by trypsinization for 3 minutes at 37°C to generate a homogenous unicellular suspension. NPCs were plated on PDL- and laminin-coated Nunc^{TM} plates at 2 x 10^6 cells/cm^2 and maintained in DMEM high glucose supplemented with 1% penicillin/streptomycin, 1% N-2 and 2% B-27 supplements, which was changed 2h, 24 and 72h after plating. All experiments were performed on day 12 of differentiation.
All cultures and differentiations were conducted by me, occasionally with the help of Nadine Fernandez-Novel Marx.

2.2. RNA extraction and RT-qPCR

RNA was extracted from approximately 1 million neurons after harvesting them with a cell scraper using the RNeasy Mini kit (Qiagen). To lyse the cells, QIAshredder columns were used, and DNA contamination was removed on-column using the RNAse-free DNase set for RNeasy columns (Qiagen). RNA concentration was measured with a Nanodrop spectrophotometer at 260 nm, and the ratio to 280 nm and 230 nm was used to assess RNA purity. For cDNA synthesis (reverse transcription, RT), at least 300 ng RNA were processed with the High Capacity cDNA Reverse Transcription kit (Thermofisher), and the resulting cDNA was directly used for qPCR measurements without an additional purification step. Quantitative PCR measurements were performed on a QuantStudio 6 Flex Real-Time PCR System using SYBR Green PCR Master Mix (Applied Biosystems). Primers used in this thesis are listed in Table 2**.** All experiments were performed by me

Table 2. List of primers used for RT-qPCR.

Primer name	Sequence (5’ to 3’)
RPL-13 Fw	AAC TTA AGC TGG CCA CCC
RPL-13 Rv	ACT CTG GCC TTT TCC TTT TTG T
Arc Fw	AGG AGA ATG ACA CCA GGT CTC AA
Arc Rv	GTG GTG TGG TGA TGC CCT TT
Fos Fw	GAC AGC CTT TCC TAC TAC CAT TCC
Fos Rv	CGC AAA AGT CCT GTG TGT TGA
Btg2 Fw	GGA CGC ACT GAC CGA TCA TTA
Btg2 Rv	GAT ACA GCG ATA GCC AGA ACC

2.3. Messenger RNA sequencing (mRNA-seq)

mRNA was isolated from total DNA-free RNA extracted with RNeasy Mini kit using the NEBNext® Poly(A) mRNA Magnetic Isolation Module (New England Biolabs®, Inc.), and libraries for sequencing were prepared using the NEBNext® Ultra RNA Library Prep Kit for Illumina sequencing (New England Biolabs®, Inc.). The concentration of RNA libraries was measured with Qubit fluorometer (Thermofisher) and RNA quality and library size distribution was assessed on the Bioanalyzer RNA 6000 Pico (Agilent). Only libraries with RNA Integrity Number (RIN) of more than 7 were pooled for sequencing in Illumina NextSeq500 sequencer, in single-end mode, aiming at 20 million 50-bp reads per sample. Library generation and pooling were done by me, and sequencing and demultiplexing were performed by GeneCore at EMBL Heidelberg.

mRNA-seq data analysis. Sequencing reads were trimmed to remove index, low quality and short reads (<20 bp) using Trim Galore! [214] (Galaxy v.0.4.3) and the remaining reads were aligned to the *Mus musculus* mm10 mouse reference genome using RNA STAR alignment tool [215] (Galaxy v.2.6.0b-2). Read counts per gene were assigned with featureCounts [216] (Galaxy v.1.6.3). Differential expression analysis was performed using the R package DESeq2 [217] (v.1.34.0) with the following model: *y ~ condition*, where *y* are the DESeq2 normalized gene counts and *condition* is either *Basal*, *Stimulated*, *Recovery* or *Re-stimulated*, being *Basal* the control situation to estimate $\log_2$ fold changes, standard errors and significance on gene expression changes using the Wald test implementation (two-sided). Only genes with more than 100 counts -in all samples together- were processed in further analysis. Additionally, to reduce the variation in the estimator of the changes in gene expression of genes with low counts or high variation across replicates, I applied the shrinkage estimator with the *apelgm* function from the DESeq2 package[218].

I defined the differentially expressed genes (DEG) with a False Discovery Rate (FDR) < 5% and an absolute $\log_2$ fold change > 0.5 in *Stimulated, Recovery* or *Re-stimulated* versus *Basal.* The DESeq2 normalized counts of the 5087 DEGs were transformed using the variance-stabilizing normalization (vsn) [219] and Z-score normalized before performing unsupervised clustering of expression changes by partitioning around medoids (PAM) clustering. I set the number of *k* medoids as 6 after applying the Elbow method (WSS: Within-Cluster-Sum of Squared Errors) for cluster number determination (**Fig.5**). The apparent optimal number of clusters is set to be 4. However, I explored the expression patterns with *k*=4, *k*=5 and *k*=6 and visualized the different clusters with heatmaps. Based on the appearance of interesting expression patterns with *k*=6, I decided to proceed with the characterization with this number of clusters.

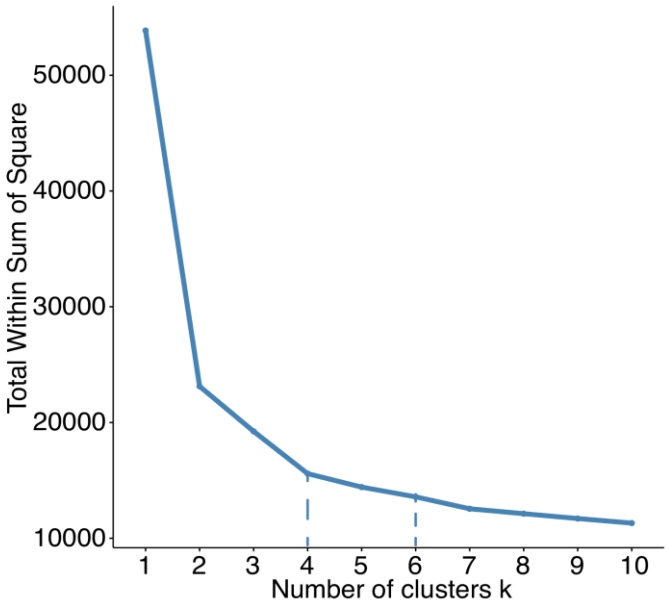

Figure 5. Elbow plot of WSS method for determination of cluster number (k) using pam clustering algorithm.

At k=4 the curve starts bending, where the optimal number of clusters is expected to be appropriate according to WSS. K=6 is also depicted as this was the final number of clusters chosen for this study.

Gene Ontology (GO) enrichment analysis of the clusters and other gene groups was performed using the clusterProfiler R package [220] (v. 4.2.2). Annotation of genes as transcription factors was performed using the CIS-BP database [221] (Build 2.0).
RNA-seq analysis was designed and performed by me, with the assistance of Sarah Kaspar, from the Center for Statistical Data Analysis at EMBL Heidelberg.

2.4. Changes in subcellular protein abundances

Subcellular protein fractionation. Neurons derived from mESC or primary neurons were harvested using a scraper and pelleted at 500 *g* for 5 minutes. 10 million neurons were washed twice with ice-cold phosphate-buffered saline (PBS) and used for subcellular protein extractions using the Subcellular Protein Fractionation kit for Cultured Cells (Thermofisher), following the manufacturer's instructions. This kit performs sequential fractionations using detergent extractions and centrifugations to separate membrane, cytosolic and soluble nuclear proteins, and extracts chromatin-bound proteins by digestion with micrococcal nuclease (MNase), leaving a pellet with cytoskeletal proteins.
Selection of the optimal protocol for MS-based subcellular proteome analysis was done together with Dr Henrik Hammarén from the Savitski lab, at EMBL Heidelberg.

Sample preparation for mass spectrometry (MS). Each of the obtained subcellular fractions was denatured in lysis buffer (50 mM HEPES-NaOH pH 8.5, 1% SDS, protease inhibitors) at 95°C for 5 minutes. Residual genomic DNA was digested using 50 U of benzonase per 100.000 cells at 37°C for 30 minutes, or at least until the solution was not viscous. For protein quantification, an aliquot was diluted 50 times and quantified using the BCA Protein Assay kit (Pierce). From each subcellular fraction (membrane, cytosol, nucleoplasm, chromatin and cytoskeleton). 10 µg of denatured, nucleic acid-free protein were used for sample preparation for MS using a modified version of the SP3 method [222]. Sera-Mag SpeedBeads (GE Healthcare) were used to precipitate proteins using 50% ethanol and 2.5% formic acid (FA) for 15 minutes at RT. Beads were washed four times on filter plates (0.22 µm pore size; Millipore) with 70% ethanol. Proteins were digested on beads overnight at room temperature with trypsin and Lys-C (5 ng/µl final concentration each) in 90 mM HEPES pH 9.5, 5 mM chloroacetic acid and 1.25 mM tris(2-carboxyethyl)phosphine (TCEP). To elute digested peptides from beads, we performed two rounds of centrifugation with 2% DMSO and eluted peptides were vacuum dried to be later on reconstituted in water.
Peptides from each sample were labelled with Tandem Mass Tags (TMT; Thermofisher) to allow for the combination of different fractions in an MS run with

increased coverage. In each experiment, biological replicates were run in separate MS runs and the different conditions (subcellular fractions and stimulations) were pooled together. Labelling was done with 4 µl of the TMT label (20 µg/µl in acetonitrile (ACN)) for 1 hour at room temperature. Hydroxylamine (1.1% final concentration) was used to quench unreactive TMT labels. After labelling, the corresponding samples were pooled together for desalting in OASIS HLB µElution plates. Peptides were washed twice with 0.05% FA and eluted in 80% ACN and 0.05% FA, and later vacuum dried. Reconstitution was done in 20 mM ammonium formate (pH 10) for high-pH reverse chromatography (HPLC). Peptide pre-fractionation was done on Ultimate 3000 HPLC (Dionex) with an X-bridge column (2.1 x 10 mm, C18, 3.5 µm, Waters) using 20 mM ammonium formate pH 10 as running buffer and ACN as elution buffer. Peptides were separated into 12 fractions and vacuum dried again before being reconstituted in reconstitution buffer (0.1% FA, 4% ACN) for nano-liquid chromatography (LC)-MS/MS.
Protein quantification and digestion and peptide labelling were performed by me together with Dr Henrik Hammarén, who carried out alone the peptide pre-fractionation.

Mass spectrometry analysis. MS analysis was performed on an Ultimate 3000 RSLC (Thermofisher) connected to a Q Exactive Plus mass spectrometer (Thermofisher) in positive ion mode. After loading the peptides onto a trapping cartridge (Acclaim C18 PepMap 100; Thermofisher) with 0.1% FA, an analytical column (nanoEase M/Z HSS C18 T3; Waters) was used for separation using a gradient of 2-40% of 0.1% FA in ACN for 120 minutes, with a constant flow of 0.3 µl/min. Full scan MS spectra with a mass range of 375–1200 m/z were acquired in profile mode using a resolution of 70,000 (maximum fill time of 250 ms or a maximum of 3e6 ions (AGC). For the isolation of precursor ions, the Top10 method was used with a window of 0.7 m/z, and isolated precursors were fragmented using 30 NCE (normalized collision energy). Tandem MS spectra (MS/MS) were acquired in profile mode with a resolution of 35,000 and an AGC target of 2e5 with a dynamic exclusion window of 30s.
Dr Henrik Hammarén conducted all the HPLC-MS/MS experiments.

Mass spectrometry data analysis. The processing of MS raw files was done using IsobarQuant[223], and the identification of proteins and peptides was achieved with Mascot (v2.5.1., Matrix Science) using a reference mouse proteome (Uniprot Proteome ID: UP000000589, downloaded 14.5.2016), which was modified to include common contaminants and reversed protein sequences.
Downstream analysis of identified proteins was done in R. After removing common contaminants, only proteins with 2 unique quantified peptides in 2 or more replicates were considered. To calculate fold changes over control (unstimulated cells), the vsn package [219] was used to normalize the protein reporter signal sums within each TMT set to get the vsn-corrected values. The

differential analysis of changing protein abundance across conditions was performed with the limma package [224].
MS data analysis was performed by Dr Henrik Hammarén following standard pre-processing pipelines by Frank Stein, from the Proteomics Core Facility at EMBL. Downstream analysis was performed by Dr Henrik Hammarén and I.

2.5. Western Blot

Neurons were washed with PBS supplemented with protease inhibitors (Sigma), harvested by scraping and snap frozen in liquid nitrogen. Cell pellets of more than 1 million neurons were resuspended in 200 µl of ice-cold PBS supplemented with 0.5% Triton-X and protease inhibitors and incubated for 30 minutes at 4°C with rotation. Cytoplasmic fraction was separated by centrifugation at 5000 *g* and 4°C for 5 minutes. The pellet containing nuclei was further resuspended in ice-cold modified Radioimmunoprecipitation Assay buffer (RIPA; 25 mM Tris pH 7.6, 150 mM NaCl, 1% NP-40, 1% Na-deoxycholate and 0.1% SDS) and subjected to sonication (6 pulses, pulse time 4s ON, 1s OFF, amplitude 40%) to shear chromatin and solubilize chromatin-bound proteins. Protein amounts were quantified using Bradford colourimetric method (BioRad) at 595 nm. Aliquots of 20µg of protein were prepared in LDS-sample loading buffer (BioRad) and heated up at 95°C for 10 minutes. Proteins were separated by size using sodium dodecyl sulfate-polyacrylamide gel electrophoresis (SDS-PAGE) with NuPAGE 4-12% Bis-Tris gels (Invitrogen) in NuPAGE MOPS SDS Running buffer for 1h at 150V. Protein transfer to polyvinylidene difluoride (PVDF) membranes with 0.45 µm pore size (Immobilon^{TM}, Merck) was achieved in NuPAGE Transfer buffer for 1h at 300 mA in a semi-dry transfer format. Membranes were blocked in 5% (w/v) milk or bovine serum albumin (BSA) in Tris-buffered saline buffer supplemented with 0.1% Tween-20 (TBS-T) for 1 hour at room temperature before incubation with primary antibodies. Primary antibodies were diluted in 5% BSA in TBS-T and incubated at 4°C overnight with mild shaking. After that, membranes were washed thrice with TBS-T and incubated with the corresponding secondary antibody for 1h at room temperature (RT). After washing the secondary antibody with TBS-T, blots were developed with chemiluminescence horseradish peroxidase substrate (Merck) and imaged with the ChemiDoc Touch imaging system (BioRad).

2.6. Chromatin Immunoprecipitation (ChIP)

For ChIP-seq experiments, neurons were cross-linked on-plate with 1% fresh formaldehyde (Electron Microscopy Sciences) diluted in PBS for 10 minutes at room temperature. Fixation was quenched by adding 125 mM glycine to the plate, which was subsequently washed thrice with PBS supplemented with protease inhibitors, and Trichostatin A (TSA; Cell Signaling Technology) when needed. Cells were collected by scraping and spun down at 500 *g* for 5 minutes at 4°C. Cell pellet was snap-frozen in liquid nitrogen. Chromatin preparation was done by resuspending cell pellets in sonication buffer (50 mM Tris-HCl pH 8.0, 0.5% SDS,

1x protease inhibitors) on ice to reach $2x10^6$ cells/100 µl of the buffer. Chromatin was sheared with 15 cycles (30s ON / 30s OFF) of sonication using the sonicator Bioruptor Pico. Soluble chromatin was collected after centrifugation at full speed for 10 minutes at 4°C and was analysed on an agarose gel to check the fragmentation pattern. Desired fragment size distribution was from 100-500 bp, corresponding to mono-, di- and tri-nucleosomal fragments.

Soluble chromatin was diluted 6 times in lysis buffer (10 mM Tris-HCl pH 8.0, 100 mM NaCl, 1% Triton X-100, 1 mM Ethylenediaminetetraacetic acid (EDTA), 0.5 mM ethylene glycol tetraacetic acid (EGTA), 0.1% NAa-deoxycholate, 0.5% N-laurolsarcosine) supplemented with protease inhibitors (and TSA if needed) and incubated with 100 µl sepharose protein A beads in a pre-clearing step to reduce unspecific binding to the antibody. Beads and lysate were incubated at 4°C for 30 minutes with rotation and beads were discarded after centrifugation at 14000 *g* at 4°C for 10 minutes. The pre-cleared lysate from $2x10^6$ cells was used for immunoprecipitation using 5 µl of the desired antibody (see Table XX) coupled to 20 µl protein G-coated beads (Thermofisher). After incubating the antibody-lysate mixture overnight at 4°C with rotation, beads were washed twice for 5 minutes with three buffers; first with RIPA buffer (10 mM Tris-HCl pH 8.0, 1% Triton X-100, 0.1% Na-deoxycholate, 0.1% SDS, 1 mM EDTA, 140 mM NaCl); then RIPA buffer with 360 mM NaCl; and with LiCl buffer (10 mM Tris-HCl pH 8.0, 250 mM LiCl, 0.5% NP-40, 0.5% Na-deoxycholate, 1mM EDTA). After the last wash, beads were quickly rinsed with Tris-EDTA (TE) buffer and resuspended in ChIP elution buffer (10 mM Tris-HCl pH 8.0, 300 mM NaCl, 5 mM EDTA, 0.5% SDS). Beads were treated with 1 µl RNase A (10 mg/ml; Thermofisher) for 30 minutes at 37 °C and with 1 µl proteinase K (20 mg/ml, Thermofisher) for 1h at 55°C. Elution of immunoprecipitated DNA was carried out at 65°C for 30 minutes while shaking samples at 1500 rpm. Beads were collected on a magnet and the supernatant was centrifuged at maximum speed for 5 minutes to remove any aggregates. DNA was purified using SPRI beads (Beckman Coulter), quantified with Qubit High Sensitivity kit and used for qPCR measurements, using 0.5 ng of DNA per reaction and the primers listed in Table 3.

Table 3. **List of primers used for ChIP-qPCR**. *Source of these primers: Gehre *et al.* [225] **Source of these primers: Callicott and Womack [226].

Primer name	Sequence (5' to 3')
Arc TSS Fw	GTC GCC GCT GAA GCT AGA
Arc TSS Rv	CAG CAT AAA TAG CCG CTG GT
GD_Chr6_Fw*	ACG CCA TAT ACA GCA AAC CA
GD_Chr6_RV*	GCC TTG ACT TGT CCC TGA TT
Telomeres Fw**	CGGTTTGTTTGGGTTTGGGTTTGGGTTTGGGTTTGGGTT
Telomeres Rv**	GGCTTGCCTTACCCTTACCCTTACCCTTACCCTTACCCT
Arc enhancer pos.1 Fw	GAG ACA CCC CCA GAG CTG AGA G

Arc enhancer pos.1 Rv	AGC CTT GAA CGC CAC CCT CTA A
Arc enhancer pos.2 Fw	TTC TCC ATC AGG GGT GGG GTT G
Arc enhancer pos.2 Rv	AGC CTT GAA CGC CAC CCT CTA A
Arc enhancer pos.3 Fw	AAA TAC CTC CCA GAG CCA GCC C
Arc enhancer pos.3 Rv	GCT GCG TCA TGG CTC AGC TAT T
Arc enhancer pos.4 Fw	AAA GGA GAG AGG CTG AGA ATA G
Arc enhancer pos.4 Rv	CAG CGC ACA GAG CCT TC

2.7. Assay for Transposase-Accessible Chromatin (ATAC) followed by sequencing (-seq)

Neurons were harvested by scraping and 50.000 cells were used for ATAC-seq. Cell pellets were washed with ice-cold PBS and spun down at 500 *g* for 5 minutes at 4°C to be resuspended in 50 µl cold lysis buffer (10 mM Tris-HCl pH 7.4, 10 mM NaCl, 3 mM $MgCl_2$, 0.1% IGEPAL CA-630). Cells were centrifuged again for 10 minutes, the supernatant was discarded and the cell pellet was placed on ice. Transposition was performed immediately using the Nextera XT DNA library preparation kit at 37°C for 30 minutes. Immediately after transposition, transposed DNA was purified using the MinElute kit (Qiagen). Following the protocol defined by the Greenleaf lab[227], the purified DNA was subjected to 5 cycles of PCR amplification using NEBNext High-Fidelity 2x PCR Master Mix (New England Biolabs) and barcoded primers from the Nextera kit to each sample. I used 5 µl of the partially amplified DNA to perform qPCR to determine the additional number of cycles for PCR amplification allowed before reaching saturation. I compared the number of cycles against ⅓ o the maximum fluorescence intensity using real-time PCR graphs on ABI7900. After performing the calculated additional PCR cycles, samples were purified using SPRI beads and quantified using Qubit fluorometer. DNA quality was determined using the High Sensitivity DNA Bioanalyzer kit (Agilent). Each barcoded library was pooled in a 1:1 molar ratio for paired-end sequencing on NextSeq500 platform at EMBL, Heidelberg Gene Core facility.
I did all ATAC-seq sample and library preparation experiments.

ATAC-seq data analysis. ATAC-seq reads were mapped to the *M. musculus* genome (build mm10) using bowtie2 (v2.3.4.1)[228] and mapped reads were used for peak calling with MACS2 (v2.2.7.1)[229], using the following parameters for paired-end samples: --nomodel --shift -75 --extsize 150 -B --SPMR --keep-dup all --call-summits. Then, called peaks and ATAC-seq reads were jointly analyzed to call differentially accessible regions using DiffBind[230]. For this, only peaks detected in at least two samples were considered and consensus peaks were generated using an overlap of 66%. LOESS normalization was applied in all ATAC-seq datasets to correct counts per peak and these were normalized using EdgeR. The following model was used to define accessibility changes (y): $y \sim$

condition, where *condition* was either *basal, stimulated, recovery* or *restimulated.* Log_2FoldChanges between conditions compared to *basal* were assessed using an Exact test (two-sided), defining differentially accessible peaks when adjusted $P < 0.05$.
ATAC-seq data analysis was performed by Victor Campos Fornes. Downstream analysis was done following discussions with Dr Kyung-Min Noh and me.

2.8. Immunofluorescence staining

Neurons were prepared for immunofluorescence on DIV11 after growing them on coverslips. Cells were washed gently with PBS before applying 4% formaldehyde to fix them for 15 minutes at room temperature. To permeabilize the cells, 0.3% Triton X-100 in PBS was applied for 3 minutes at room temperature. Subsequently, cells were washed thrice for 10 minutes at room temperature with washing buffer (1xPBS, 2% BSA, 25 mM glycine) and incubated for 1h at room temperature with the primary antibodies at the corresponding dilution in washing buffer (Table 4). Again, coverslips were washed in washing buffer three times each for 10 minutes at room temperature and the fluorescently labelled secondary antibodies were applied at 1:1000 dilution in washing buffer (Table 4). Excess of antibody was washed 3 times with 1x PBS for 10 min at room temperature and cells were mounted with Mowiol (2.4 g Mowiol 4-88; 6 g glycerol, 6 mL H2O, and 12 mL 0.2 M TRIS/HCl (pH 8.5)).

Image acquisition. For the acquisition of images, Dr Jennifer Heck used a Nikon Ti-2 widefield microscope controlled by NIS 5.2.02 software (Nikon) to acquire Z-stacks of 10-15 planes at 500 nm steps in 2x2 segments, stitching planes together based on a 15% overlap. The used objective was a CFI P-Apo DM 60x Lambda oil objective (Nikon), coupled to an ORCA-Fusion CMOS camera (Hamamatsu), and the light source was a SPECTRA III light engine (Lumencor). To excite the fluorophores, 395 nm (DAPI) and 555 nm (Cy3) wavelengths were used. The emission was filtered by a 595/30 nm filter for Cy3 emission. Images were processed with background and drift correction as maximum projections using ImageJ software (v. 2.3.0/1.53q) and plugins (Template Matching and Slice Alignment [231]).
All immunofluorescence stainings, image acquisition and processing were done by Dr. Jennifer Heck from the Saka and Noh labs at EMBL Heidelberg.

Table 4. List of antibodies used for immunofluorescence.

Target	Host	Dilution	Supplier
c-fos (monoclonal)	Rabbit	1:1000	Cell Signalling Technologies
macroH2A1.2 (polyclonal)	Rabbit	1:250	Cell Signalling Technologies
Cy3 anti-rabbit IgG (H+L)	Donkey	1:1000	Jackson ImmunoResearch Labs

CHAPTER 3:

RESULTS

With the following exceptions, the experiments and analysis presented in this chapter were designed and performed by me with discussion and guidance from Dr Kyung-Min Noh.

The content of chapter 3.1 has been published in the following manuscript:

Ignacio L Ibarra*, Vikram S Ratnu*, Lucia Gordillo*, In-Young Hwang, Luca Mariani, Kathryn Weinand, Henrik M Hammarén, Jennifer Heck, Martha L Bulyk, Mikhail M Savitski, Judith B Zaugg, Kyung-Min Noh (2022) *Molecular Systems Biology*. **Comparative chromatin accessibility upon BDNF stimulation delineates neuronal regulatory elements**.

*: indicates equal contribution

Chapter **3.1.1** describes RNA-seq and ATAC-seq datasets that were generated by Dr Vikram Ratnu, and the pre-processing and differential gene expression and accessibility analysis were performed by Dr Ignacio Ibarra del Rio. The generation of the CRISPR lines containing a deletion of a putative *Arc* enhancer mentioned in chapter **3.1.4** was also performed by Dr Vikram Ratnu.

The design of the subcellular proteome fractionation described in chapter **3.1.2** was done by Dr Mikhail Savitski and Dr Henrik Hammaren with input from Dr Kyung-Min Noh and me. The mass spectrometry and corresponding data analysis were performed by Dr Henrik Hammaren.

Victor Campos Fornes analyzed the ATAC-seq data described in chapters **3.2.5** and **3.2.6**.

Dr Jennifer Heck performed the immunofluorescence stainings on primary neurons and acquired and processed all images.

3.1. BDNF-specific chromatin responses in postmitotic neurons

As described in the previous section, the study of the neuronal response to stimulation is an interesting system to understand signal integration on chromatin since stimulation regulates neuronal connectivity and synaptic features through specific transcriptional programs[232,233]**.** The specificity of these programs relies primarily on the initial duration and type of stimuli[102], which activates particular membrane receptors and distinct signalling pathways to transduce the signal to the nucleus. In the nucleus, the reorganization of chromatin factors results in the modification of the chromatin landscape in a stimulation-specific manner, which will affect the transcription of inducible genes[234–236].

The neurotrophin BDNF is naturally produced in the central nervous system to regulate neuronal differentiation, maintenance and plasticity of mature neurons through binding tropomyosin receptor kinase B (TrkB)[237]**.** The effects of BDNF on neuronal function are dependent on the BDNF-induced transcriptional response[238]. Although great efforts have been made to investigate both the transcriptional mechanisms that trigger BDNF synthesis in the presynaptic cell[239] and the physiological effects of BDNF on postsynaptic neurons[176], little is known about the effect of BDNF on transcriptional regulation.

In this chapter, the main goals I sought to address are:

- To characterize the neuronal transcriptional and chromatin responses in different stimulation systems to dissect the BDNF-specific effects (section 3.1.1)
- To generate a proteomic dataset in response to stimulation to provide insights into transcriptional regulatory proteins involved in the BDNF response (section 3.1.2)
- To understand the role of Fos in the regulation of BDNF-dependent transcription (sections 3.1.3 and 3.1.4)

3.1.1. Transcriptional response and chromatin changes upon BDNF and KCl stimulations

In order to understand the transcriptional regulation upon neuronal stimulation, the first task was to identify the responsive genes and their expression dynamics in the chosen stimulation set-up. My colleague Dr. Vikram Ratnu generated an mRNA-seq dataset on mouse primary neurons stimulated with BDNF and KCl for 1h, 6h and 10h to address this question, and Dr. Ignacio Ibarra del Rio analyzed

the data to identify the differentially expressed genes (DEG) in each condition compared to the unstimulated control. Overall, this study revealed that BDNF induces >1000 DEGs and this number of DEGs remains constant over the time course (1h: 1268 DEGs, 6h: 1156 DEGs, 10h:1124 DEGs; **Fig.6A**). On the contrary, KCl-induced gene expression changes peaked after 6h and were, in general, higher in number than for BDNF (1h: 1551 DEGs, 6h: 2641 DEGs, 10h: 2109 DEGs). Despite the mild overlap in the DEGs induced after 1h of both stimuli (452 upregulated DEGs and 207 downregulated DEGs), the majority of the changes were BDNF- or KCl-specific, as seen in **Fig.7A**.

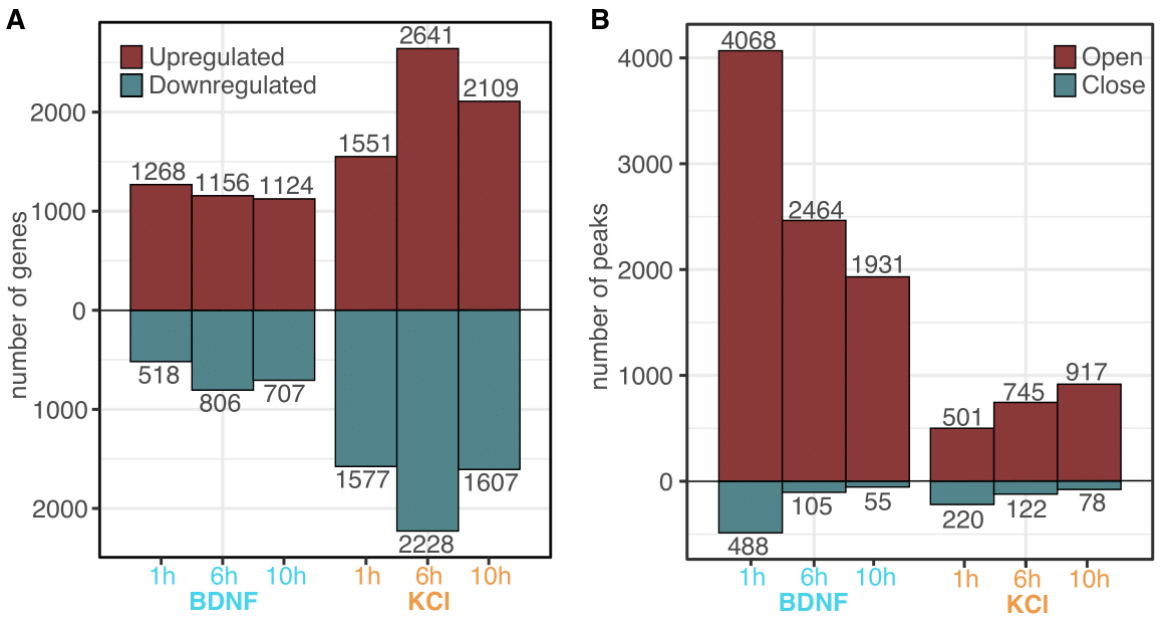

Figure 6. Changes in gene expression and chromatin accessibility upon BDNF and KCl stimulation for 1h, 6h and 10h in mouse primary neurons
(A) Number of DEGs and (B) number of DARs or peaks (FDR 1%, logFC >0 versus unstimulated control) after 1h, 6h and 10h of BDNF and KCl treatments. Figure adapted from Ibarra, Ratnu, Gordillo et al. [210]

Next, my colleagues and I aimed to investigate if the gene expression changes were conditioned at the level of chromatin accessibility. For that, Dr. Vikram Ratnu performed ATAC-seq on the same primary neuronal cultures stimulated for the above-mentioned time points and Dr. Ignacio Ibarra del Rio called the differentially accessible regions (DARs) compared to the unstimulated control (**Fig.6B**). We observed that BDNF stimulation for 1h induces the highest number of DARs (4068 opened, 488 closed) and that this number decreases over time (6h: 2464 opened, 105 closed; 10h: 1931 opened, 55 closed). Surprisingly, although KCl affected more DEGs than BDNF, at the level of chromatin accessibility it induced a reduced set of loci (1h: 501, 6h: 745, 10h: 917) and an even smaller set of peaks closed in a KCl-dependent manner (1h: 220, 6h: 122, 10h: 78). The overlap between the affected genomic regions by 1h of BDNF and KCl was considerably low (238 regions) with respect to the BDNF-specific (3830) opening DARs, and closing peaks were strictly KCl- or BDNF-specific (220 and 488, respectively;

Fig.7B). Furthermore, the affected genome regulatory elements by each stimulus also differed: whilst most of the BDNF-responsive DARs were annotated to be intronic regions, likely corresponding to distal enhancers, promoter regions were over-represented in KCl-responsive DARs (**Fig.8**).

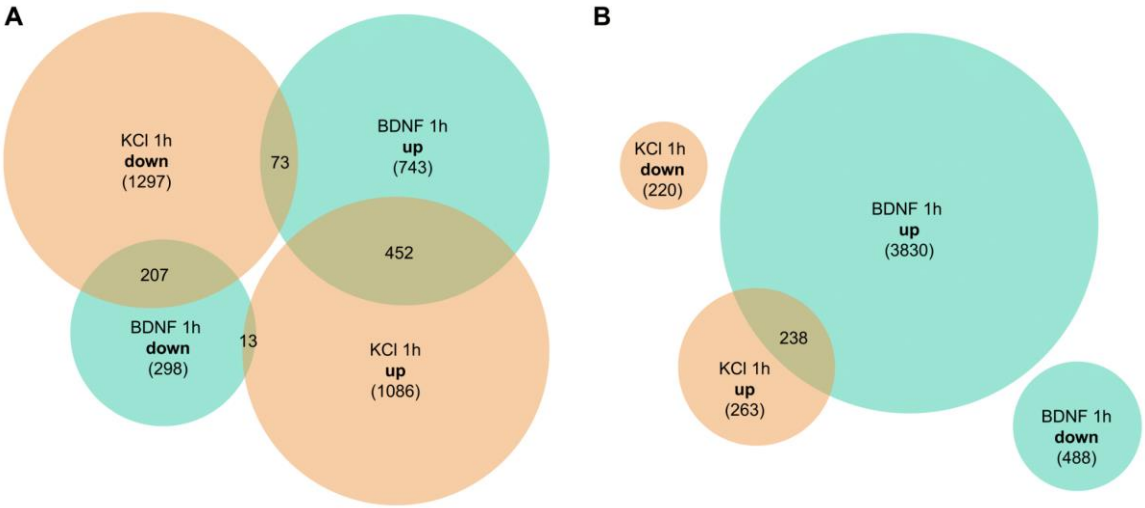

Figure 7. Overlap between DEGs and DARs for 1h of BDNF and KCl stimulations
(A) Venn diagram showing overlapping DEGs and (B) DARs in 1h of BDNF (yellow) and KCl (blue) stimulations.

Both stimuli displayed distinct transcriptional and chromatin accessibility profiles, with BDNF affecting a greater extent of genomic regions mostly annotated as distal regulatory elements in spite of inducing fewer gene expression changes. To investigate if the DARs have a direct role in the regulation of differential gene expression, Dr.. Ignacio Ibarra del Rio associated each peak to the closest gene within a 2-20 kb distance and correlated the changes in accessibility with the changes in gene expression of the peak-gene pairs (described in Ibarra, Ratnu, Gordillo *et al*.[210], **Appendix Fig.1**). He found the strongest significant correlation between the DAR and DEG after 1h of BDNF treatment (odds ratio = 5.8 for enhancers; 20.8 for promoters; adjusted $P = 2 \times 10^{-18}$, two-sided Fisher's exact test with BH correction). In the case of KCl, a significant relationship between gene expression and accessibility could only be found after 6h and 10h of treatment. This means that the chromatin remodelling upon BDNF stimulation is an early event directly linked to gene expression changes, which is not the case for KCl-regulated transcription. It is likely that the KCl-induced accessibility changes at 1h have a delayed effect on gene expression changes, given that a significant relation peak-to-gene only appears later in time (described in Ibarra, Ratnu, Gordillo *et al*.[210], **Appendix Fig.1** and **Appendix Fig.2**)

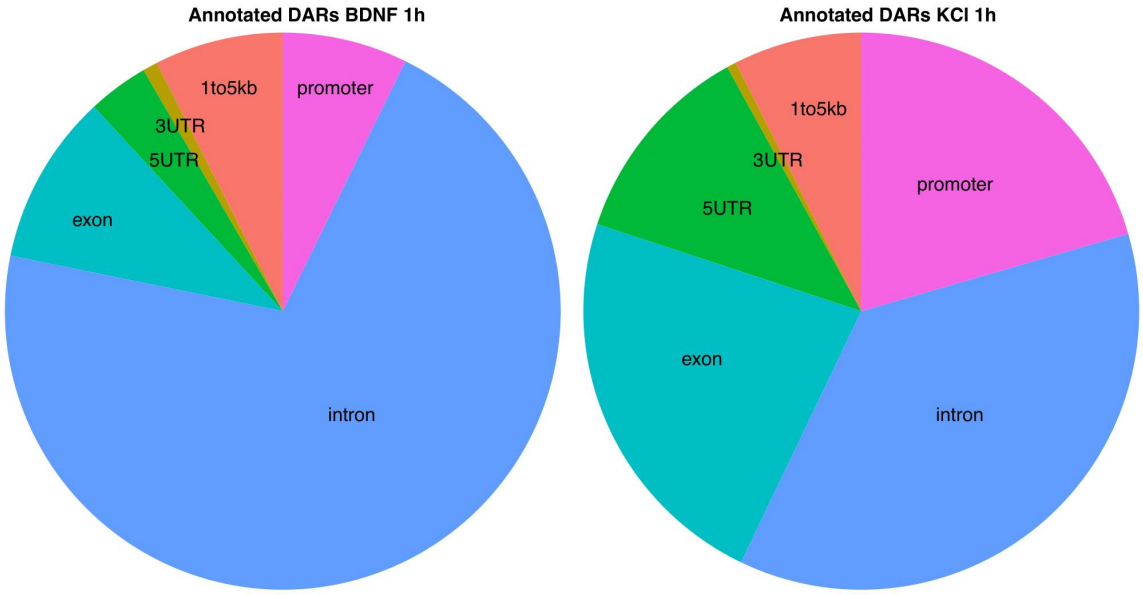

Figure 8. Genomic annotations of DARs after 1h of stimulations.
Pie charts depicting the percentage of DARs after 1h of BDNF (left) or KCl (right) annotated as introns, exons, 5'UTRs, 3'UTRs, promoter or regions 1 to 5kb proximal to promoters in the *annotatr* package[240] using the mm10_basicgene shortcut.

3.1.2. MS analysis of subcellular proteomes shows stimulus-specific reorganization of proteins

The chromatin landscape plays a crucial role in the regulation of gene expression[241–243]. Given that BDNF stimulation strongly affected chromatin accessibility, which was directly linked to gene expression changes, I sought to characterize the transcriptional regulators that play a relevant role in chromatin regulation in a BDNF-specific context at the protein level. To enhance the detection of transcriptional regulators, such as transcription factors and histone readers or modifying enzymes, which are naturally low abundant in the cell[207,208], I applied an enrichment protocol for chromatin-bound and nuclear-soluble proteins. In brief, this protocol comprises a sequential fractionation using detergents with different properties to disrupt specific components of the cell. Additionally, in order to solubilize chromatin-bound proteins, I added an MNase digestion to chromatin DNA.

Performing mass spectrometry on the subcellular proteomes showed enrichment in nuclear proteins for both the soluble-nuclear and chromatin-bound fractions compared to the cytosolic fraction or the total lysate **(Fig.9**, **Appendix Fig.3** and **Appendix Fig.4**).

Figure 9. Enrichment of proteins annotated as nuclear or cytosolic in the subcellular proteomes.
The percentage shown in the bar plots corresponds to the vsn-normalized intensity values for proteins annotated to be nuclear (GO:0005654, GO:0005634, GO:0031965, GO:0044428, GO:0005654, GO:0044451, GO:0005730), cytosolic (GO:0005737, GO:0005829, GO:0044444) or ambiguous (annotated in both categories) with respect to the total intensity of all proteins detected (top panels) of a representative sample. The bottom panel shows only proteins annotated to be either nuclear or cytoplasmic, for a better comparison.

After having established the fractionation efficiency of the protocol, I aimed to compare the enriched proteins in each subcellular compartment after 15 and 60 minutes of stimulation with BDNF and KCl versus an unstimulated control. Due to the limitations in obtaining enough primary cellular material from mouse neurons for proteomics experiments, this study employed two different sets of neurons. The first set comprised primary cortical neurons dissected from E15.5 mouse embryos and stimulated on DIV7 for 15 minutes with either BDNF, KCl, or left unstimulated. A total of 2991 proteins were detected, of which I annotated 57 to be transcription factors or transcriptional coregulators (GO:0001216, GO:0003712, GO:0000981, GO:0001217, GO:0098531). For the second set of neurons, I differentiated mESC for 12 days *in vitro* to glutamatergic neurons and stimulated them for 60 minutes. In this case, 5509 proteins were detected, of which 180 were transcription factors or coregulators. To identify differentially abundant proteins after each treatment, I used the Limma package[224] to compare the normalised protein intensities in each stimulation time point versus the unstimulated control, for each subcellular compartment. The cut-off for calling significant proteins was FDR < 0.1 and |logFC| > 0. The first question I asked was

how comparable the changes induced by BDNF and KCl were in each compartment, in a time-specific manner. Some of the differences between the time points may have been related to the differences between the neuron type, primary or mESC-derived, rather than the time points themselves. Therefore, I inspected only the differential changes compared to the unstimulated control that was generated from the same batch of stimulated groups. Further to this, the protein BDNF was found highly abundant in all the cultures stimulated with BDNF for 60 minutes, which likely corresponds to the exogenously applied BDNF than the endogenously produced peptide (**Fig.10**).

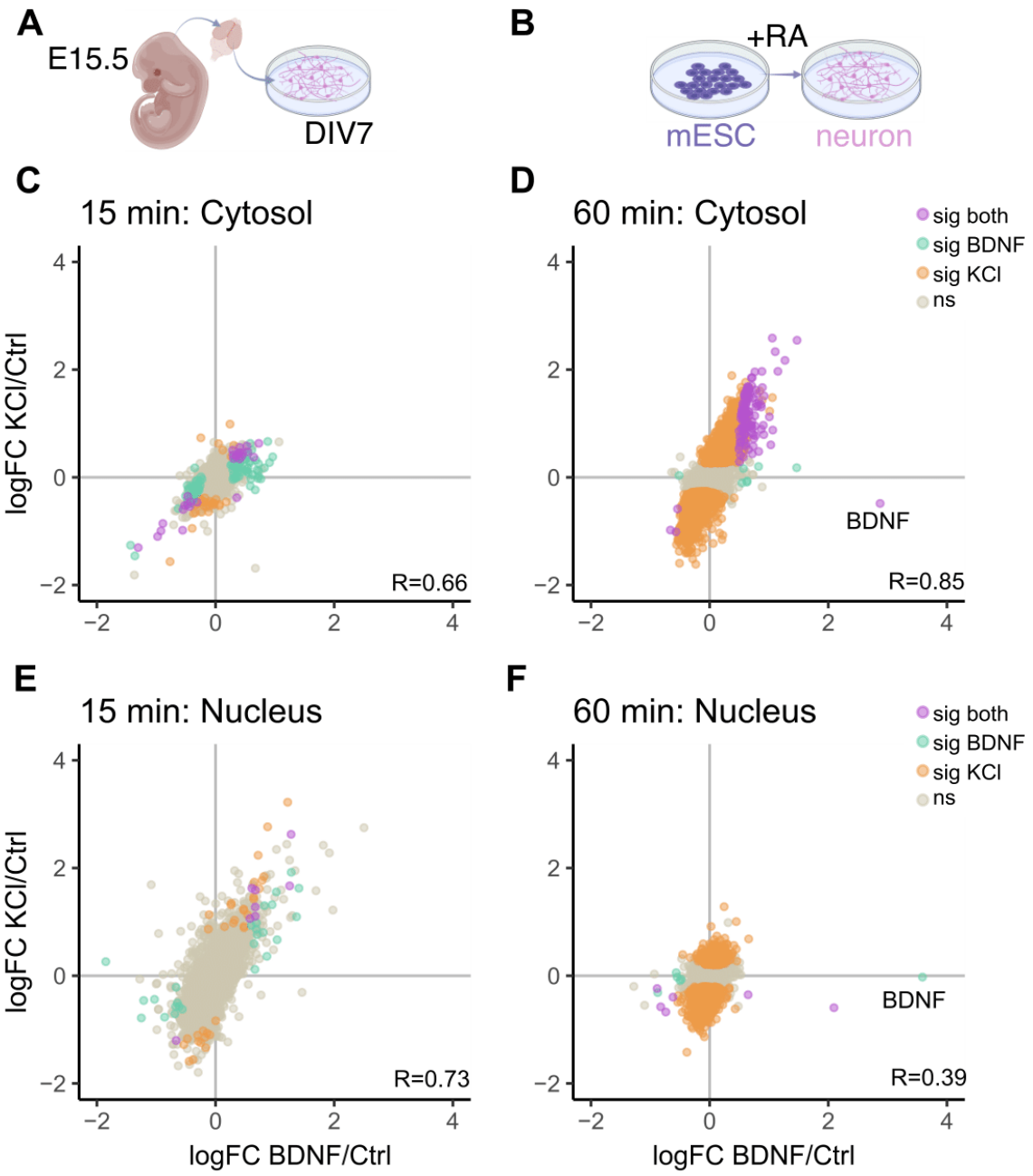

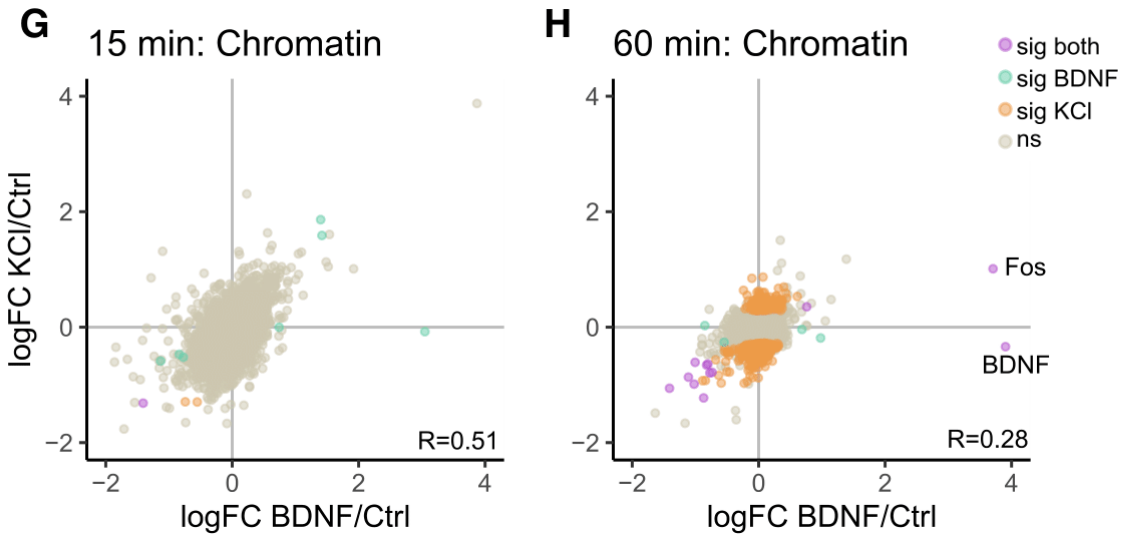

Figure 10. Comparison of the differentially abundant proteins in KCl and BDNF stimulated neurons versus unstimulated control.
MS analysis of protein abundances in primary neurons stimulated for 15 minutes (A, C, E, G) and mESC-derived neurons (B, D, F, H) stimulated for 60 minutes. Scatterplots compare the changes in BDNF versus control (x-axis) and KCl versus control (y-axis) in the cytosolic compartment (C, D), soluble in the nucleoplasm (E, F) and bound to chromatin (G, H). The colour of the dots indicates if the protein was found significantly enriched (*FDR* <0.1 and absolute logFC > 0) in both treatments (*sig both*; magenta), only in KCl (*sig KCl*; golden), only in BDNF (*sig BDNF*; blue) or not significant (*ns*; grey). For each plot, the Pearson correlation coefficient (*R*) of the linear correlation between the changes in BDNF and in KCl is shown. BDNF protein is labelled for the 60 min dataset since this protein corresponds most likely to the exogenously applied BDNF rather than to the endogenously produced BDNF.

In both datasets, the highest number of differentially abundant proteins (DAPs) was found in the cytosolic compartment, followed by the nucleoplasm and chromatin (15 min: 157/69/10 DAPs in the cytosol, nucleus and chromatin, respectively; 60 min: 3486/1831/552 DAPs in the cytosol, nucleus and chromatin, respectively; **Fig.10** and **Appendix Table 1**) considering together KCl and BDNF stimuli. Regarding the response to KCl, the highest number of changes was found in mESC-derived neurons treated for 60 minutes -in all compartments-, compared to the primary neurons treated for 15 minutes. Although the source of the neurons differs, the higher impact after 60 minutes versus 15 minutes implies that the effect of KCl on protein abundance increases or accumulates over time. Overall, KCl-dependent protein changes were greater than the number of changes caused by BDNF. KCl affected 510 and 5852 proteins after 15 and 60 minutes, respectively, considering all compartments, whilst BDNF only affected 209 and 149 proteins after 15 and 60 minutes. In fact, upon BDNF treatment, the number of significant protein changes did not differ much in primary neurons stimulated for 15 minutes or mESC-derived neurons stimulated for 60 minutes, which indicates that BDNF stimulation differs from KCl dynamic behaviour by maintaining the impact in the number of affected proteins over time. Alternatively, this could also mean that the types of neuronal cultures, primary or mESC-derived, display

different time dynamics in response to BDNF, possibly due to the maturation state of the neurons.

The highest correlation between the effect of BDNF and of KCl was found in the cytosolic proteins after 60 minutes (R=0.85). The responsive cytosolic proteins to 1h of KCl treatment (*N*=3366) were involved in cytoskeleton organisation, synapse and proteasomal complex, as indicated by the GO analysis (**Fig.11**). Proteins commonly induced by BDNF and KCl were related to transcriptional regulation, nuclear pore complex and mRNA transport. Enrichment of KCl-induced proteins in chromatin and nucleus was related to terms associated with transcriptional regulation, histone modification, RNA splicing and chromatin remodelling. In particular, chromatin proteins were also enriched in DNA damage response, which could be related to DNA break-mediated stimulus-dependent transcription[244,245]. No specific enrichment could be found for BDNF-induced changes, probably due to the low number of differentially abundant proteins.

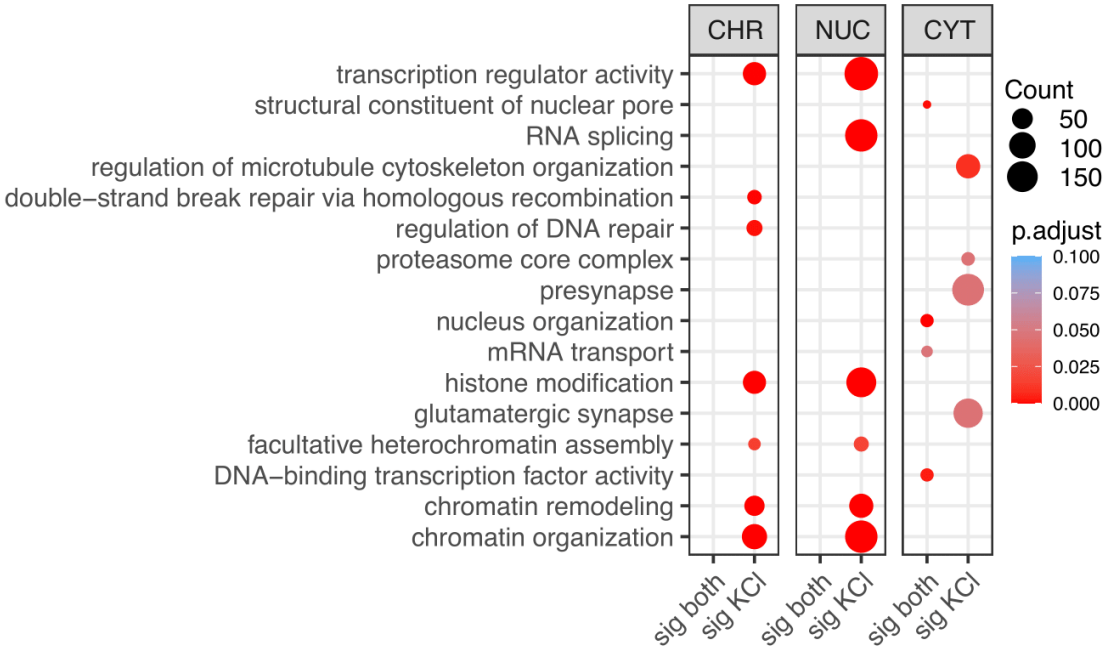

Figure 11. Gene Ontology enrichment analysis of differentially abundant proteins in chromatin, nucleus and cytosol after 1h of stimulation.
Enriched terms for proteins significantly enriched after KCl (sig KCl) or in KCl and BDNF treatments (sig both). Nuclear and chromatin fractions did not show any specific enrichment for proteins significantly different in both stimuli.

To investigate if the changes in protein abundances after 1h of stimulations were regulated at the level of gene expression, I correlated the protein changes after the treatments considering all detected proteins (*N* = 5509) with the changes in gene expression described in Chapter **3.1.1** considering only the DEGs in each condition (N_{BDNF_1h} = 770, N_{BDNF_6h} = 931, N_{BDNF_10h} = 876, N_{KCl_1h} = 1254, N_{KCl_6h} = 2000, N_{KCl_10h} = 1572) (**Fig.12**). Gene expression changes triggered by KCl treatments significantly correlated with the proteome in all conditions, possibly due

to the higher number of analyzed proteins accompanied by differential gene expression. Surprisingly, I could detect significant negative correlations between the gene and protein changes specific to the cytosolic compartment after KCl (R_{KCl_1h} = -0.21, R_{KCl_6h} = -0.20, R_{KCl_10h} = -0.22) but not BDNF treatments (correlations not significant). This could point out a transcription-independent regulation of cytosolic protein abundances upon KCl treatments, possibly due to adjustments in protein stabilities through post-translational modifications or subcellular shuffling of existing proteins. On the other hand, the nuclear and chromatin-bound proteomes after 1h of BDNF treatment displayed stronger associations with gene expression triggered by 1h of both BDNF and KCl stimulations (Chromatin: R_{BDNF_1h} = 0.15, R_{KCl_1h} = 0.14; Nucleus: R_{BDNF_1h} = 0.23, R_{KCl_1h} = 0.27), meaning that the abundance of nuclear proteins, among which transcriptional regulators are comprised, is more likely to be regulated at the transcriptional level. Additionally, focusing on the stimulus specificity, I could notice that although BDNF transcriptional changes do not correlate significantly with the KCl proteome, KCl-triggered transcriptional changes can explain not only the KCl nuclear and chromatin-bound proteomes, but also the BDNF ones, interestingly also at later time points (BDNF nuclear proteome: R_{KCl_1h} = 0.27, R_{KCl_6h} = 0.15, R_{KCl_10h} = 0.22). In this study, I did not generate proteomic datasets for later stimulation time points to test time-wise correlation, yet this data could already indicate that transcriptional-dependent protein changes in the nucleus after BDNF treatments are specific for early time points (1h) for BDNF, while for KCl early proteomic changes still correlate with later transcriptional responses, which could point to more stable or delayed protein changes as a transcriptional consequence.

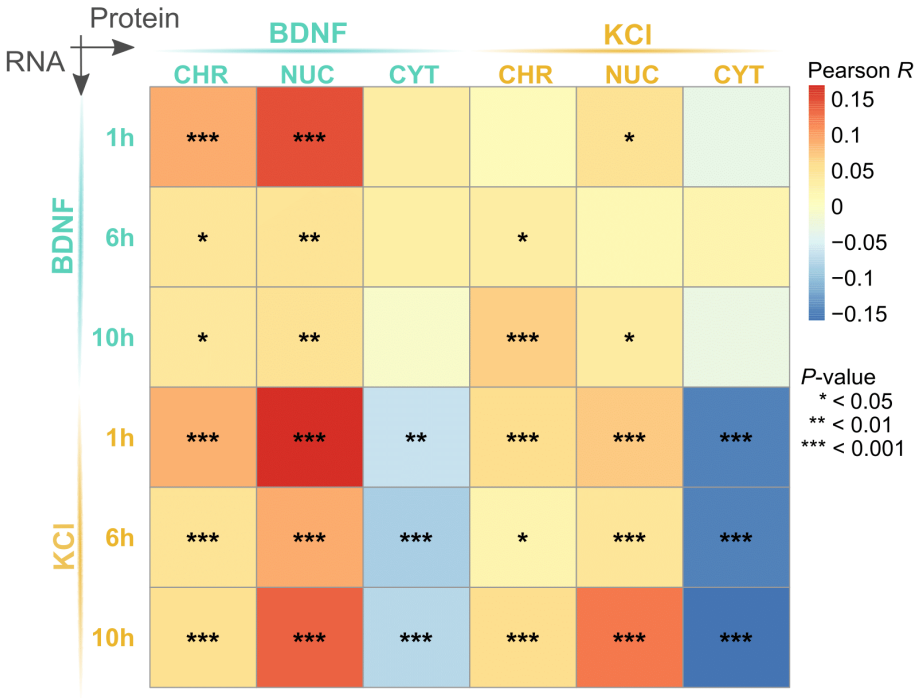

Figure 12. Correlation between the changes in DEGs and protein abundances after BDNF and KCl treatments compared to unstimulated control.

The heatmap colour code shows the Pearson correlation coefficient (*R*) and the asterisks within the squares indicate the significance of the correlation based on a two-sided *t*-test. Conditions from RNA-seq experiment can be read as rows and samples from the proteomics experiment, as columns. Numbers of correlated protein-gene pairs were the intersection between the detected proteins (N = 5509) and the DEGs in each condition. For all compartments: N_{BDNF_1h} = 770, N_{BDNF_6h} = 931, N_{BDNF_10h} = 876, N_{KCl_1h} = 1254, N_{KCl_6h} = 2000, N_{KCl_10h} = 1572.

3.1.3. BDNF induces the recruitment of Fos and other TFs to chromatin more than KCl

I noted that the changes in the nuclear-soluble and chromatin-bound proteins differed in BDNF compared to KCl after 60 minutes (**Fig.10**; R=0.39 for the nucleus and R=0.28 for the chromatin). This led me to think that specific nuclear proteins such as transcriptional regulators might drive the differences between KCl and BDNF responses. Indeed, when I compared the changes in proteins annotated as transcription factors or transcriptional coregulators (hereafter referred to jointly as TFs) versus the changes in the rest of the proteins, a significant increase in TF proteins for BDNF in all compartments compared to KCl appeared (**Fig.13**). The change in TF abundance was greater compared to other non-TF protein amounts in the chromatin and cytosol. Notably, most of the detected TFs in the nucleus and chromatin were downregulated upon KCl treatment, but the TFs found in the cytosol after KCl stimulation were upregulated compared to the unstimulated control.

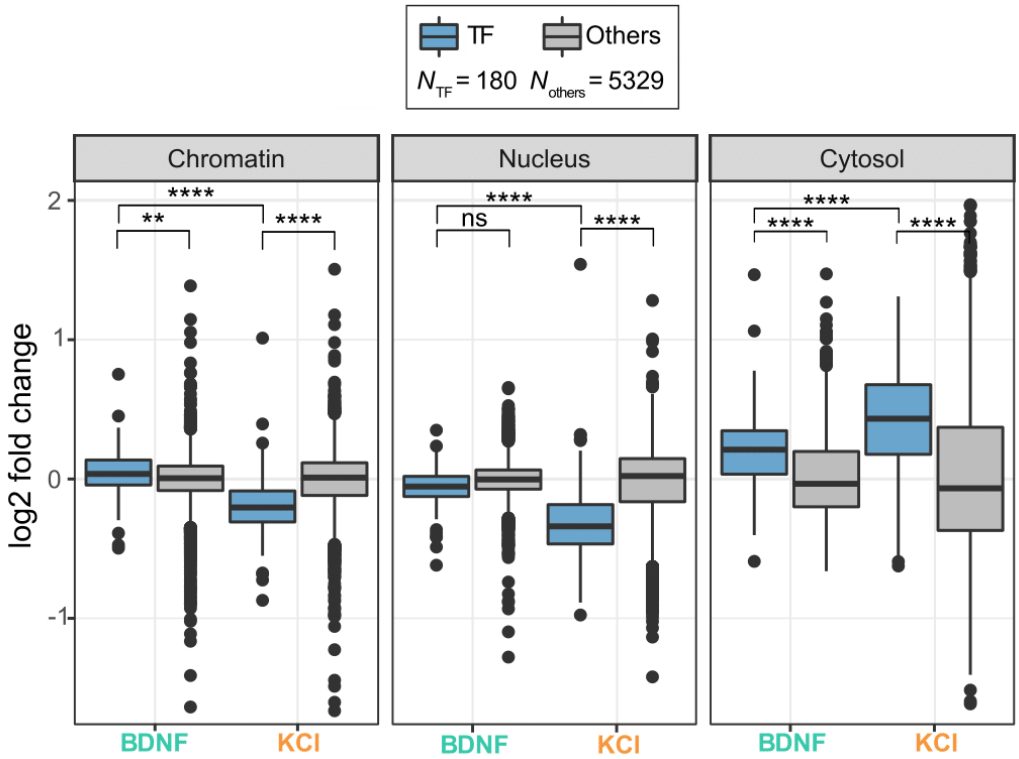

Figure 13. Transcription factor protein abundance changes after 60 minutes of stimulation. Comparison of the logFC over unstimulated control of all detected TF proteins (blue, *N*=180) and all other detected proteins (grey, *N*=5329) after 60 minutes of BDNF and KCl treatments, in

chromatin (left), nucleus (centre) and cytosol (right). Asterisks indicate *P* values from a two-sided t-test (** = $P < 0.01$; *** = $P < 0.001$; **** = $P < 0.001$; ns = not significant).

Next, I performed a TF-target enrichment analysis using DoRothEa gene regulatory network database[246] on proteins detected in the cytosol, nucleus or chromatin after BDNF of KCl stimulations based on their significance value. The transcription factors with the top 10 normalized enrichment score (NES) for each condition can be seen in **Fig.14**. Overall, each condition displayed a specific set of TF-target enrichment. Proteins regulated by Tead1, which regulates cortical development[247], were enriched in most of the conditions. Certain immediate early genes (IEG) - stimulus-responsive transcription factors- targets were specifically enriched for KCl, such as Egr1 and Klf6, whilst Fos, Nr5a2 and Mef2a targets were specific to BDNF (**Fig.14**).

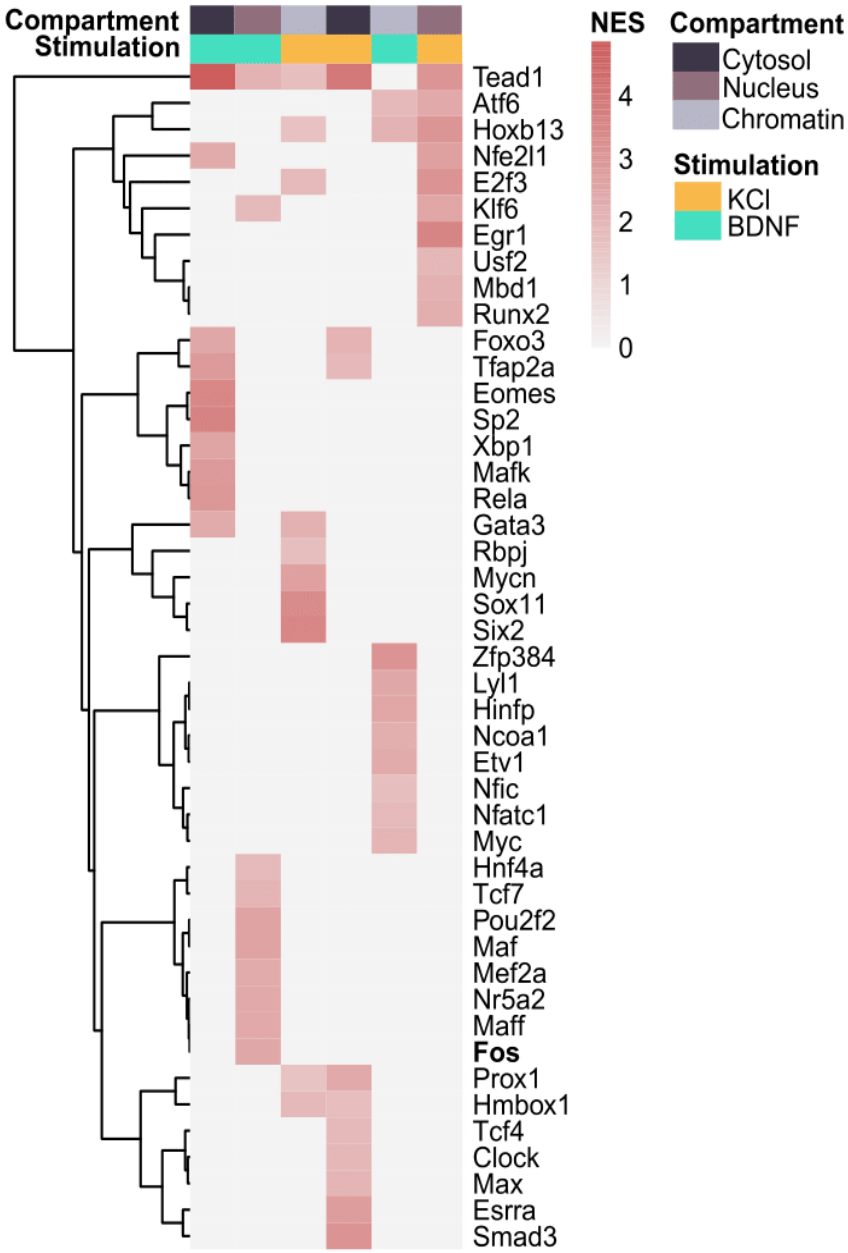

Figure 14. TF target enrichment analysis after 60 minutes of stimulation.

Heatmap showing the TFs with the top 10 normalised enrichment score (NES) for their targets reported in DoRothEa (levels A, B and C, v.1.7.2) [246]. The NES was calculated from the *p*-values of all proteins detected in each subcellular compartment and stimulation condition.

I focused on transcription factor Fos as it plays a major role in chromatin accessibility by recruiting chromatin remodellers and is known for being a pioneer factor. The abundance of the transcription factor Fos was higher in BDNF than in KCl for all compartments (**Fig.10**), with a logFC over control of 4.5 in the nucleoplasm and 3.7 in chromatin, whilst KCl only induced 1.5 and 1 fold enrichment over control for each compartment (**Fig.15A**). I verified the higher abundance of Fos protein after 1h of BDNF treatment compared to KCl by western blot (**Fig.15B**). Interestingly, although Fos protein abundance is diminished after 6h of BDNF stimulation, for KCl Fos levels are much higher after 6h than 1h of treatment. The difference in the protein expression dynamics of a pioneer factor such as Fos could explain the delayed correlation between gene expression changes and chromatin accessibility in the KCl- versus BDNF-induced responses, as described in **Chapter 3.1.1**.

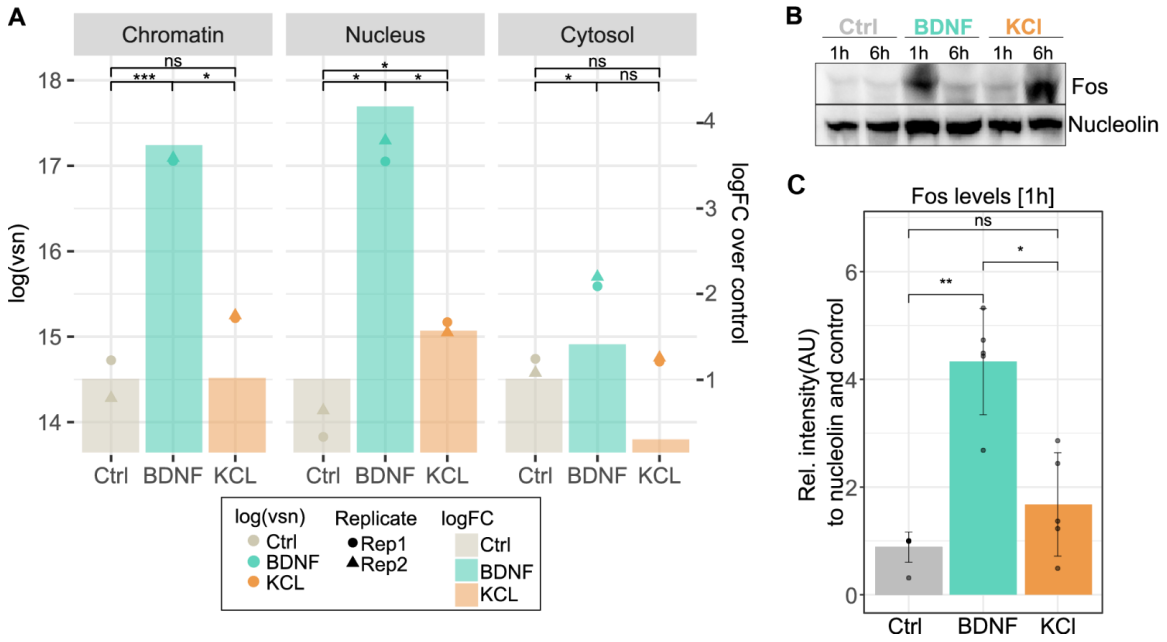

Figure 15. Change in Fos protein intensities in chromatin, nucleus and cytosol 60 minutes after BDNF and KCl stimulation.
(A) Barplot depicts the logFC over unstimulated control (right y-axis) and dots represent the log(vsn) values for each replicate (left y-axis). Asterisks indicate *P* values from a two-sided *t*-test (* = $P < 0.05$; *** = $P < 0.001$; ns = not significant). (B) Western blot analysis of Fos abundance after 1h or 6h of BDNF or KCl treatments, and unstimulated control (left) and (C) quantification of Fos levels after 1h of stimulation normalized to nucleolin for $N = 5$ experiments.

3.1.4. Cooperativity between Fos and EGR enhances the expression of the Arc gene through a novel BDNF-specific enhancer

To investigate the role of Fos in the BDNF-dependent regulation of gene expression, Dr. Ignacio Ibarra del Rio performed a TF motif overrepresentation analysis on the DARs and studied those containing Fos binding motifs (bZIP motif). The centrality of the motif within the opening peaks[210,248] confirmed the pioneering role of Fos[249]. He also found that the accessibility in the Fos motif-containing peaks was significantly greater at sites that contained other TF motifs such as Homeobox or POU. However, the presence of other TFs like EGR and KLF did not increase accessibility but affected neighbouring gene expression. Hence, while Fos may be responsible for pioneering accessibility, other TFs such as POU and Homeobox further enhance accessibility without affecting gene expression. In contrast, co-presence with EGR and KLF seems necessary to modulate BDNF-induced gene expression (described in Ibarra, Ratnu, Gordillo *et al*.[210], **Appendix Fig.5**). To test this, Dr. Vikram Ratnu aimed at disrupting a genomic region where the Fos motif and other TFs were present to test the effect on gene expression. He selected a distal region from the *Arc* gene, a regulator of synaptic plasticity[250], strongly induced upon BDNF stimulation and not so much in response to KCl. This region displayed differential accessibility upon BDNF treatment and showed properties of an active enhancer (H3K27ac and H3K4me1) when Dr. Ignacio Ibarra overlaid the ATAC-seq signal with publicly available epigenomics data. Furthermore, this region comprised a Fos binding motif (bZIP) together with EGR and HIC1 motifs (**Fig.16**).

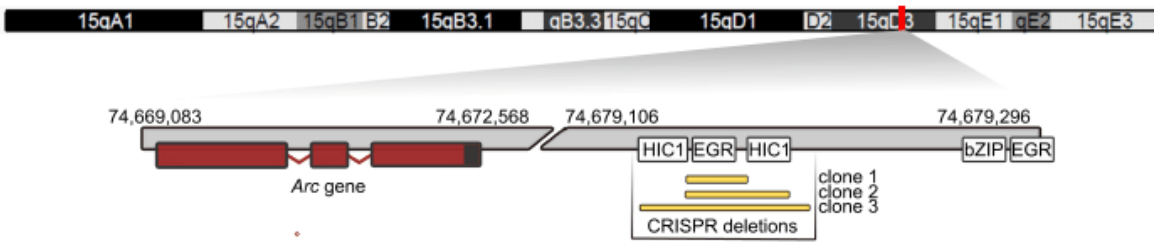

Figure 16. Schematic representation of a novel BDNF-specific Arc enhancer targeted with CRISPR-Cas9.
The genomic region in chromosome 15, ~6kb upstream of the *Arc* gene comprising bZIP, EGR and HIC1 motifs was targeted with CRISPR-Cas9 to generate 3 clonal lines with different deletion profiles (clones 1, 2 and 3). Numbers with flanking arrows indicate the binding sites for qPCR primers.

To validate the binding of Fos and Egr transcription factors to this locus, I performed chromatin immunoprecipitation followed by qPCR (ChIP-qPCR) using Fos and Egr1 antibodies on mouse primary neurons stimulated with BDNF or KCl for 1h. I designed qPCR primers that were specific for the EGR and bZIP motifs (**Fig.16**), for the *Arc* TSS as a positive control, and for gene-free regions in

chromosome 6 (Chr6) and telomeres as negative controls. The Fos ChIP presented technical challenges related to the antibody specificity that prevented me from repeating the experiment with an adequate number of biological replicates that would allow statistical testing of Fos enrichment. Nevertheless, the overall tendency was a higher binding of Fos to this putative enhancer after BDNF stimulation than with KCl, as well as to the *Arc* TSS (**Fig.17A**). In addition, I could detect a significant enrichment for Egr1 binding in all the positions (pos. 1 to 4) in BDNF-stimulated neurons but not KCl or unstimulated neurons, indicating that the binding of Egr1 to this locus is BDNF-specific (**Fig.17B**).

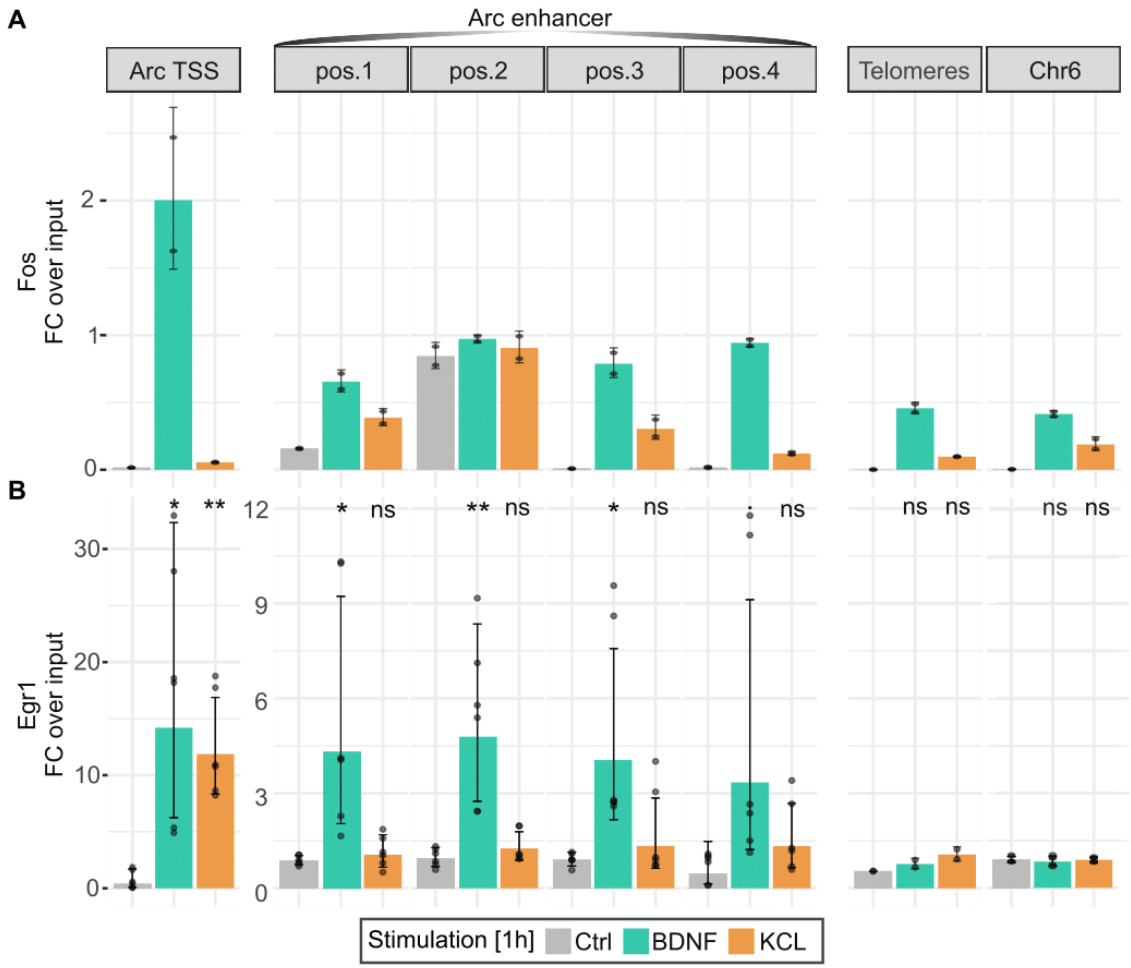

Figure 17. Validation of Fos (A) and Egr1 (B) binding to the novel BDNF-specific Arc enhancer by ChIP-qPCR.
Relative enrichment over input of BDNF- or KCl-stimulated, and unstimulated neurons was measured using primers annealing on 4 positions across the selected locus (**Fig.16**), on Arc TSS (positive control) and on gene-desert loci in chromosome 6 (Chr6) and in the telomeric region (negative controls). *N* = 3 biological replicates measured in 2 technical replicates for Egr1 ChIP, and *N* = 1 biological replicate measured in 2 technical replicates for Fos ChIP. Asterisks on (B) indicate the *p*-value measured by *t*-test (*$P < 0.05$, **$P < 0.01$, ns: not significant).

Using CRISPR-Cas9 technology, Dr. Vikram Ratnu generated three mESC clonal lines with a deletion in the putative enhancer (**Fig.16**). Each line presented a deletion in the EGR motif, although the deletion also affected HIC1 motifs to a

different degree. I differentiated these clones into glutamatergic neurons, stimulated them with BDNF for 1h and measured the expression of *Arc* by RT-qPCR. In both cases, BDNF induced the expression of *Arc* >3 fold over unstimulated control. However, in the CRISPR KO lines, a significant decrease in *Arc* expression could be detected (t = -3.1482, P = 0.01436, two-sided t-test), meaning the presence of an EGR motif close to a bZIP motif positively regulates gene expression in a BDNF-dependent manner (**Fig.18A**).

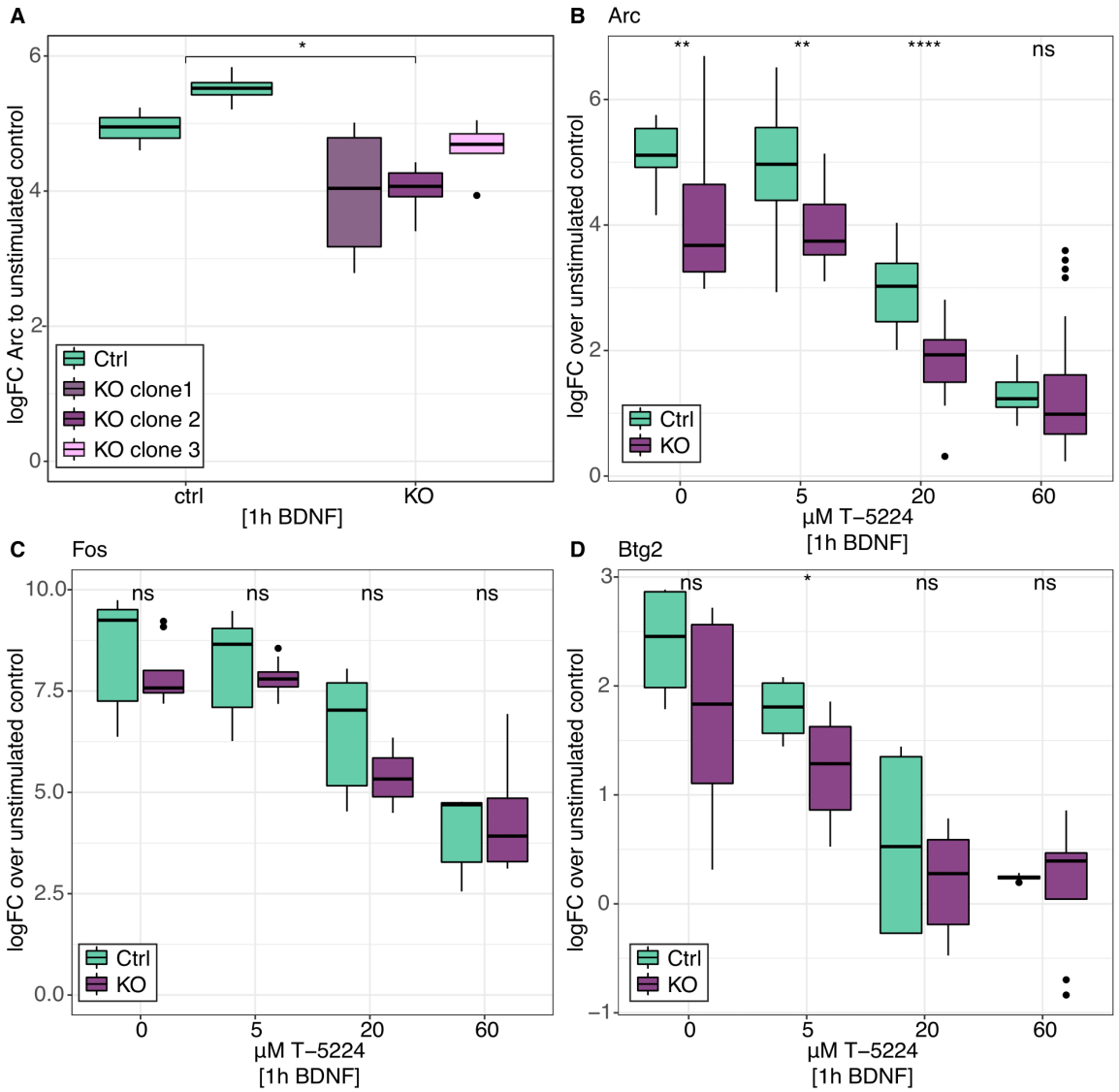

Figure 18. Changes in gene expression relative to a novel BDNF-specific enhancer
(A) *Arc* expression after 1h of BDNF stimulation measured by RT-qPCR in CRISPR control lines (*N*=2, blue) and KO lines (*N* = 3, shades of magenta) containing a deletion in a novel putative enhancer (2 technical replicates per line). (B) *Arc*, (C) *Fos* and (D) *Btg2* expression after 1h of BDNF stimulation in CRISPR control (blue, *N* = 2) and KO (magenta, *N* = 2 (clones 1 and 3)) lines cultured with different concentrations of T-5224. Expression fold changes are with respect to unstimulated control and housekeeping gene *Rpl-13*. Asterisks indicate *P* values from two-sided *t*-test (* = $P < 0.05$; ** = $P < 0.01$; *** = $P < 0.001$; **** = $P < 0.0001$; ns = not significant).

To study the possible cooperativity between EGR and Fos in that particular putative enhancer on the regulation of *Arc* expression, I made use of a Fos inhibitor (T-5224[212]) in our CRISPR control and KO lines. I hypothesized that disrupting Fos binding to this enhancer plus the deletion of the EGR motif could have an additive effect on *Arc* expression due to their cooperativity. To test this hypothesis, I titrated the concentration of T-5224 to see the decreased rate of *Arc* expression in both control and KO lines (**Fig.18B**). Increasing concentrations of the inhibitor significantly reduced *Arc* expression after 1h of BDNF stimulation and fully inhibited *Arc* induction at 60 µM, both in control and KO lines. Yet, the inhibitor treatment yielded significantly less *Arc* expression in the KO lines, confirming EGR's role in *Arc* gene expression. Fitting both datasets to linear regression (*Arc* expression ~ Inhibitor concentration) revealed a more dramatic effect in control than in the KO lines, as seen by the slope of the regression (ctrl slope = -0.58, R = -0.65; KO slope = -0.34, R= -0.42). I then applied two models to describe *Arc* expression depending on the presence of the EGR motif and the degree of Fos inhibition. A simple model considered *Arc* expression to be dependent on EGR (motif deletion) and Fos (inhibitor concentration): Arc ~ EGR + Fos. On the other hand, a complex model considered EGR, Fos and, in addition, their interaction on the regulation of *Arc* expression: Arc ~ EGR + Fos + EGR:Fos. Indeed, performing a Likelihood Ratio Test confirmed that the complex model could describe this data significantly compared to the simple model ($\chi^2(1)$ = 4.3438, P = 0.03714). The more dramatic decrease in *Arc* expression in the control line could then be seen as a consequence of eliminating two terms of the linear relation, Fos and Fos:EGR interaction. To validate the specific effect of Fos:EGR cooperativity related to this novel enhancer, I additionally investigated the expression of *Fos* (**Fig.18C**) and *Btg2* (**Fig.18D**), both being differentially expressed upon BDNF treatment and known to be regulated by Fos itself. In this case, the expression of *Fos* and *Btg2* is better explained by the simple model relying solely on the Fos term and not by the additional interaction term Fos:EGR (*Fos*: Likelihood Ratio Test, $\chi^2(1)$ = 2.8148, P = 0.2448; *Btg2*: Likelihood Ratio Test, $\chi^2(1)$ = 4.476, P = 0.1067). Thus, I concluded that BDNF-dependent gene expression is regulated through the pioneering role of Fos, which would grant chromatin accessibility to other TFs to bind regulatory sites. In turn, Fos cooperativity with these other TFs, such as EGR, allows fine-tuning of neighbouring gene expression.

3.2. Transcriptional adaptation to reiterated BDNF treatments

The study of chromatin responses to BDNF revealed a massive reorganization of chromatin, specifically at enhancers, which made accessible multiple regulatory elements for up to 10 hours of BDNF treatment[210]. The motivation of this chapter is to test the hypothesis that these chromatin changes could be maintained and therefore prime the neurons in subsequent encounters with BDNF. This would be defined as the phenomenon of transcriptional memory to stimuli, where the response to an initial experience changes the transcriptional responsiveness to the same environmental stimulus[251]. Specific cell types such as immune cells have undergone this phenomenon[252]. Several epigenetic mechanisms have been reported as the source of adaptation to stimulations, such as RNA polymerase pausing, exchange of histone variants, DNA methylation, interaction with the nuclear pore complex and dimethylation of the lysine 4 residue of histone H3[253]. It is reasonable to think that neurons, responsible for storing memories in response to experiences, could also display the capacity of transcriptional memory. Additionally, BDNF induces synaptic plasticity, an adaptation in the strength of the synapses over time in response to neuronal activity and this process is transcription-dependent and could possibly undergo stable modifications of chromatin that conditions the neuron to adapt.

The aims of this chapter, therefore, are:

- To assess if previous exposure to BDNF can condition the transcriptional response in subsequent encounters with the neurotrophin
- To identify differential transcriptional patterns in naive and primed neurons with BDNF
- To study possible epigenetic mechanisms that contribute to the differences in the transcriptional patterns, by enhancing or lessening the response to BDNF

3.2.1. Prior exposure to BDNF primes the transcriptional response in mouse cortical neurons

Having defined the transcriptional response upon BDNF stimulation, I sought to investigate if this response differs when neurons have been previously exposed to the neurotrophin, in an attempt to study a putative neuronal-specific phenomenon of transcriptional memory[251]. To test this, I developed an experimental system in which neurons were either primed with BDNF for 1h (when most of the chromatin accessibility changes already take place[210]) or left unstimulated. Two days later,

when most of the first stimulation effect (e.g., transcriptional changes) was gone, both sets of neurons, primed and naive, were stimulated in the same way with BDNF for 1h (**Fig.19**). I studied four stages in this set-up, which could be considered as a pseudo-time-course for a better understanding. The control group, called *basal,* describes cells that had never been stimulated with BDNF. Then, the *stimulated* neurons recapitulate the BDNF stimulation for 1h, only once. Subsequently, the *recovery* condition represents neurons that had been exposed to BDNF for 1h two days before. And finally, a *re-stimulated* condition encompasses neurons that had been treated twice with BDNF for 1h each time, with a 48h recovery interval between rounds.

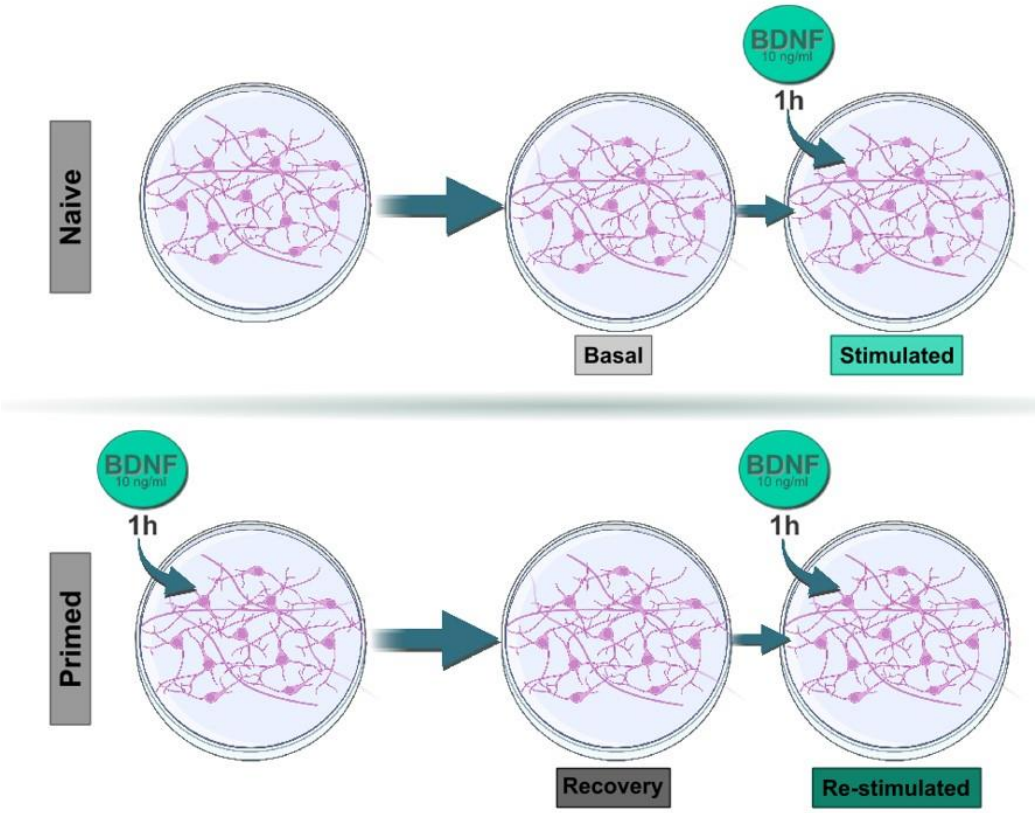

Figure 19. Experimental set-up for double BDNF stimulation of primary neurons.
Cells were collected at the *basal*, *stimulated*, *recovery* and *re-stimulated* stages for subsequent experiments.

To investigate if neurons display different transcriptional responses to the same stimulus (1h of BDNF), conditioned by the previous exposure to it, I performed RNA-seq on mouse cortical primary neurons that underwent the treatments shown in **Fig.19**. Dimensionality reduction of the variability across the top 5000 most variable genes showed that most of the variation across samples came from exposure to BDNF regardless of the number of stimulation rounds. Nonetheless, 15% of the variation could be explained by the number of encounters with BDNF (*stimulated* and *restimulated*; **Fig.20**).

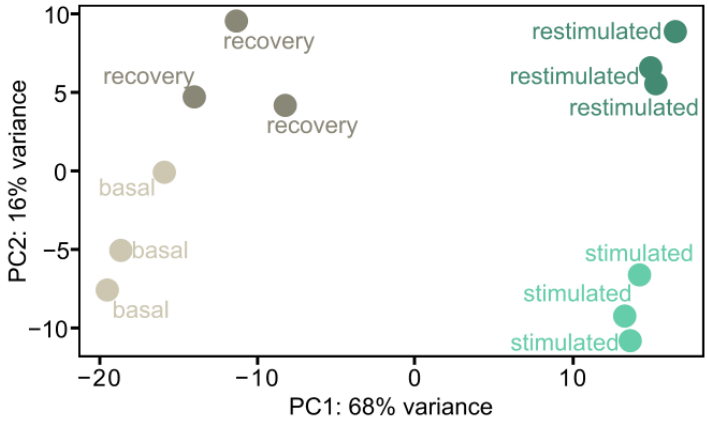

Figure 20. Principal component analysis of top 5000 most variable genes

Next, I performed a differential expression analysis using DESeq2[217] to identify differentially expressed genes in *stimulated*, *recovery* and *restimulated* conditions versus the *basal* control, with a 5% FDR and a fold-change threshold of 1.4 ($log_2FC = 0.5$). I identified a total of 4901 genes differentially expressed in at least one of these conditions compared to unstimulated *basal* control. The first stimulation with BDNF triggered 1347 upregulated and 1570 downregulated genes (**Fig.21**). Almost all of these changes were reverted in the *recovery* condition. However, 107 genes were still upregulated and 573 genes remained downregulated. Interestingly, the second treatment with BDNF led to a higher number of changes, with 1605 up- and 2629 downregulated genes.

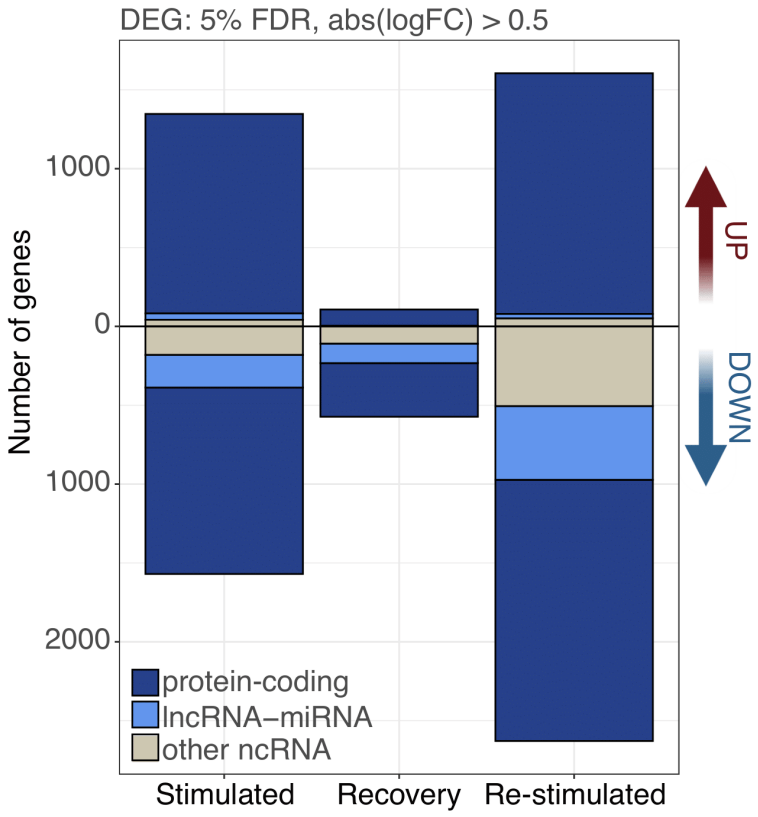

Figure 21. Number of differentially expressed genes in stimulation, recovery and re-stimulation compared to basal condition

The threshold for significance was FDR 5% and abs(log2FC) > 0.5. Annotation of transcripts (protein-coding, lncRNA, miRNA and others) according to Ensembl[254].

Not only did the two BDNF stimulation rounds differ in the number of DEGs but also in the genes themselves. The upset plot in **Fig.22** shows the number of genes that are DE specifically in the first or second BDNF treatment rounds. I observed that the largest group of genes was downregulated after the second BDNF treatment (*N* = 1071), followed by the group of shared downregulated (*N* = 961) and upregulated (*N* = 871) genes between the first and second rounds. From the 1605 upregulated genes in the *restimulated* condition, 639 had not been induced in the *stimulated* sample (nor in the *recovery* stage), meaning these genes may undergo some kind of transcriptional priming during the first BDNF treatment in order to be expressed later on. Likewise, a small group of genes was not DE in the *stimulated* condition but appeared DE in the *recovery* stage and in the *restimulated* sample (219 downregulated and 35 upregulated). I concluded that these genes are late responders to the first stimulation, whose induction could have been orchestrated after the first treatment but their increase could only be detected later on and was carried over up to the second treatment round.

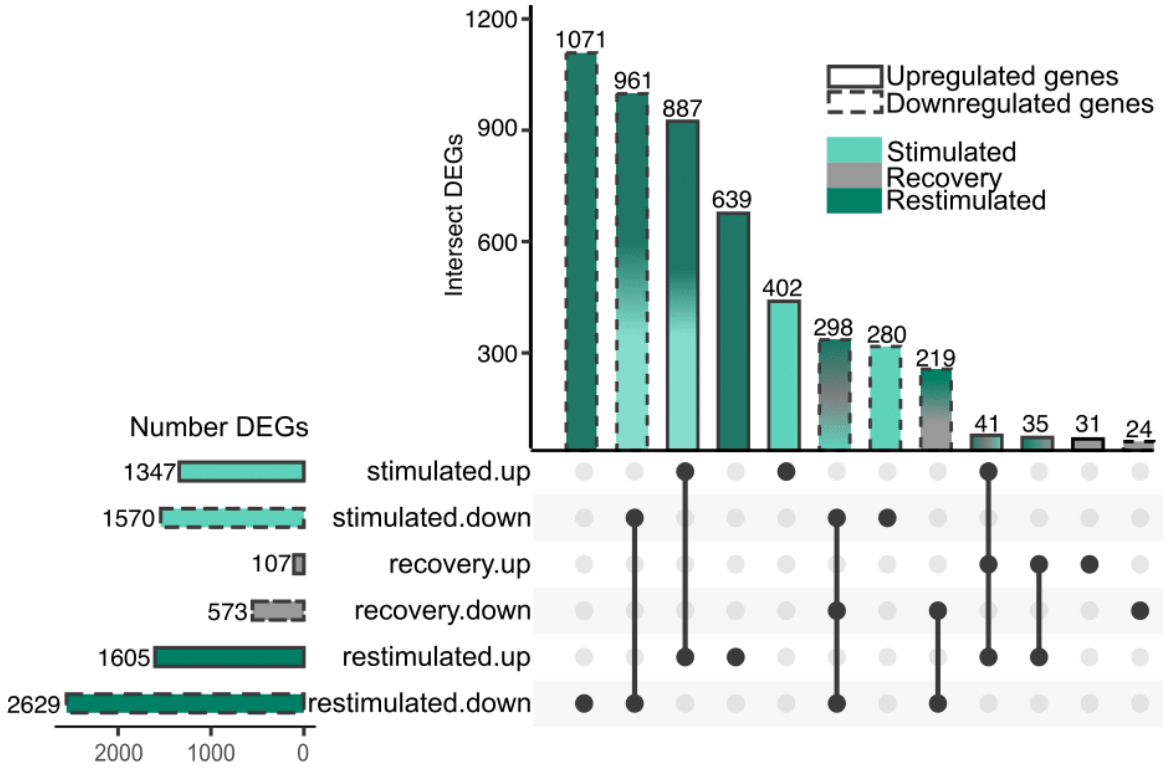

Figure 22. Number of common and specific DEGs, upregulated or downregulated, between the stimulated, recovery or restimulated samples.
The threshold for significance was FDR 5% and abs(log2FC) > 0.5.

3.2.2. BDNF-responsive long non-coding RNAs are more repressed in primed neurons

The higher number of downregulated genes was in part driven by non-coding transcripts (ncRNA), such as long non-coding RNA (lncRNA, total DE lncRNA = 526) or micro-RNAs (miRNA, total DE miRNA = 11) (**Fig.21**). Other ncRNAs annotated according to Ensembl mm10 genome[254] included small nucleolar RNAs (snoRNA), small nuclear RNA (snRNA), small Cajal body-specific RNA and pseudogenes[1]. I found the expression levels of these lncRNAs to be significantly reduced upon BDNF treatment, and they remained at similarly low levels until *recovery*. Therefore, primed neurons that would encounter BDNF again have lower levels of these regulatory RNAs than in the *basal* condition, possibly yielding differences in *restimulation* compared to the first *stimulation*. Indeed, repeating the BDNF application led to a stronger downregulation of these lncRNAs, significantly more than in the first treatment round (**Fig.23A**)**.**

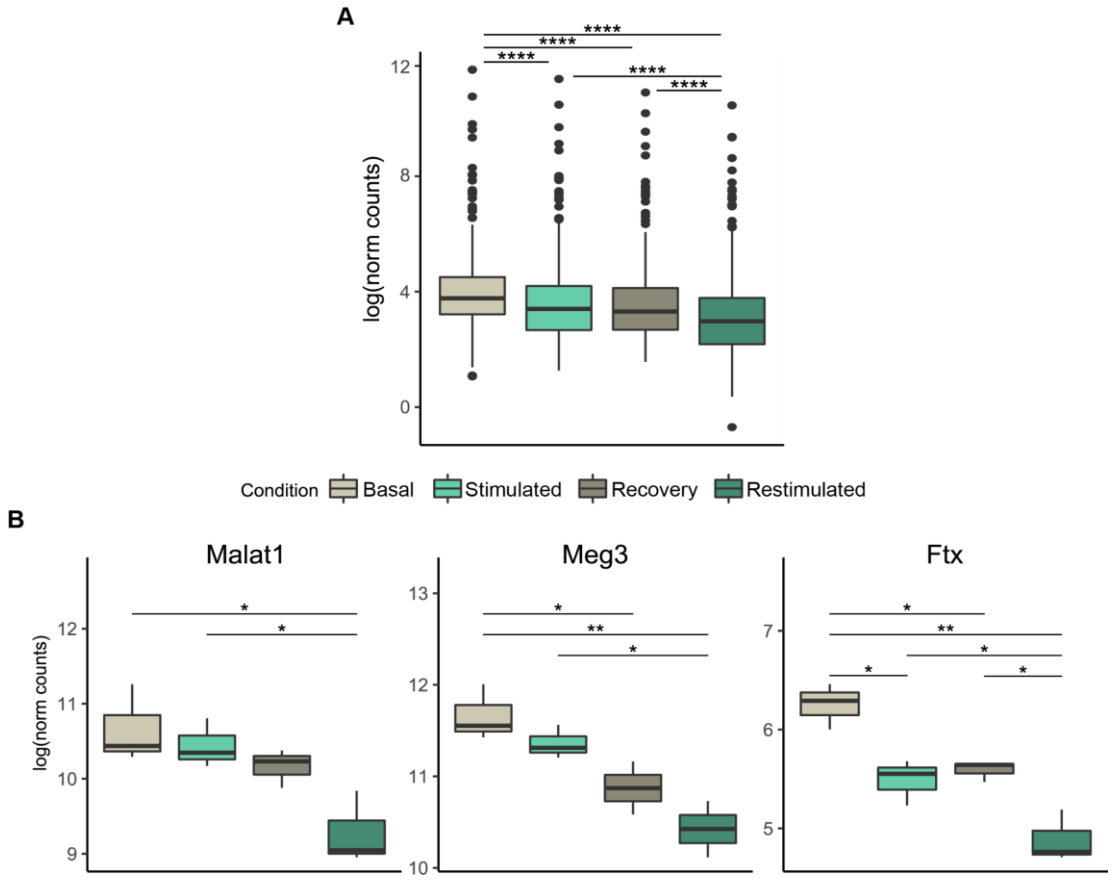

Figure 23. Expression pattern of DE lncRNA

[1] Ensembl definitions of ncRNA biotypes: *snoRNA* - small nucleolar RNAs involved in post-transcriptional modifications of other RNAs, *snRNA* - small nuclear RNAs involved in pre-mRNA processing, *pseudogene* - homologous gene to protein-coding gene with a disrupted open reading frame by a frameshift or stop codon.

(A) DESeq normalized counts for 526 lncRNA that were found differentially expressed in any of the conditions versus basal. (B) DESeq normalized counts for *Malat1*, *Meg3* and *Ftx.* Two-sided *t*-test, only significant contrasts ($P < 0.1$) are shown (**** = $P < 0.0001$, ** = $P < 0.01$, * = $P < 0.05$).

Given the traditional functional role of lncRNAs as repressors of their target genes[63], this could be a potential adaptation mechanism to BDNF, where the expression of the lncRNA target genes would be presumably enhanced in a second encounter to the neurotrophin due to downregulation of the regulatory lncRNAs. However, I could not detect this inverse relation between the abundance of lncRNA with their target genes, since most of the annotated targets also appear to be downregulated in the second response. For example, *Grin1* (Glutamate Ionotropic Receptor NMDA Type Subunit 1) and its associated lncRNA, *Grin1os,* display both lower fold changes in the *restimulation* (log_2FC_{Grin1}=0.21, $log_2FC_{Grin1os}$=-0.89) than in *stimulation* (log_2FC_{Grin1}=0.36, $log_2FC_{Grin1os}$ =0.31), as happens to the lysine demethylase 6b (*Kdm6b*) and lncRNA *Kdm6bos* (*Stimulation*: log_2FC_{Kdm6b}= 2.40, $log_2FC_{Kdm6bos}$= 2.21*; Restimulation:* log_2FC_{Kdm6b}= 1.81, $log_2FC_{Kdm6bos}$= 0.23). Given the complexity of lncRNA effects on gene expression, this could point to a different regulatory mechanism. Given that both, coding and non-coding transcripts, in these cases emerge from the same locus, they may share a common regulation of their expression, and the consequences of the lncRNA differential transcription are seen in another layer of regulation, i.e., post-transcriptional.

Three interesting examples of neuronal regulatory lncRNA that were differentially expressed in this system were *Malat1* (Metastasis- associated lung adenocarcinoma transcript 1)*, Meg3* (Maternally Expressed Gene 3) and *Ftx* (Five prime to Xist). All of them showed very low expression levels, especially in the *restimulated* condition (**Fig.23B**). *Malat1* showed a strong response to BDNF in the second treatment round, whilst *Meg3* showed a progressive decrease from the *stimulation* through *recovery* up to *restimulation*. *Ftx* displayed a strong downregulation already after the first BDNF treatment. The transcript abundance remained at a similar level 48h later, to experience an even stronger downregulation in the *restimulated* condition. The difference between *Ftx* levels in *basal* and *recovery* could explain the stronger downregulation in the second encounter to the neurotrophin.

These three lncRNAs regulate neuronal functions that are often attributed to BDNF. During neurodevelopment, *Malat1* has been linked to the promotion of neurite outgrowth through the activation of ERK/MAPK and to the prevention of developmental cell death[255]. In cultured hippocampal neurons, *Malat1* regulates gene expression programs to trigger synaptogenesis[256]. On the other hand, both *Meg3* and *Ftx* are imprinted genes. *Meg3* is induced by neuronal activity[257,258] and implicated in ischemic stroke, where it mediates neuronal death[259] as well as in Alzheimer's disease, where it induces necroptosis[260]. In contrast to this cell death promoting-role in Alzheimer's and ischemia, a rat epileptiform model revealed that

Meg3 enhances cell viability by inhibiting apoptosis through activation of PI3K/AkT/mTOR pathway[261]. Interestingly, *Meg3* has repeatedly been associated with PI3K/Akt pathway in neurons[257] and other cell types such as macrophages[262]. Specifically, in neurons, the reduction of *Meg3* levels over-activates this pathway and decreases AMPAr activation in LTP, linking it to a role in synaptic plasticity[257]. Furthermore, *Ftx* has been recently associated with hippocampal neuronal apoptosis in the context of epilepsy, and its overexpression reduces neuronal death *in vivo*[263], although the mechanism by which this takes place is still unknown. Given that BDNF also induces ERK/MAPK and PI3K/Akt pathways, it is reasonable to believe that the above-described roles of these lncRNAs could be similar in the BDNF stimulation paradigm. Performing further experiments with overexpression of these non-coding transcripts would shed light on which BDNF-specific genes are regulated by them, and which BDNF-induced neuronal processes are affected, e.g. neurite outgrowth, synaptogenesis or increased neuronal survival.

3.2.3. PI3K/Akt pathway is less responsive to BDNF in primed neurons

Having assessed the distinct number of gene expression changes and the overlap between BDNF treatment rounds, I wondered if the genes differentially affected by each round were a result of distinct signalling pathways, in particular those induced by BDNF. To test this, I employed the Pathway RespOnsive GENes for activity inference (PROGENy) database[264]. This resource defines genes that are responsive to certain signalling pathways, obtained from signalling perturbation experiments from publicly available data. If several genes that are annotated as the endpoint of a specific signalling pathway show differential expression, this pathway will display a higher enrichment score. The result of inferring pathway activities with the weighted mean statistical method can be seen in **Fig.24**. From my transcriptome data set, ROGENy identified responsive genes of 14 different pathways, among which NFκB, MAPK, p53 and PI3K are known BDNF-responsive pathways through $p75^{NTR}$ [179] or TrkB activation [121,174]. I focused on the differences between these pathways. All of them were underrepresented in both *basal* and *recovery* conditions, verifying that in the absence of BDNF the pathway-responsive genes are not induced. Upon the first BDNF treatment, NFκB, MAPK and PI3K showed a high enrichment score, whereas p53-responsive genes were not affected. On the contrary, a second BDNF treatment did induce this pathway and, in addition, the NFκB pathway was found slightly more active. These two pathways, mostly induced by BDNF binding to the $p75^{NTR}$ receptor, establish a balance to regulate cell survival, with p53 and NFκB transcription factors competing for p300 binding to regulate transcription of pro-apoptotic or survival genes[265]. MAPK-responsive genes were found equally induced in both rounds, indicating that the most associated pathway to BDNF response is highly robust and is not altered by BDNF priming.

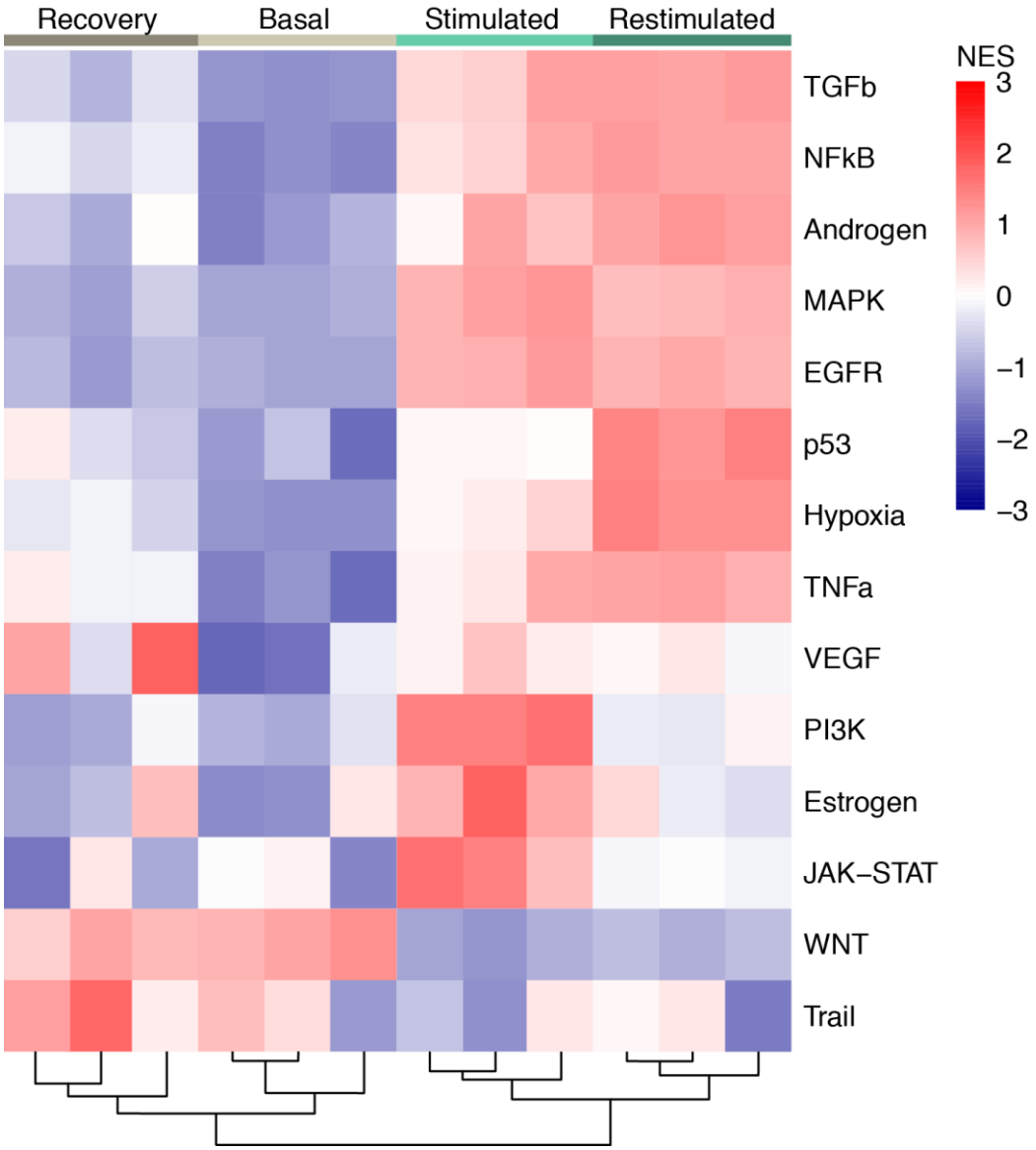

Figure 24. Pathway-responsive gene enrichment analysis using the PROGENy[264] database
The DESeq2 normalized counts for the 4901 differentially expressed genes were tested for enrichment against the PROGENy database by activity inference with weighted mean (NES: normalized enrichment score). Hierarchical clustering of the samples represented with the dendrogram at the bottom of the heatmap.

Interestingly, the PI3K pathway was less activated in the second stimulation. From the top 500 annotated genes responsive to PI3K, 227 were significantly expressed in *stimulation* or *restimulation*. The majority of these genes were induced similarly in both treatments, but several upregulated genes in the *restimulation* were not induced in the first encounter with BDNF (**Fig.25**). One example is the transcription factor Foxo4 (forkhead member of the class O-4), with a $\log_2$FoldChange of 0.48 in *restimulated* and 0.02 in *stimulated*. Foxo4 is known to be induced when the PI3K signalling pathway is inhibited[266] and it has been related to the reduction of oxidative stress in neurons[267], which could contribute to the role of BDNF in neuroprotection.

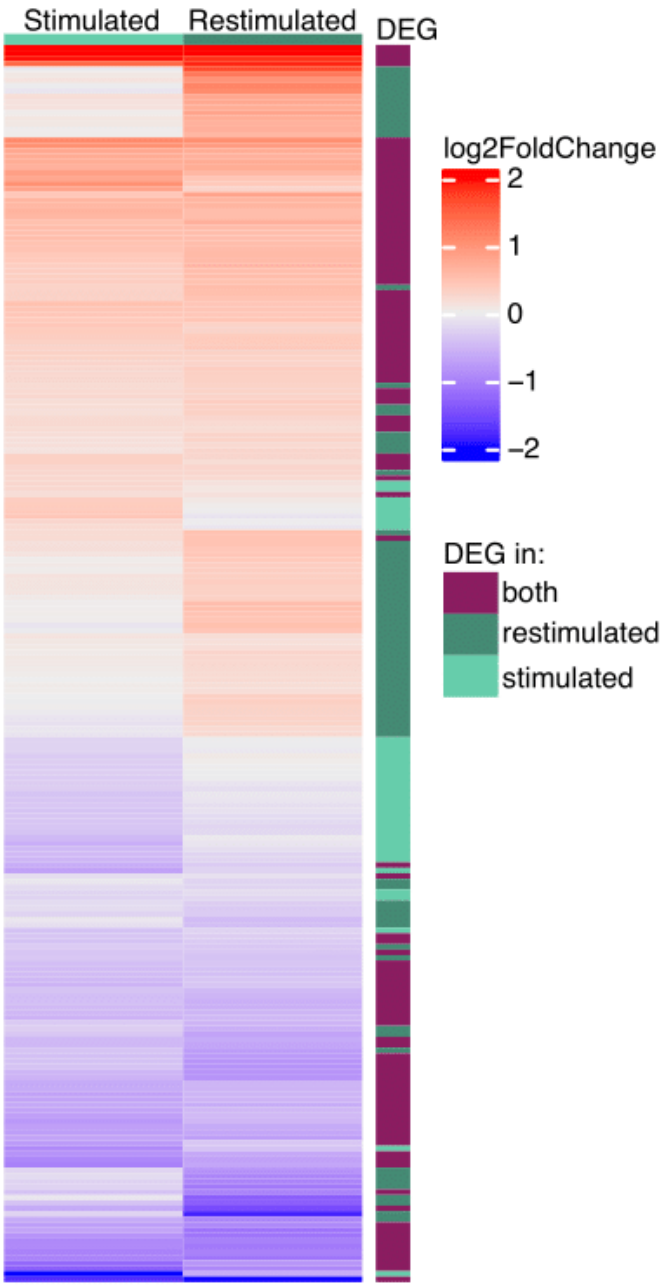

Figure 25. Differentially expressed genes in stimulated and/or restimulated that are annotated to participate in the PI3K pathway according to the PROGENy database.
Heatmap colour code indicates the log2FoldChange versus *basal* condition, and the colour bar next to the heatmap shows if the gene was found significantly DE in *stimulated*, *restimulated* or in both (*N* = 227 genes).

How PI3K and its downstream genes are affected upon a second treatment with BDNF and not by a single one is still inconclusive. The PI3K/Akt pathway is associated with BDNF neuroprotective effect, with BDNF repressing PI3K/Akt/mTOR signalling to induce autophagy in response to cellular damage[268]. At the molecular level, the mTOR signalling regulates the translation of dendritic mRNAs in response to stimulation (**Fig.4**)[184,186,269]. It is possible that some of the adaptations to BDNF stimulations are regulated at the posttranscriptional level, i.e. dendritic mRNA translation.

3.2.4. Identification of transcriptional patterns throughout BDNF treatment rounds

Next, I sought to define patterns of transcriptional changes across the treatment rounds. I performed unsupervised hierarchical clustering with the partition around medoids (PAM) algorithm in order to identify different transcriptional groups. The 4901 DEGs were separated into six distinct clusters (**Fig.26**). The first 3 clusters comprised upregulated genes in response to BDNF ($N_{cluster1}$ = 577, $N_{cluster2}$ = 499, $N_{cluster3}$ = 958), whilst downregulated genes were grouped in the latter 3 clusters ($N_{cluster4}$ = 1046, $N_{cluster5}$ = 1296, $N_{cluster6}$ = 525). Genes in clusters 3 and 4 displayed the same expression response in the first and second stimulations with BDNF. At the *recovery* stage, their transcriptional levels almost fully reversed to the *basal* condition, showing a highly reversible profile to allow induction (cluster 3) or repression (cluster 4) in the same manner as in the first encounter with BDNF.

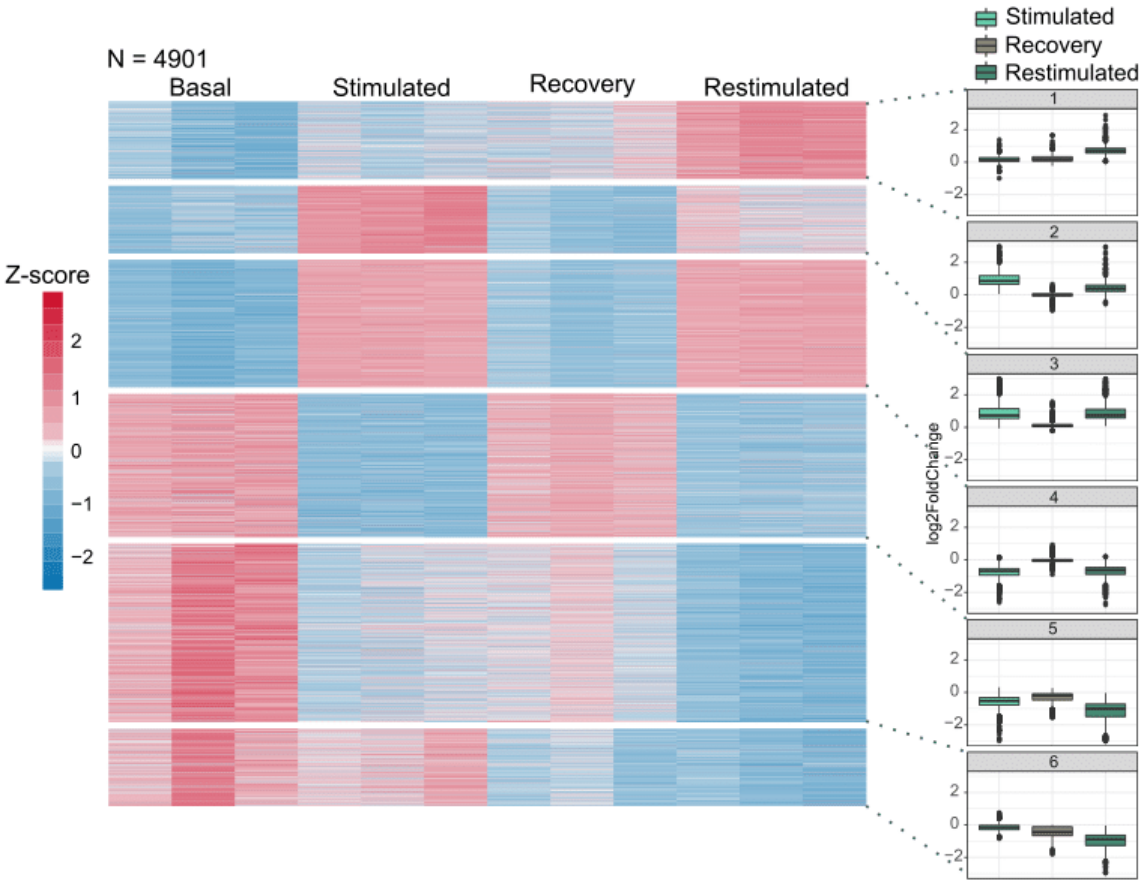

Figure 26. Unsupervised hierarchical clustering of DEGs revealed 6 different transcriptional behaviours in response to BDNF treatments.
(Left) Heatmap of z-scored normalized counts of 4901 DEGs in any condition versus basal clustered by PAM algorithm (k=6) and (right) boxplot of the log2FoldChange of the genes belonging to each cluster.

Performing a pathway enrichment analysis using the Reactome database[270] on genes from cluster 3 resulted in canonical terms related to the response to

neurotrophins, which included many of the immediate early genes, e.g. *signalling by Ntrks* (*Fos*, *Egr4*, *Junb*, *RhoA*), *regulation of MAPK pathway* (*Dusp1*, Kras, *Ubb*) and *diseases of signal transduction by growth factor receptors* (*Calm1*, *Psmb4*, *Tgfbr1*) (**Fig.28**). This indicates that the classical response to BDNF is conserved across stimulation rounds.

Fos and Egr are major TFs contributing to the BDNF response. Given that their transcriptional induction was similar between BDNF stimulation rounds, I performed western blot analysis of Fos and Egr1 to assess their protein abundances in the *basal*, *stimulated*, *recovery* and *restimulated* conditions (**Fig.27A**) and could confirm that these proteins are not expressed at the *basal* nor *recovery* stages, and are induced in the same manner in both treatment rounds. Activation of the MAPK signalling pathway can be assessed by studying the phosphorylation of ERK1/2. The same western blot analysis showed that phosphorylation of ERK1/2 happened equally in both stimulation rounds, and was not present prior to stimulation with BDNF. I further analysed the homogeneity of the response at the single-cell level using immunofluorescence microscopy with the help of Dr. Jennifer Heck. She stained the BDNF-treated neurons with anti-Fos and MAP2 (a neuronal-specific marker) antibodies and observed that not all the neurons induced Fos protein expression equally (**Fig.27B**). The violin plots in **Fig.27C** show the distribution of the Fos fluorescence values for the neuronal populations. We noticed that in the *restimulation* condition there was a larger proportion of cells falling onto the lower part of the distribution than in the *stimulation*, indicating that there were two populations of neurons: one with an average Fos induction similar to the *stimulation* and another smaller group that did not induce Fos. In addition, the *recovery* group displayed a subpopulation of neurons that did not fully repress Fos induction as in the *basal* state. This finding made clear that neuronal primary cultures present some variability, possibly due to the establishment of neuronal connectivity networks, that affect the response to stimulation at the single-cell level. Conceivably, the use of bulk omic technologies to investigate the effect of BDNF will not be able to capture the full complexity of the response due to the lack of single-cell resolution, although it will be able to capture global and robust events.

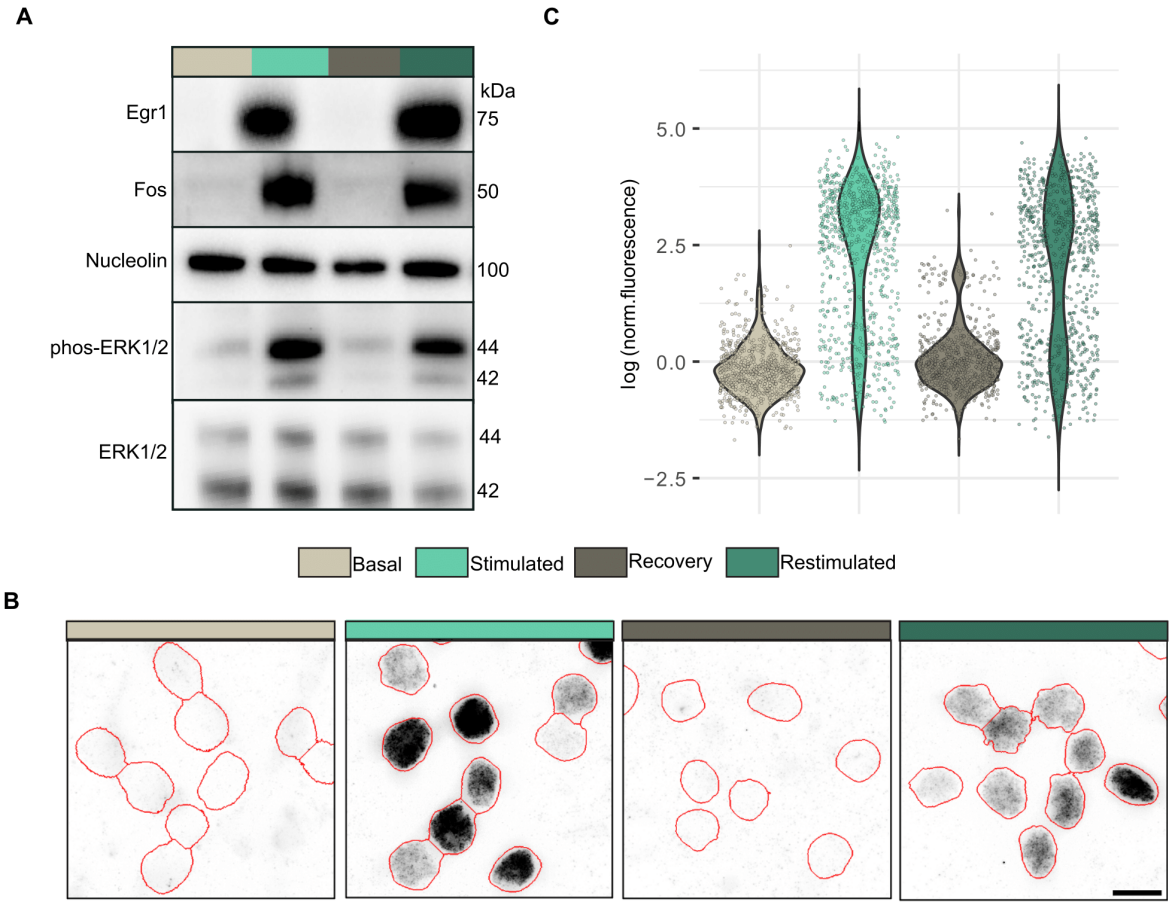

Figure 27. Analysis of immediate early gene protein expression and MAPK activation by western blot (A) and immunofluorescence (B, C).
(A) Representative western blot analysis using antibodies against Egr1, Fos, Nucleolin (control), phosphorylated ERK1 (44 kDa) and ERK2 (42kDa) and total ERK1/2 in mouse primary neurons stimulated repeatedly with BDNF. (B) Representative Fos immunofluorescence in mouse primary cortical neurons at DIV12. Images are maximum projection with inverted LUT. Nuclear regions, indicated by red outlines, have been segmented from DAPI staining. Scale bar corresponds to 10 µm. (C) Quantification of Fos protein levels from fluorescence values normalized to DAPI signal (*N* = 2 independent experiments, total of 751 cells). Neuronal cultures were stained, and the corresponding images were acquired, processed and quantified by Dr. Jennifer Heck.

On the other hand, cluster 5, which presents a conserved downregulated response throughout treatments did not show a similar result or any terms related to BDNF neuronal physiology. Performing Gene Ontology enrichment analysis identified gene groups belonging to *cillium organization* (TMEM and TTC families), *RNA modification* (*MettL8*) and *glycolipid biosynthetic process* (PIG family) terms. Hence, the transcriptional response to BDNF stimulations is partially conserved and comprises upregulated signalling and regulatory factors of the response to neurotrophins, whilst downregulated genes do not have a regulatory but rather a physiological function.

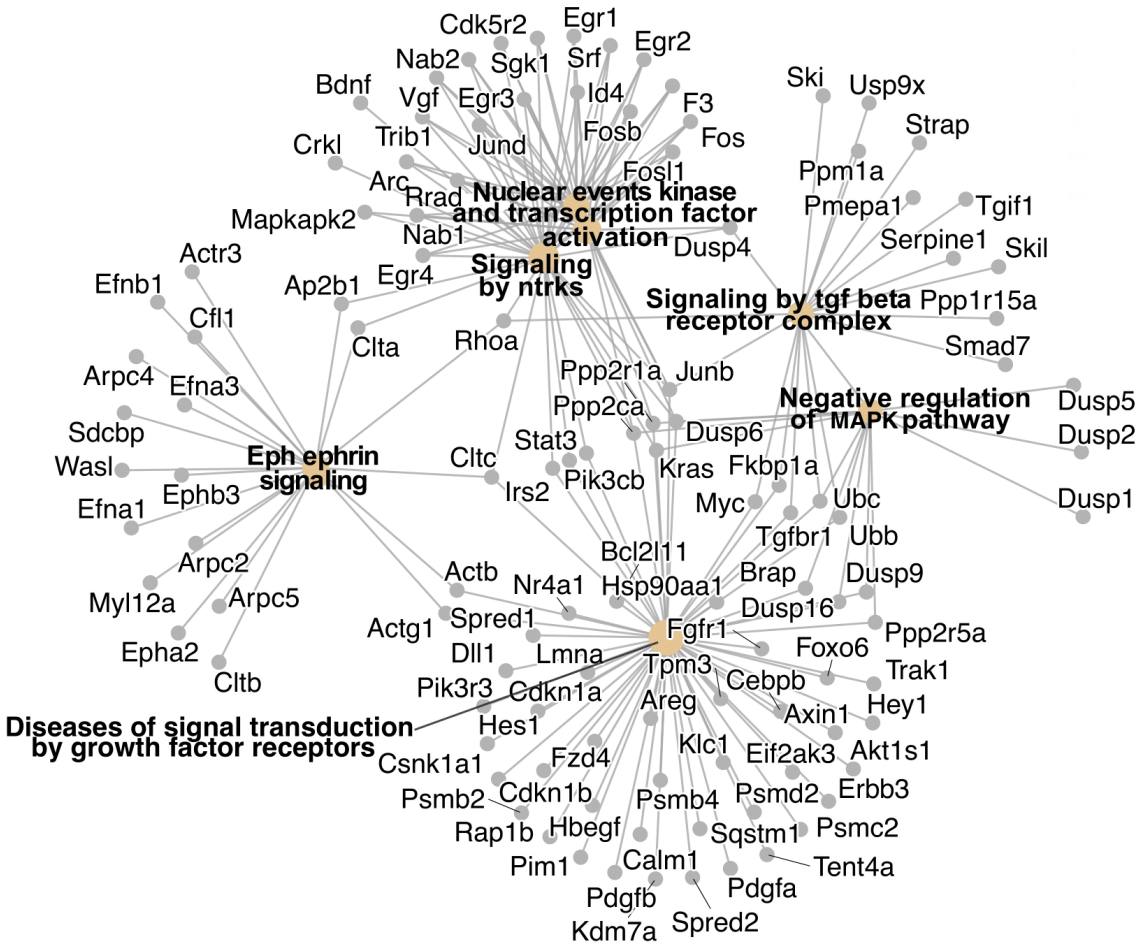

Figure 28. Pathway enrichment analysis of genes in cluster 3 using Reactome pathway database (10% FDR cutoff).

Although both BDNF treatment rounds shared commonalities in the transcriptional response (**Fig.22**; clusters 3 and 4 in **Fig.26**), clusters 1 and 6 were composed of genes that only induced a differential response in the second encounter with BDNF. Interestingly, these genes started being upregulated (cluster 1) or downregulated (cluster 6) in the *recovery* stage, suggesting that they could be late responders to the first treatment and applying a second BDNF treatment induced (cluster 1) or repressed (cluster 6) these genes faster. For these genes, I hypothesize that priming with BDNF could have lowered the threshold to induce their activation or repression, probably through a feedback regulatory loop due to the residual levels carried over to the *recovery* stage, prior to the *restimulation*. These two groups presented genes with different functions, but all related to neuronal physiology. Cluster 1 was enriched in *synaptic* (e.g., *Snca*) and *neuropeptide signalling* (e.g., *Calca*), *neuronal precursor proliferation* (e.g., *Mdk*), *neuronal death* (e.g., *ApoE*), and *calcium transport* (e.g., *Cav2*). For cluster 6 only two terms were significantly enriched: *constituent of the extracellular matrix* (collagen family) and *calcium channel complex* (*Cacna* genes) (**Fig.29**).

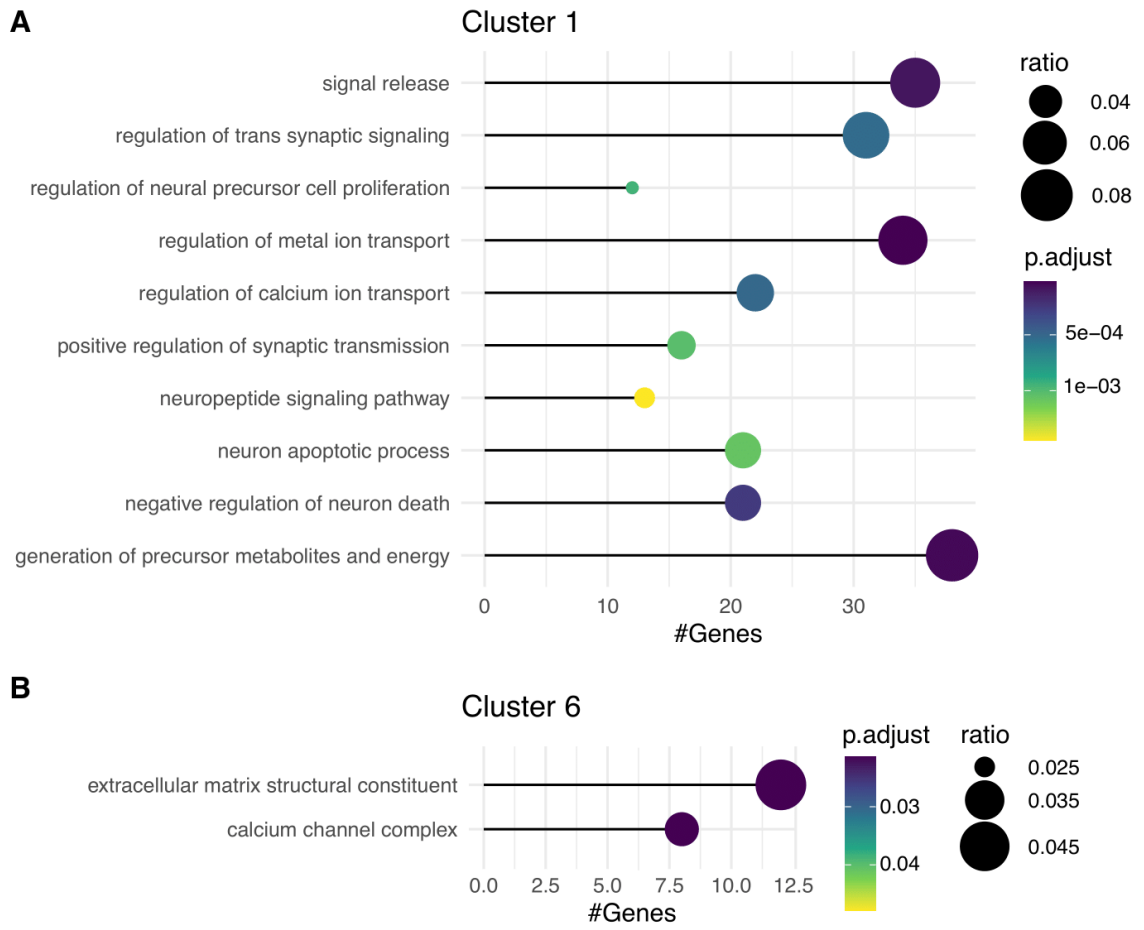

Figure 29. Gene ontology enrichment analysis on genes from clusters 1 (A) and 6 (B).
The circle size depicts the ratio of input genes annotated under each term, and the circle colour indicates the adjusted p-value using Benjamini–Hochberg's correction.

Finally, clusters 2 (upregulated) and 5 (downregulated in response to BDNF) had the shared characteristic of fully returning to *basal* levels 48h after the first treatment round. In the case of cluster 2, the *restimulation* led to a milder induction of genes associated with regulatory roles in transcription and signalling (*kinase activity*: *CamkkI*, *Mapk6*) as well as a role in *mRNA binding* (*Ago2*; **Fig.30**). Among the transcriptional coregulators, I could identify histone deacetylases (*Hdac5*) and acetyl-transferases (*p300*) and subunits of the mediator complex (*Med14*). Additionally, several transcription factors, such as *Npas4*, *Klf4*, *5* and *6*, *Nr4a2* or *Mef2d*, known to be induced by BDNF and neuronal activity were also less expressed.

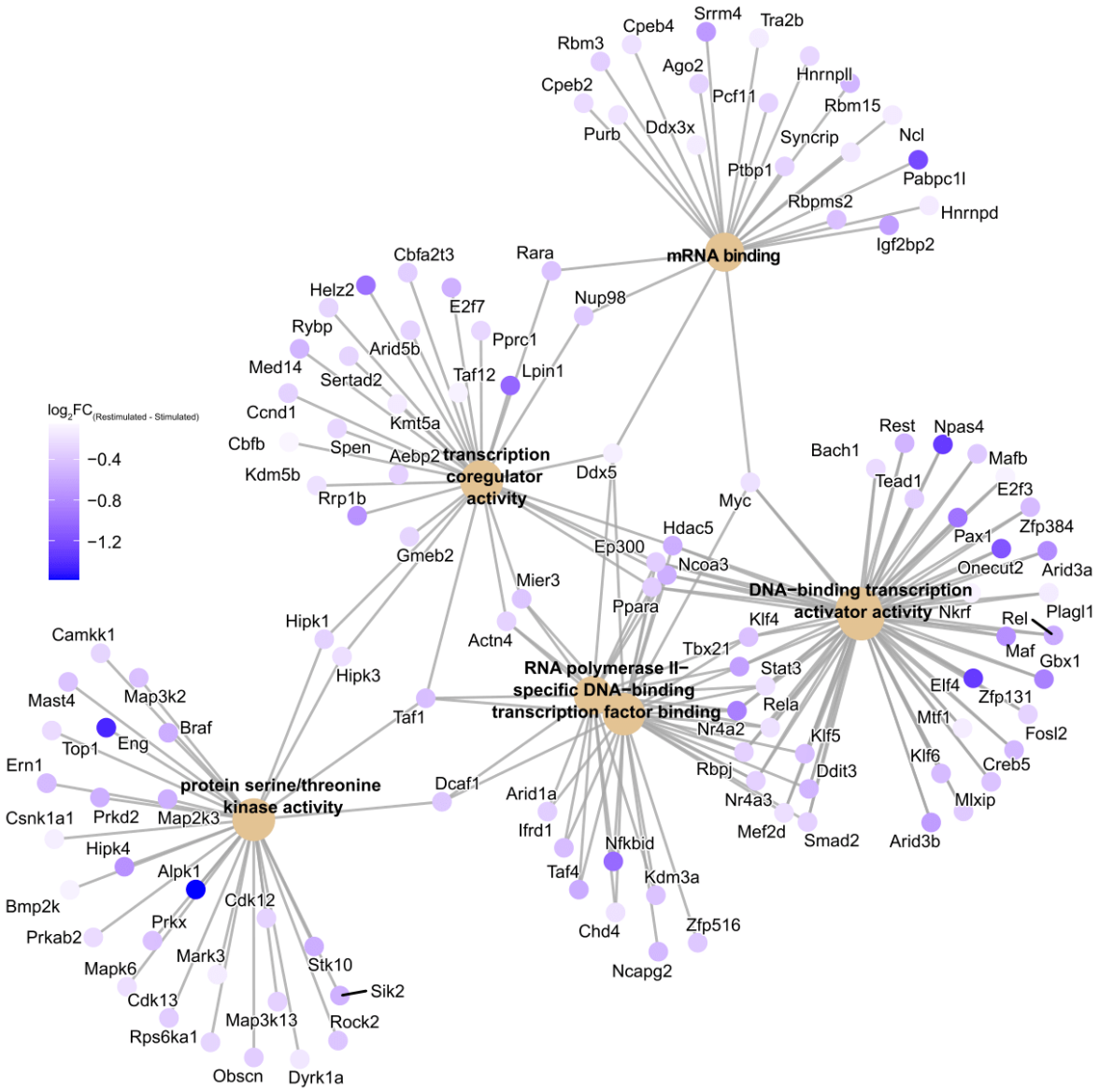

Figure 30. Gene ontology enrichment analysis on genes from cluster 2.
The colour of the circles with gene names indicates the difference in log_2FoldChange between *restimulation* and *stimulation*.

Comparing the magnitude of the changes between treatment rounds revealed that genes belonging to cluster 2 (*p300*, *Mef2d*, *Hdac5*, *Npas4*, *Rest*, *Atf3*, *Nr4a2*) had a milder response to BDNF than the genes in cluster 3 (*Fos*, *Egr1*, *Egr4*, *Arc*, *Jun*). Nevertheless, these less-induced genes were the main source of variability between the treatment rounds with greater differences in their fold change versus *basal*(**Fig.31**).

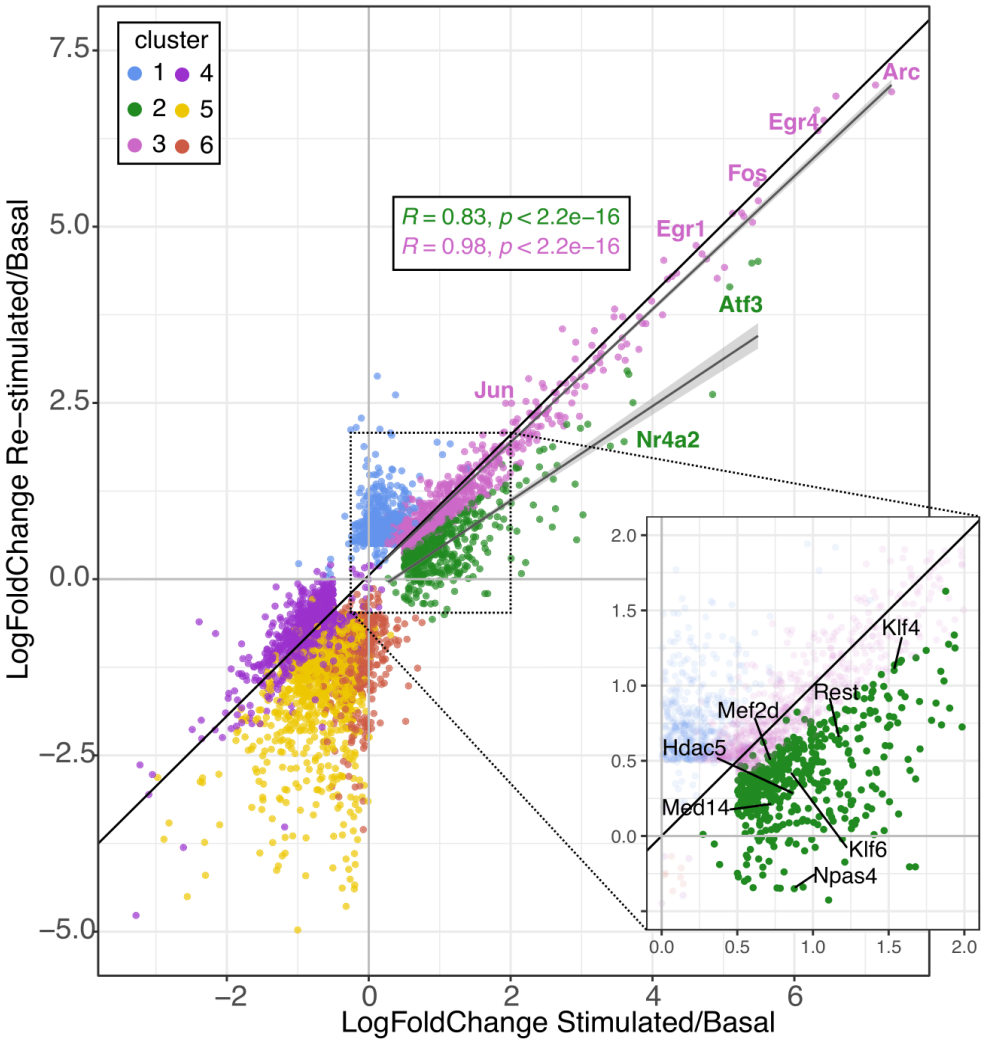

Figure 31. Scatter plot comparing the changes in stimulated (x-axis) and restimulated (y-axis) versus basal.
The colour code depicts the cluster to which each gene was assigned. Black lines with a grey halo indicate the fit to a linear regression of cluster 2 (green) and cluster 3 (pink), to which the Pearson correlation coefficient (R) and *p*-values are indicated in the same colour. The plot in the lower right corner shows a magnification of cluster 2. The names of representative transcriptional regulators are shown in the colours representing each cluster (main plot) or black (amplified plot)

Finally, cluster 5 seemed to encompass genes that are repressed after two BDNF treatment rounds. Gene ontology enrichment analysis exhibited few enriched terms, related to cellular physiology (*mitochondrial respiratory chain defects* and *axoneme assembly*) but also terms possibly related to transcriptional regulation: *double-strand break repair* and *catalytic activity on DNA*, both including topoisomerases and helicases (**Fig.32**). It has recently been described that neuronal activity-dependent transcription requires double-strand breaks to induce transcription [244]. Why the proteins regulating these processes are downregulated in response to BDNF is beyond the scope of this work.

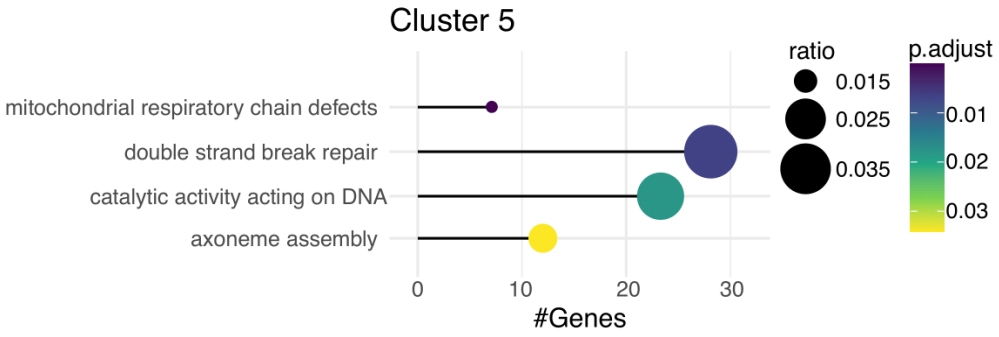

Figure 32. Gene Ontology enrichment analysis of genes belonging to cluster 5.

3.2.5. BDNF-dependent chromatin accessibility changes are plastic and reversible

The identification of different transcriptional patterns in response to BDNF in primed neurons encouraged me to investigate possible mechanisms that could condition the changes in gene expression to the same stimulus. Given that BDNF stimulation led to a massive opening of chromatin regions, particularly at enhancers (chapter **3.1.1**), I sought to test if these BDNF-affected loci remained accessible up to the *recovery* stage and could therefore influence the transcriptional response in the next encounter with BDNF. To address this question, I performed chromatin accessibility profiling with ATAC-seq on the same neuron samples that were used for RNA-seq. Victor Campos Fornes conducted a peak calling with MACS2 and differential analysis versus the *basal* condition using DiffBind and EdgeR normalization, after generating a consensus peak set considering the overlapping regions among 66% of the samples. He investigated the variability across the different conditions performing a PCA of the identified peaks by DiffBind and we observed that most of the differences come from the BDNF treatment itself and not from the number of encounters with BDNF.

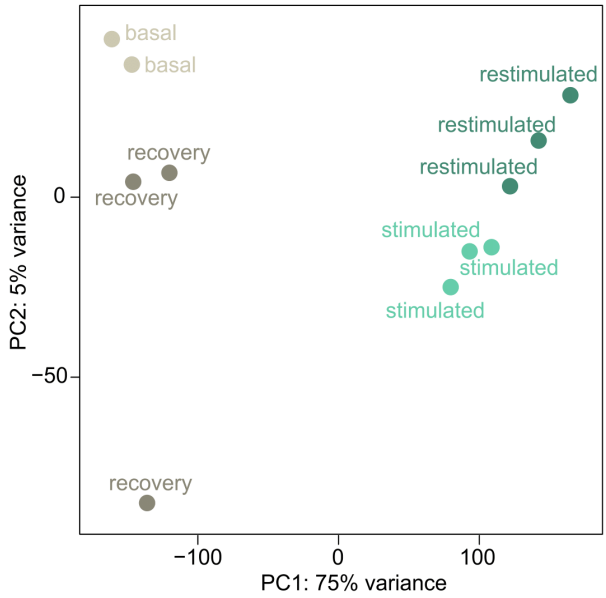

Figure 33. Principal component analysis of N = 54996 peaks identified by DiffBind.

From 54996 called peaks, 16153 were found to be differentially accessible (FDR < 1%) against *basal* in at least one condition (*stimulated, recovery* or *restimulated*). The first treatment with BDNF opened 8261 and closed 5399 regions. Surprisingly, two days later, at the *recovery* stage, all these changes were reverted and no DARs were found compared to the *basal* state (**Fig.34A**). This indicates that after BDNF stimulation ceases, the chromatin accessibility landscape is able to return to the previous state, showing a highly dynamic and plastic feature. The reiterated application of BDNF led to very similar numbers of DARs to the first encounter (N_{open} = 8134, N_{close} = 5433), indicating that the magnitude of the chromatin response is highly maintained across treatment rounds. Additionally, in both treatment rounds, the annotated genomic regions of affected chromatin accessibility were identical, with a high incidence on intronic regions possibly corresponding to distal regulatory elements (**Fig.34B**).

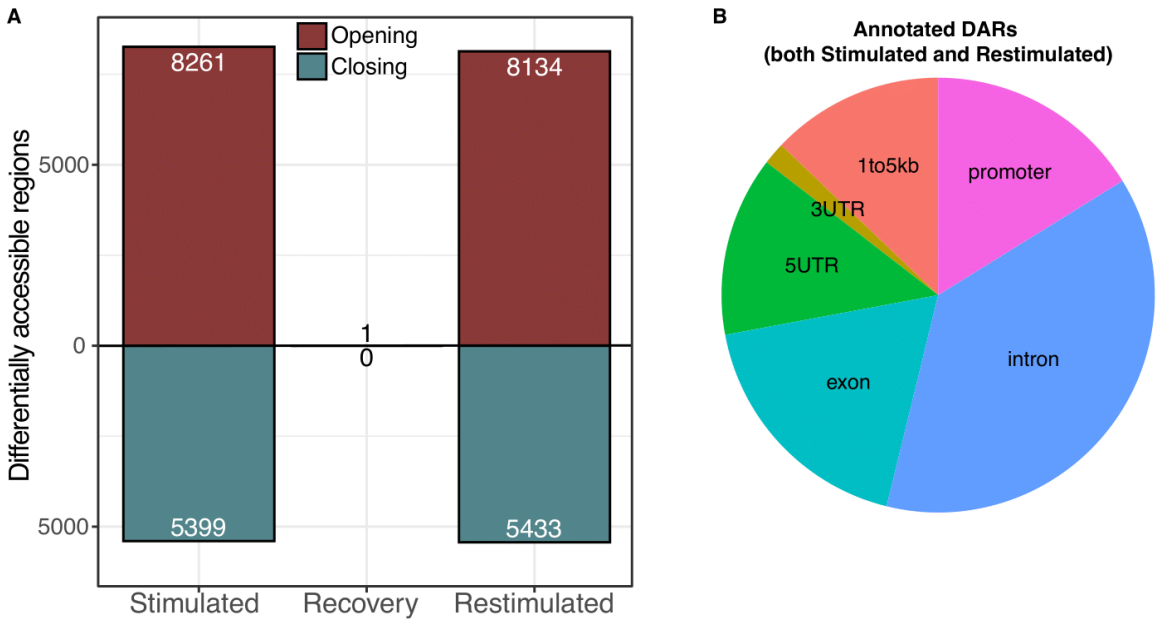

Figure 34. Number of differentially accessible regions across treatment rounds (A) and their annotated genomic features (B).
(A) Differentially accessible regions against *basal* were identified using DiffBind with a significance threshold of 1% FDR. Red: opening peaks, blue: closing peaks. (B) Proportion of peaks with specific genomic features across the DARs in the *stimulated* sample. The *restimulated* condition displayed identical proportions.

Although the number of changes induced by BDNF in both treatment rounds was highly similar, the affected loci differed slightly between the two. More than 7000 peaks opened and almost 4000 closed in the same manner in both rounds. However, a subset of peaks displayed differential accessibility in one of the rounds only (**Fig.35**).

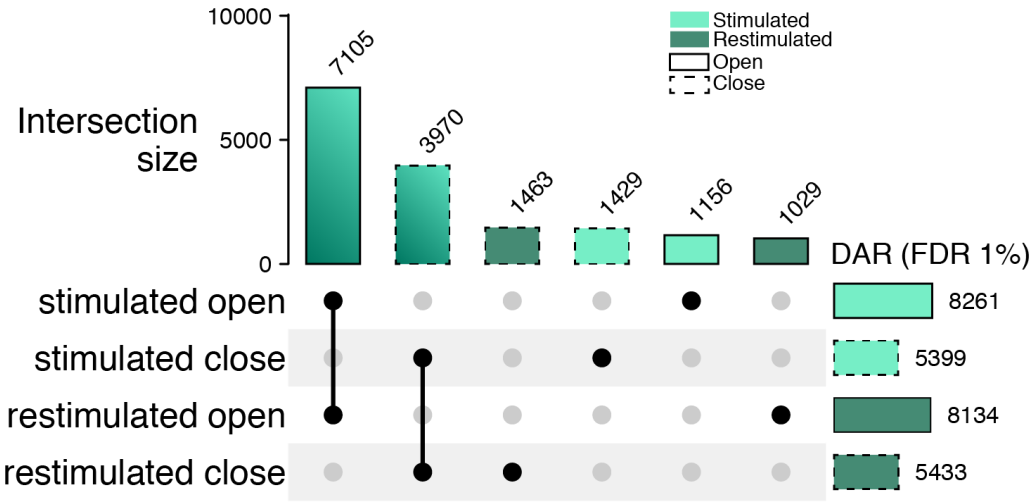

Figure 35. Number of overlaps between the DAR (FDR 1%) in stimulated and restimulated neurons.

3.2.6. Promoter and enhancer accessibility do not explain gene expression changes specific to BDNF stimulation rounds

Next, Victor and I wondered if the loci affected by each treatment round could explain the gene expression changes described in section **3.2.4.** To test that, Victor selected the DAR with a milder significance threshold (FDR 5%) and associated them with the closest DEG, separating promoters (0-2 kb from TSS) and putative distal enhancers (2-50 kb). He then grouped the peaks into 6 clusters depending on the cluster that they gene they had been associated to belonged (**Fig.26**) and which inspected the relative fold-change against the *basal* condition in the *stimulated*, *recovery* and *restimulated* samples (**Fig.36**). Overall, all the clusters displayed similar behaviours, both for promoters and distal peaks and they all showed a strong reversibility in the response, as seen in **Fig.34**, with an average fold-change in the *recovery* peaks close to 0, for both promoters and enhancers. We could identify bimodal distributions of the fold-changes for all gene clusters, meaning that these peaks open and close in response to BDNF although the associated genes are specifically upregulated (clusters 1, 2 and 3) or downregulated (clusters 4, 5, 6). Nevertheless, promoter peaks in clusters 4 and 6 had a higher density towards negative values (closing peaks), which would explain better the downregulation of the associate genes.

The absence of specific accessibility behaviours associated with the gene expression clusters indicated that our association study did not explain the gene expression changes. Hence, we could not identify a mechanism for memory or adaptation based on changes in chromatin accessibility that could represent the transcriptional differences across the stimulation rounds.

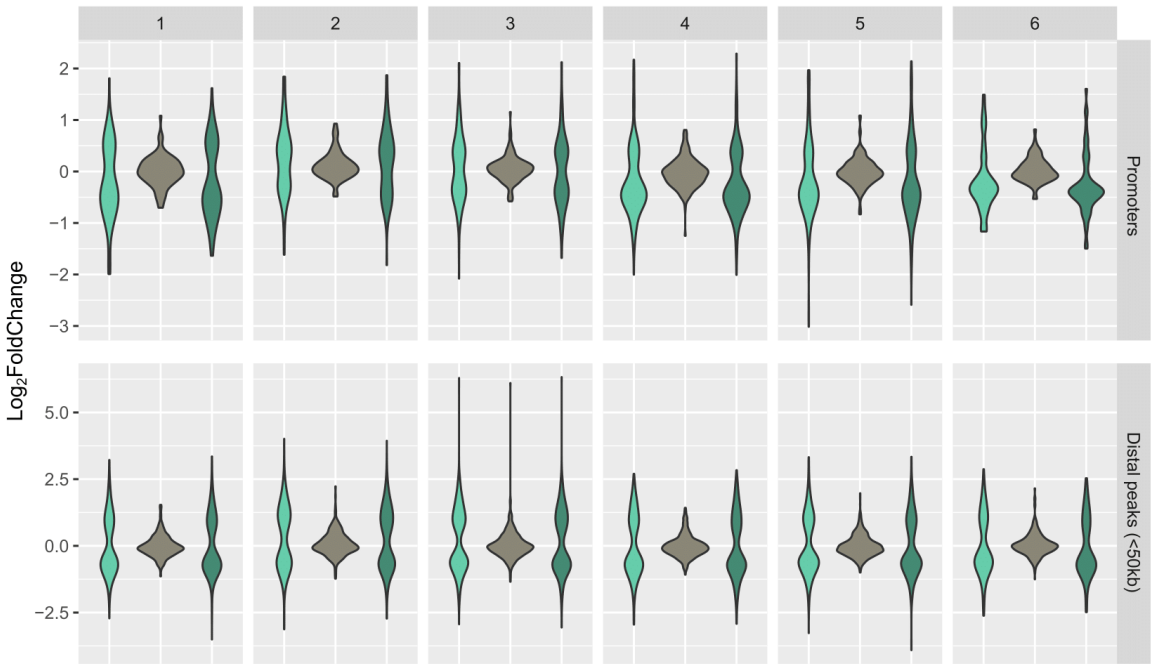

Figure 36. Changes in accessibility at promoters (top) and distal regions (< 50 kb, bottom) associated with differentially expressed genes per cluster.
Only peaks with a FDR< 0.05 are included. Log_2FoldChange computed by DiffBind using EdgeR normalization versus the *basal* condition. *N* per cluster indicated in **Appendix Table 2**.

3.2.7. MS analysis of double BDNF treatments reveals macroH2A as a possible regulator of transcriptional adaptation

Priming of cortical neurons with BDNF resulted in a distinct transcriptional outcome in response to the same stimulus. However, I was unable to identify a pattern in chromatin accessibility that could explain the gene expression changes between the two stimulation rounds. Therefore, I reasoned that, although chromatin accessibility returned to the *basal* state, chromatin regulators, such as transcription factors or chromatin modifying enzymes could be differentially abundant in the *basal* and the *recovery* condition, which would create a distinct chromatin landscape to allow a different transcriptional program. Additionally, posttranslational modifications on these proteins or on effectors belonging to BDNF-responsive pathways could lead to a change in how the signal is transduced into the nucleus to trigger a different transcriptional response.

To identify changes in protein abundances that could influence the differences in the transcriptional response to BDNF in primed neurons, I carried out a subcellular proteome analysis as the one described in chapter **3.1.2** using mouse primary cortical neurons stimulated as in **Fig.19**. In this occasion, the limited amount of cellular material led to a lower protein detection power, and only 1065 proteins were identified with at least 2 unique peptides among all conditions and compartments. To understand if the changes in gene expression were

accompanied by changes at the protein level, I correlated the abundance of the 1065 detected proteins per treatment and compartment with the expression levels of the corresponding transcripts. From the 1065 input proteins, 997 were also differentially expressed at the transcriptional level and used for the linear correlation analysis. Among all the comparisons, the strongest positive significant correlation was found for the DEG after *recovery* and *restimulation* and the chromatin-bound proteins after *restimulation* (**Fig.37**). A similar relationship was also found for the whole-cell lysates (WCL) of the *recovery* and *restimulation* transcriptomes. This indicates that the changes in gene expression only start being translated into protein changes at later times (48 hours after the first treatment round) and this seems to be regulating particularly chromatin-bound proteins.

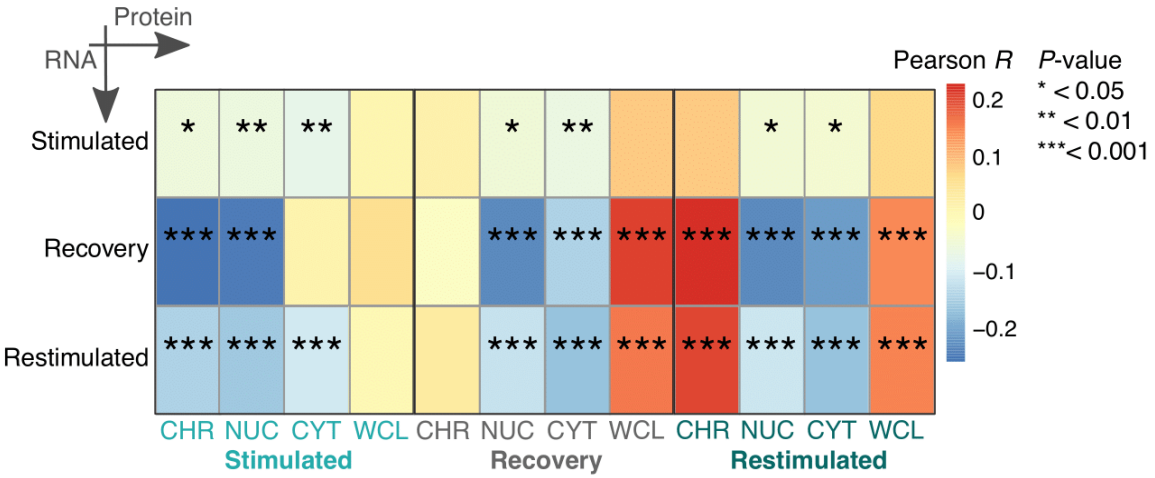

Figure 37. Correlation between protein abundance changes and gene expression changes in stimulated, recovery and restimulated neurons.
The heatmap colour code shows the Pearson correlation coefficient (*R*) and the asterisks in the squares indicate the significance of the correlation based on a two-sided *t*-test. Conditions from RNA-seq experiment can be read as rows and samples from the proteomics experiments, as columns. Only detected proteins which were differentially expressed at the level of gene expression were considered (*N* = 997 out of 1065 detected proteins). CHR: chromatin-bound proteins, NUC: nucleoplasmic proteins, CYT: cytosolic proteins, WCL: whole-cell lysate.

From the 1065 detected proteins, only 51 showed differential abundance in at least one sample against the *basal* condition in the corresponding subcellular compartment (FDR < 10%). The majority of these changes (29) appeared in the soluble nuclear fraction of the *restimulated* neurons. Among those, I noticed the enrichment of the histone variant macroH2A. There are three macroH2A protein isoforms: macroH2A1.1 and macroH2A1.2, two splice variants from the same gene, *H2afy*, and macroH2A2, from the gene *H2afy2*. The distinction between isoforms 1.1 and 1.2 by MS was not possible since they only differ in eight amino acids, making the assignment of each peptide to one of the isoforms a challenging task. Nevertheless, the isoforms produced from the gene *H2afy*, macroH2A1.1 and macroH2A1.2, were found in the *restimulated* and in the *recovery* condition (**Fig.38**). The macroH2A isoform 2 (*H2afy2)* was also enriched in the *restimulation* sample but not in the *recovery.*

In addition, I observed the enrichment of DNA methyltransferase 3a (DNMT3A) in the *restimulation* sample. DNMT3A responsible for *de novo* DNA methylation in response to extracellular stimuli[271,272] and necessary for learning and memory formation in postmitotic neurons [273]. During memory consolidation, the promoter of BDNF gets demethylated, which is associated with a decrease of DNMT3A in the nucleus of hippocampal neurons[272]. However, in the paradigm of reiterated BDNF stimulations, which displayed several gene clusters being downregulated or less induced in primed neurons, DNMT3A could have an additional function by which it would aid in desensitizing the induction of responsive genes that are no longer needed in a second treatment round. Further analysis of differential DNA methylation at the promoter of BDNF-responsive genes could shed light on a putative adaptation mechanism that could explain partially the gene expression patterns described in **Fig.26** with less transcriptional levels in primed neurons.

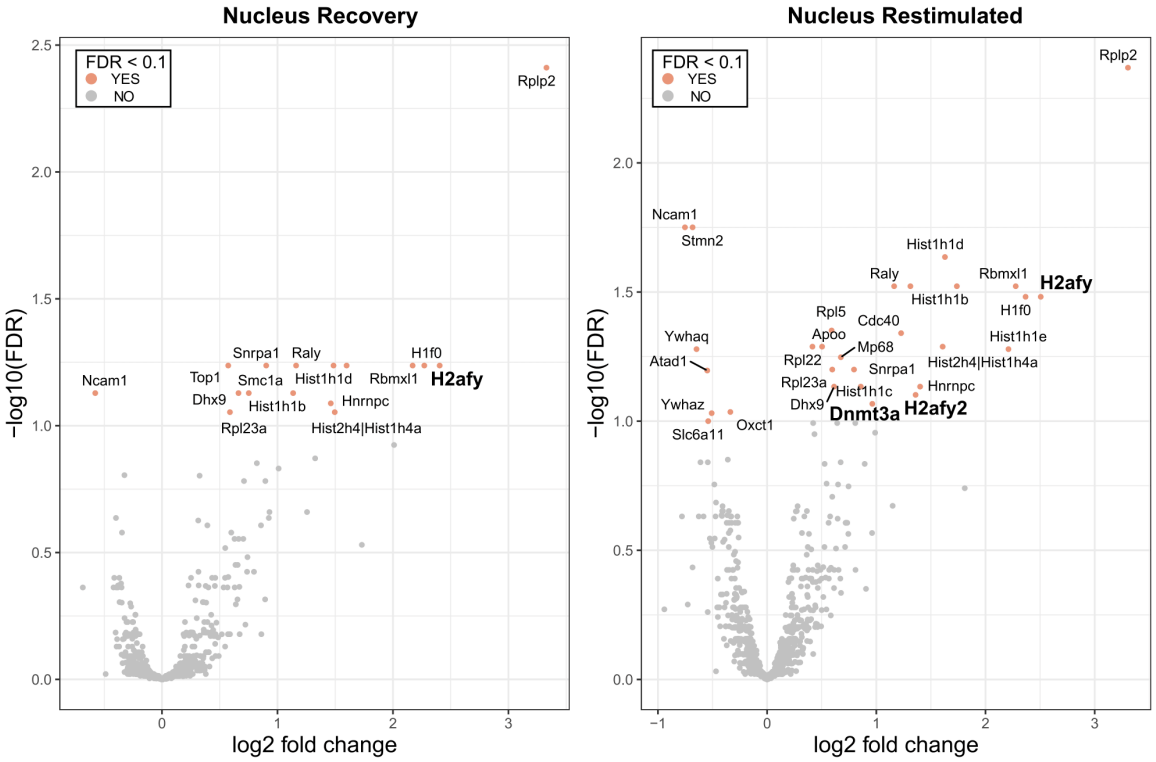

Figure 38. Volcano plots of the significantly abundant proteins in the nucleoplasm of recovery (left) and restimulated (right) conditions.
Significance threshold 10% FDR.

The mass spectrometry results were further validated by immunofluorescence stainings using an antibody against MacroH2A isoform 1.2, with the help of Dr. Jennifer Heck. Quantification of the signal indicated that macroH2A1.2 was already significantly more abundant in the nucleus of *stimulated* neurons, and the protein levels were maintained throughout the *recovery* and the *restimulation* conditions (**Fig.39A**). This was also validated by western-blot analysis (**Fig.39 B**). MacroH2A is a histone variant of the canonical histone H2A. Similarly to DNMT3A, macroH2A has attributed a transcriptional repressive function, although

it has also been associated with the augmentation of stimulus-triggered transcription in other cell types[57]. MacroH2A is deposited along large chromatin domains (>500 kb) and often colocalizes with the trimethylation of lysine 27 in histone H3 (H3K27me3) or with the constitutive heterochromatin mark trimethylation of lysine 9 in histone H3 (H3K9me3), which supports the role of macroH2A in the repression of gene expression [274]. Given that the increase in macroH2A signal can also be seen in the first response to BDNF and stays up to the second encounter, it is reasonable to think that higher macroH2A deposition on chromatin would occur in a BDNF-specific manner and that this deposition could repress the induction of BDNF-responsive genes in the latter stimulation (**Fig.26** cluster 2) or induce a direct downregulation of other genes (**Fig.26** clusters 5 and 6). To validate this hypothesis, further work should be performed to assess if macroH2A is indeed differentially deposited on the promoter of these genes in a BDNF-dependent manner by ChIP-seq or similar approaches.

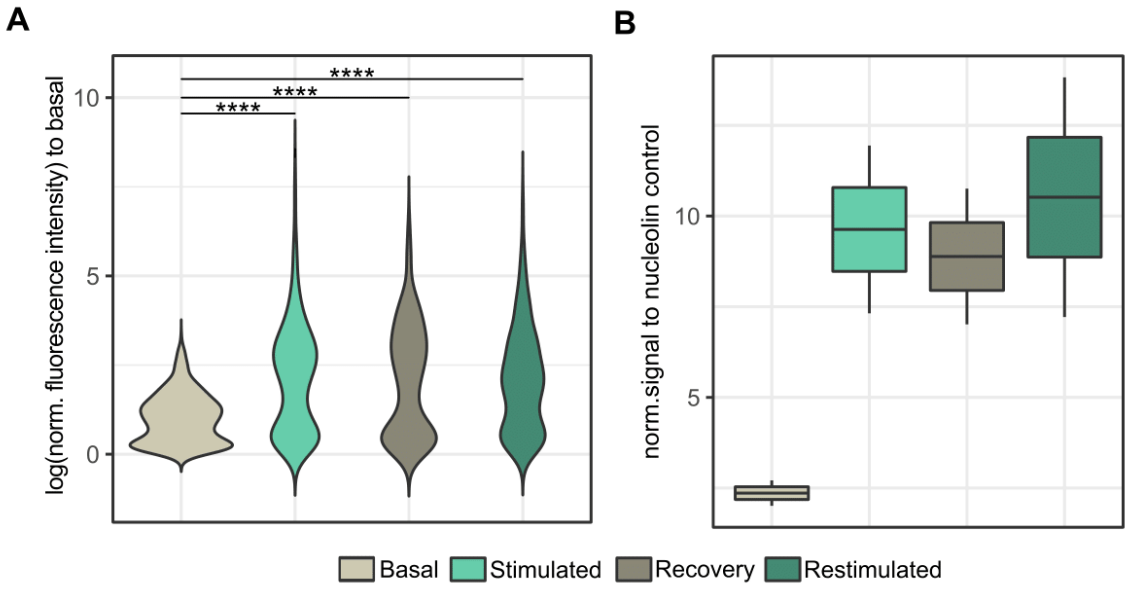

Figure 39. Analysis of macroH2A1.2 abundance in primary neurons stimulated with BDNF by immunofluorescence (A) and western blot (B).
(A) Fluorescence signal normalized to *basal* (data generated and analyzed by Dr Jennifer Heck; *N* = 1 experiment, with 409 analyzed cells. (B) Quantification of macroH2A1.2 signal in western blot experiments normalized to nucleolin (*N* = 2 independent experiments).

CHAPTER 4

DISCUSSION AND OUTLOOK

The results presented in this thesis provide a better understanding of the BDNF-regulated transcriptional response in mouse cortical neurons. BDNF is the most abundant neurotrophin in the central nervous system, with numerous roles in neuronal physiology and human disease[275]. During development, BDNF is necessary for the neurogenesis and the correct differentiation of neuronal precursor cells, while in mature neurons, BDNF mediates the maturation of neuronal processes, synaptic plasticity and connectivity[123]. Lower levels of BDNF have been associated with depression[203], schizophrenia[202] and Alzheimer's disease[200]. Therefore, clinical efforts are being driven towards increasing BDNF levels in the central nervous system of these patients, recently by means of gene therapy[276]. Nevertheless, comprehending the downstream effects of BDNF binding to its receptors can shed light on new areas of therapy. This work has been focused primarily on the chromatin responses to BDNF and consequential transcriptional adaptations to it as the ultimate consequence of BDNF-induced processes.

To better understand the BDNF-specific chromatin responses, I generated a subcellular proteomics dataset describing the changes in protein abundances in neurons after BDNF and KCl treatments and correlated these changes with the differentially expressed genes in response to both stimuli. As a result, I could identify the transcription factor Fos as the main player in BDNF-regulated transcription through early enhancer activation. Together with my colleagues, we identified a novel BDNF-specific enhancer that regulates *Arc* expression, a regulator of synaptic plasticity[250], through the cooperativity between Fos and TFs from the EGR family. I validated this finding using mESCs carrying a deletion of this enhancer differentiated *in vitro* to neurons, combined with a small molecule inhibitor of Fos binding to DNA. Finally, I aimed to evaluate if BDNF chromatin responses could prime future neuronal responses to the neurotrophin, describing a putative phenomenon of transcriptional adaptation. To this end, I could identify six different transcriptional patterns, four displayed variations between the BDNF-primed and naive neurons. I investigated the role of chromatin accessibility in the regulation of these transcriptional differences, but I was not able to identify an accessibility trace on BDNF-affected regions that could prime the response. Ultimately, I propose three hypothetical mechanisms that could lead to the transcriptional priming of the neurons, such as lncRNA regulation, desensitisation of the PI3K pathway and macroH2A deposition, which will be discussed in the following sections.

Challenges in dissecting stimulation-specific effects in neurons

The diversity of cell types in the brain generates difficulty profiling chromatin responses at a bulk level. The high variability across cell types increases the background, reducing the signal-to-noise ratio and hindering the detection limit of sequencing technologies. To circumvent this issue, I employed dissociated cultures of mouse cortical neurons in an attempt to have a homogenous population that would enable the study of transcriptional changes and their regulatory mechanisms. However, even among these homogeneous cultures, the responses to BDNF seemed variable from cell to cell. As shown in **Fig.27B**, only a portion of the cells induced Fos protein to the same level, and this variability increased when the cells had been previously primed with BDNF. It should be noted that the chromatin responses are extremely specific to the type and duration of stimulation, as well as to the physiological state of the neurons, i.e., maturation state or connectivity networks. The regulatory nature of BDNF itself provides additional consideration to this phenomenon since BDNF activation of TrkB induces more BDNF production in the target cells. Cells that stochastically perceive more BDNF would synthesize a larger amount of BDNF. This endogenously-produced BDNF could activate more TrkB receptors in the producer cell and neighbouring cells. Locally released BDNF would create subclusters of cells receiving higher BDNF concentrations, leading to differences in the downstream effects. Furthermore, BDNF also elicits neuronal activity through membrane depolarization[277], which could complicate the regulatory landscape, with simultaneously ongoing signalling cascades masking the initial impact of the neurotrophin itself. The additive effect of BDNF self-regulation plus the elicitation of other activity-dependent pathways limit the capacity to dissect stimulus-specific responses. To reduce the impact of spontaneous neuronal activity and increase the signal-to-noise ratio of the induced response, I treated the neurons with tetrodotoxin, a voltage-gated sodium channel blocker that also increases neuronal excitability[278]; and D-AP5, an NMDA receptor antagonist[279]. Although this usage may compromise some of the effects of the neurotrophin on neuronal physiology (e.g., on dendritic outgrowth[280]), it has been widely used by other labs[281–283] to reduce the noise of the transcriptional response when performing genomic studies.

The chromatin accessibility response to KCl showed a direct effect on promoter elements, and only at later time points, the effect of KCl on enhancers could be directly associated with changes in gene expression (**Appendix Figure 1**). Intriguingly, neuronal activity triggers BDNF production and release from depolarized cells[151]. Therefore, this delayed enhancer activation could correspond to a lagged response to BDNF in addition to the KCl-mediated depolarization. This confounding effect would interfere with determining KCl-specific mechanisms at later time points. Moreover, induction of cellular depolarization by elevated

potassium chloride concentrations activates L-type voltage-sensitive calcium channels (L-type VSCCs)[284]. Although we and others[102,282] intended to use this *in vitro* system as a representation of neuronal activity, it has been reported that KCl-mediated depolarization may not be translated into the generation of an action potential. One possible reason is that depolarization could exhaust the pre-synaptic cell and cause neurotransmitter depletion, preventing subsequent rounds of activity[285]. However, this does not preclude the increased intracellular calcium (Ca^{2+}) levels, which would mediate the biological effects of KCl depolarization[286,287]. BDNF transcriptional effects depend on Ca^{2+} signalling since TrkB activation increases intracellular Ca^{2+} release through the PLCγ pathway. Therefore, similarities in KCl- and BDNF-dependent transcriptional responses could be explained by the commonalities in the usage of Ca^{2+} as a second messenger.

I also want to discuss the stimulation-specific responses in the mESC-derived neurons. The deletion of the novel *Arc* enhancer, based on its BDNF-specific gained accessibility and the presence of Fos and EGR binding sites was performed in mESC using CRISPR-Cas9. Given that the efficiency of the CRISPR-Cas9 protocol in mutant generation is low, we selected clones and expanded them, which is only possible in dividing cells. To generate glutamatergic neurons[213,288] from the obtained mESC clonal lines, we employed an *in vitro* differentiation protocol using retinoic acid, which induces the commitment to the neuronal lineage[289]. The claim that the novel *Arc* enhancer is specific to BDNF came from the fact that this region gained accessibility in primary neurons treated with BDNF but not KCl. The experimental validation with mESC-derived neurons carrying the deletions could confirm that it responded to BDNF treatment and displayed the cooperativity of Fos and EGR. Interestingly, in contrast to the primary neurons, these mESC-derived neurons could not induce *Arc* expression upon KCl depolarization for 1h. I could not rule out Fos:EGR cooperativity in the KCl-stimulation setup because it could happen to other KCl- and BDNF-responsive genes. The differences in the physiological or maturation state of the mESC-derived neurons versus the primary neurons are correlated with the differences in *Arc*-inducing mechanisms upon BDNF or KCl treatments. This result emphasizes the need for a better characterization of neuronal model systems before extrapolating assumptions from the model to the *in vivo* context of the brain.

Fos: the protagonist in BDNF-dependent transcription

As seen in section 3.1.1, the transcriptional responses to BDNF treatments and KCl-depolarization over a time course (1h, 6h and 10h) were specific in a time- and stimulus-dependent manner. What are the mechanisms that regulate these differences at the transcriptional level? The analysis of the chromatin accessibility changes upon the different treatments carried out by Dr. Ignacio Ibarra revealed that BDNF affects *cis*-regulatory elements more than KCl, which induces a direct

opening of promoters to regulate gene expression. BDNF displayed a complex mechanism, right from the start, by opening a larger number of genomic locations corresponding to distal elements, i.e., enhancers. Using MS-based proteomics, I could identify significantly higher recruitment of the transcription factor Fos to chromatin upon 1h of BDNF stimulation than after 1h of KCl treatment. This implied that Fos has a significant role in BDNF-regulated transcription. We also observed that the opening regions in response to 1h of BDNF stimulation presented a 1.3-fold enrichment in Fos motifs over KCl stimulation[210]. Furthermore, the increase in Fos protein abundance triggered by KCl was comparable to the one by BDNF only at later time points (**Fig.15B**). This observation presents a deviation in Fos dynamics depending on the stimulation condition and duration, pointing out mechanisms for regulating the specificity of the response. Hence, my colleagues and I concluded that the TF Fos plays a more decisive role in BDNF-induced transcription based on early enhancer activation through its role as a pioneer TF[249,290].

My colleagues Vikram Ratnu and Ignacio Ibarra observed that Fos transcript levels were higher after 1h of KCl than 1h of BDNF, indicating a discrepancy in Fos protein and transcript levels. This is not fully surprising given the complex self-regulatory mechanism that Fos, as part of the AP-1 complex, undergoes. Fos protein exerts a negative autoregulation on the *Fos* gene[113,291,292]. Phosphorylation of the C-terminal domain of Fos by ERK stabilised the protein[112,293,294] and this event is related to downregulated *Fos* expression[113,291,292]. Apart from the stabilization by phosphorylation, Fos heterodimerization with Jun enables the complex to bind AP-1 binding sites[295,296] found upstream of the *Fos* gene, downregulating its own transcription[297]. However, Fos-Jun binding also influences Fos protein stability, by inducing Fos degradation mediated by the proteasome-ubiquitin system[24]. The complex equilibrium between Fos protein stabilization and degradation could be easily affected by the differential induction of *cis*- and *trans*-regulatory features by BDNF or KCl. Overall, BDNF stimulation seems to enhance Fos protein stability leading to a decrease in *Fos* transcript levels, which appears to be less the case for KCl.

I illustrated the effect of Fos:EGR cooperativity in the regulation of *Arc* expression, considering one locus presenting both motifs. This locus was selected based on differential accessibility of the region, significantly greater in BDNF over KCl and control neurons and, in addition, had been found to present enhancer marks (H3K4me1 and H3K27ac) upon depolarization with KCl[282]. I validated Fos and Egr1 binding to this locus, but we did not confirm that enhancer marks were deposited differentially in BDNF versus KCl and control conditions. Although the cooperativity study employed the inhibitor T-5224, which prevents Fos activity at a global level, the usage of CRISPR KO lines for this particular region conferred specificity to the studied locus, as can be seen when observing the expression results of the negative controls *Btg2* and *Fos* (**Fig.18C, D**). Nevertheless,

performing this study on a genome-wide scale would enable the characterization of BDNF-enhancer regulation by assessing if TF cooperativity is required for only a subset of specific enhancers, for instance, affecting only IEGs, or if it is a genome-wide phenomenon.

Last but not least, the pioneering role of Fos can select the activation of specific enhancers through the recruitment of other protein complexes such as remodelers[249]. Investigating the differential protein-protein interactions in the diverse contexts of stimulations could uncover other mechanisms by which Fos would regulate stimulation-specific transcription. Depending on the stimulation-induced changes in the nuclear proteome, putative Fos interactors may be more or less likely to establish functional associations, leading to different transcriptional outcomes.

Transcriptional adaptation to BDNF: possible mechanisms of transcriptional memory

The second aim of this thesis was to investigate the phenomenon of transcriptional memory and adaptations to BDNF stimulations. This hypothesis arose because half of the accessibility changes triggered by BDNF stimulation lasted up to 10 hours (**Fig.6**). I reasoned that this could be a priming mechanism to allow for a different transcriptional outcome in future encounters with BDNF. To this end, I identified six distinct transcriptional profiles depending on their reaction to both encounters with BDNF (**Fig.26**).

A prototypical example of transcriptional memory and adaptation can be found in the inflammatory immune response. Exposing immune cells to a pathogen primes the inflammation response to be faster and more efficient in later encounters with the infection. This is known as the basic principle of cellular memory response, where the cell incorporates the acquired information from the previous event and presents a readiness state to respond to stimuli conditioned by the experience. Foster *et al.*[298] performed one of the first studies that linked immune memory mechanisms to epigenetic modifications. They identified two groups of differentially responsive genes to Toll-like receptor activation by lipopolysaccharide (LPS) in macrophages. The first group presented altered histone acetylation and accessibility profiles that rapidly recruited RNA polymerase II to induce faster transcription in later rounds of LPS treatment. After LPS removal, the active histone marks H3K4me1 and H3K4me3 were not removed from the enhancers and promoters, respectively[35,299], of these genes, with the concomitant maintained accessibility state[298] allowing enhanced induction later on. Conversely, the second group displayed decreased accessibility after the removal of LPS that lasted for long periods, in what they called the “tolerance” phase. If LPS were administered during this phase, these genes would not be induced due to their decreased accessibility, which prevented excessive inflammation[298].

From this finding onwards, several studies described various epigenetic mechanisms conferring immune transcriptional memory. As mentioned in the *Introduction*, the lncRNA UMLILO can prime the promoters of responsive genes to retain the H3K4me3 mark enhancing their sensitivity to subsequent inflammatory cues[62]. Furthermore, the deposition of the repressive histone mark H3K9me2 was found to be decreased in response to LPS by the reduced activity of the TF ATF7[300]. Reduced H3K9me2 at the promoter of LPS-responsive genes increased their basal levels, enhancing the resistance to pathogens[300]. Apart from mechanisms based on histone modifications, the activation of stimulus-responsive TFs was found essential to establish transcriptional memory in the memory response to inflammation[301,302]. In particular, Fos, as part of the AP-1 complex, has been reported as a pioneer TF that confers accessibility to responsive genes in order to allow stimulus-independent TFs to bind them. Long after the stimulation and the AP-1 complex are gone, these pre-existing, stimulus-independent TFs remain bound to these loci preserving the accessibility[301].

All these events happening in immune cells are plausible mechanisms affecting neuronal cells. Similarly to the immune system, the brain continuously receives external inputs and needs to react to and learn from them. Epigenetics, i.e., chemical modifications of histone tails and genomic DNA, appears as an attractive mechanism to store information on chromatin. In particular, it has been described that the basis of memory formation lies in DNA methylation since DNMTs are upregulated in the hippocampus upon experience, and their inhibition prevents memory formation[303]. The methylation of promoters of memory-suppressing genes and the demethylation of memory-promoting genes are necessary for the memory process[303]. The synaptic activity also induces global *de novo* demethylation of activity-dependent genes, and this mark persists long after the activation ceases[304]. An interesting theory speculates that global neuronal activity-induced demethylation generates a permissive chromatin accessibility landscape that could enhance the transcriptional response in the process of reactivation[305]. Furthermore, the histone modifications described in immune transcriptional memory acquisition have also been reported in memory formation and consolidation, such as H3K4me3 deposition at promoters of responsive genes[306] or H3K9me2 mark removal[307]. The relevance of these marks in the memory processes has been assessed by association studies using pharmacological approaches and behavioural tests. However, the direct consequence on the transcription of their targeted genes during memory formation and reinduction has been less investigated. Recently, Marco *et al.*[308] reported that chromatin accessibility changes induced during memory formation are maintained for longer times during memory consolidation and that these changes correlate with promoter-enhancer interaction frequencies. They also identified distinct transcriptional clusters behaving differently across activation (memory formation) and reactivation (memory consolidation). They reported that, although these genes presented enhanced promoter-enhancer contacts and incremental

accessibility at enhancers, there was no specific accessibility behaviour corresponding to each transcriptional pattern. To my understanding, a precise mechanism connecting chromatin contacts and accessibility and transcriptional patterns was still missing.

Although the final outcome of acquired transcriptional memory is commonly regarded as enhanced transcription, either faster or stronger, the second response to BDNF encounters described here was, overall, milder. Of the three downregulated clusters, two displayed a stronger downregulation. Cluster 2, which comprised BDNF-upregulated genes (*Npas4*, *Nr4a2*), was induced, yet to a lesser extent in the second round. Finally, cluster 1 (*Snca*, *Calca*) did show a stronger response when neurons had been previously exposed to BDNF. It is interesting that BDNF did not manage to induce them in the first encounter. One possibility is that their induction is initially slow, hence I do not capture it with this experimental setup. Reinduction with BDNF could accelerate their response, enabling their detection in the selected time window. How their transcriptional kinetics is accelerated remains unanswered.

Having observed these transcriptional differences, I investigated a possible priming effect on chromatin accessibility since most of the histone marks described as responsible for priming immune cells are accompanied by accessibility changes. Additionally, it had been described that the repression of stimulus-responsive genes was maintained after the removal of the stimulus by limiting accessibility[298]. The analysis performed on the ATAC-seq dataset did not reveal any left-over chromatin accessibility changes that could explain this phenomenon. Although I could identify specific peaks that only opened or closed in one of the stimulation rounds (**Fig.35**), I did not detect any influence on associated gene promoters or enhancers (**Fig.36**) or a correlation with the features of the gene expression clusters. Gene-to-peak associations were made based on genomic distance and may not be actual associations, especially for distal regulatory elements such as enhancers, whose main characteristic is the regulation of gene expression regardless of their location and orientation. Additional computational efforts need to be made to further dissect information from this data, including other strategies to delineate gene-enhancer associations.

Investigating the memory component at the proteome level did reveal some interesting hints. Both DNMT3A and macroH2A were found to be more abundant after a second BDNF treatment. Furthermore, macroH2A levels were significantly greater already in the first treatment and maintained in the recovery stage, as seen by WB and IF (**Fig.39**). As described above, DNMT3A has been reported in mechanisms of epigenetic memory in neurons, hence it would be a hint worth pursuing. Identifying differences in the methylation profile of primed neurons would provide a causative mechanism for transcriptional adaptation. On the other hand, a higher macroH2A deposition on chromatin upon the first encounter with BDNF could lead to a novel mechanism of adaptation to stimuli since the role of

this histone variant in postmitotic neurons is not fully defined. The association of macroH2A with the genes displaying different transcriptional responses across the treatment rounds would be the initial step to uncovering a potential mechanism since it still needs to be fully understood how macroH2A triggers the repression of target genes. Structurally, macroH2A has been linked to stabilizing the compacted chromatin architecture in differentiated cells[309], contributing to constitutive heterochromatic regions decorated with H3K9me3[274]. In addition, macroH2A co-localizes with H3K27me3[57,310], a mark for facultative heterochromatin that can be deposited differentially in response to extracellular cues[311,312], indicating that the deposition or removal of macroH2A could potentially be regulated by external cues.

From another point of view, the differences in the transcriptional responses could be a consequence of different signalling cascades being activated in response to $p75^{NTR}$ or TrkB if the balance between both receptor abundances or between pro-BDNF and mature BDNF had been affected in between stimulation rounds. Similarly, the signal transduction to the nucleus to trigger a transcriptional response highly relies on posttranslational modifications of the receptors and the proteins involved in the signalling cascades. Proteomic analysis of these membrane receptors and the post-translational status of the regulatory proteins could unveil the lack of induction or over-activation of some proteins in specific pathways, providing further insights into the pathway enrichment analysis performed in this work (**Fig.24**).

The massive downregulation of lncRNAs in the second encounter with BDNF is a puzzling event. Although lncRNAs are known to play regulatory roles in neurons[104,257] and, in particular, in response to BDNF[63], additional work is required to investigate the downstream consequences of this downregulation. Some of the consequential effects of this phenomenon may be better appreciated at later time points. As seen in section 3.1.1, transcriptional and accessibility responses vary over time, and therefore the effects of lncRNA downregulation may be correlated with events taking place later. Overall, with the employed approaches, I was able to observe snapshots of these processes, and relevant events happening before or after the study window may be missed. Likewise, this could apply to some of the genes in cluster 2 defined in **Fig.26**. My current conclusion is that these genes are desensitized to BDNF by showing a milder induction. However, their expression could have been induced faster, and by the time of measurement, their transcript levels could have been returning to the basal level, leading to confounding conclusions.

Conclusions and outlook

In this study, a comprehensive analysis of the neuronal transcriptional and chromatin responses to stimuli was conducted to identify specificity mechanisms of transcriptional regulation. My colleagues and I identified BDNF-characteristic

events, such as early enhancer activation with concomitant gene expression changes regulated by TF recruitment to chromatin that orchestrate transcription in a cooperative manner. In particular, the TF Fos seemed to have a stronger role in BDNF-induced transcription thanks to the synergistic effect with other TFs, such as EGRs and KLFs. In addition to the computational TF cooperativity analysis, I believe that the identification of these cooperativity events by experimental means could shed light on the mechanisms underlying gene specificity. Current approaches such as proximity labelling proteomics offer the possibility to identify neighbouring partners of a protein of interest[313], even of nuclear regulatory proteins such as TFs[314]. To gain a full view of the role of stimulus-specific interactions, the identification of bound genomic regions by the interacting partners should be considered. Disrupting the interactions, by means of small molecule inhibitors, could further help in understanding the relevance of such complexes.

When investigating the adaptation of the transcriptional response to BDNF, I could identify groups of genes whose response to BDNF was enhanced (cluster 1) or desensitised (cluster 2) in primed neurons. Several other genes experienced a stronger downregulation in the second treatment event, with many lncRNAs following this behaviour. In the search for a bookmarking mechanism that could condition the second transcriptional response as a consequence of the first treatment, I investigated the chromatin accessibility landscape and changes in the subcellular proteome. Chromatin accessibility revealed itself as a very plastic event, responding almost fully equally in both rounds, and completely going back to the basal state after the first treatment without leaving a fingerprint that would provide an explanation for the differences in transcription. Technical difficulties hindered a deeper study of the proteomic changes, yet I was able to identify two candidates that could transcriptionally prime neurons after BDNF stimulations: DNMT3A and macroH2A. Due to time limitations, I could not conduct further experiments to validate the role of these factors on BDNF-dependent transcription. For instance, performing ChIP-seq experiments to investigate their genomic distribution would aid in associating the differentially induced genes by BDNF treatments with this adaptation mechanism. These association studies would require further investigation to assign a causative role to these elements. In the case of DNMT3A, assessing differential methylation profiles would verify the role of DNA methylation in regulating this phenomenon. Perturbing DNMT3A function and observing the consequences not only on the DNA methylation status but also on the transcription of the BDNF-responsive genes could directly associate this epigenetic regulator with the transcriptional adaptation to BDNF. Likewise, profiling other chromatin states through histone PTMs (H3K4me1/3, H3K27ac/me3) or other chromatin binding factors (BRDs, CTCF) by performing ChIP-seq, with relation to macroH2A deposition could provide a mechanism for the regulation of these genes.

The development of single-cell sequencing technologies has been an important breakthrough in the field of neurobiology, allowing the identification of cell type-specific transcriptomes and epigenomes that give rise to the complexity of the brain[315]. Until then, studying distinct neuronal populations had been restricted to imaging essays or complex reporter-based sorting protocols that require high material amounts of materials and that are not always applicable to primary samples. The cell-to-cell variability observed in this study encourages the use of these technologies, to be able to trace the magnitude of the responses based on the degree of activation of each cell. This would aid in the direct association of gene expression and chromatin changes in response to a certain degree of activation and epigenomic landscape. An even deeper understanding of the transcriptional adaptations in response to reiterated stimulation events would go through the live tracking of the cellular responses. Identifying the degree of response of a specific cell and investigating the effect of subsequent encounters with the stimulus on the same particular cell would be an extremely valuable source of knowledge to identify adaptation mechanisms.

Appendix

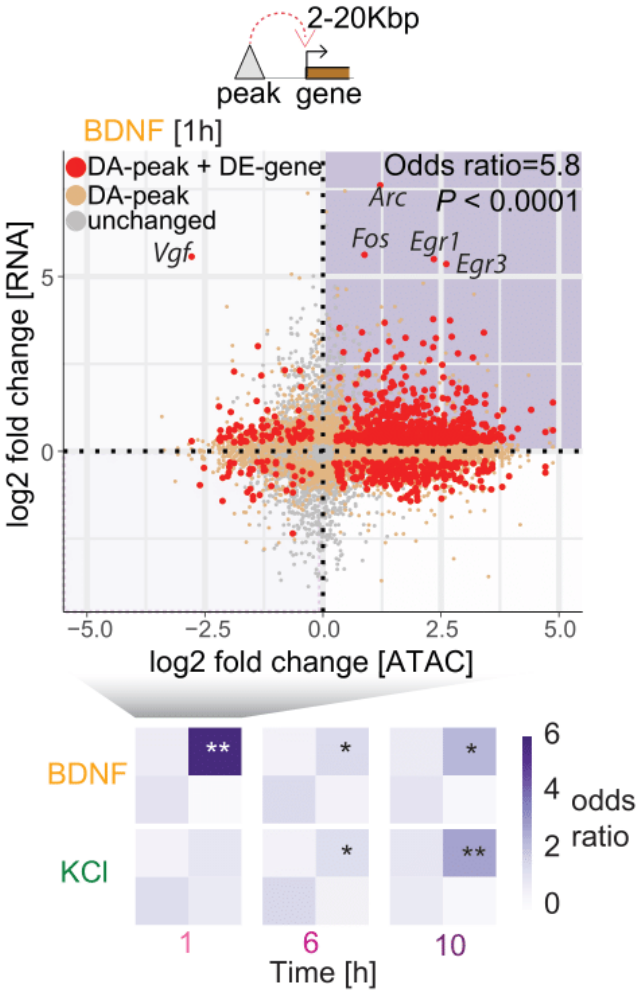

Appendix Figure 1. Correlation between ATAC-seq and RNA-seq changes at enhancers from Ibarra, Ratnu, Gordillo et al. [210].
In the main top panel, each ATAC peak was associated with the closest peak within 2-20 kb distance and log2FoldChanges in accessibility and expression for the peak-gene pair is shown. The main scatter plot refers to BDNF 1h stimulation, and the lower panels show schematics of the rest of the comparisons (BDNF 6h, 10h, KCl 1h, 6h, 10h). Purple colour intensity represents the odds ratio by a two-sided Fisher's exact test with BH correction. Asterisks in lower panels indicate *P*-values as corrected by a Benjamini–Hochberg procedure (*$P < 0.05$; **$P < 0.01$)

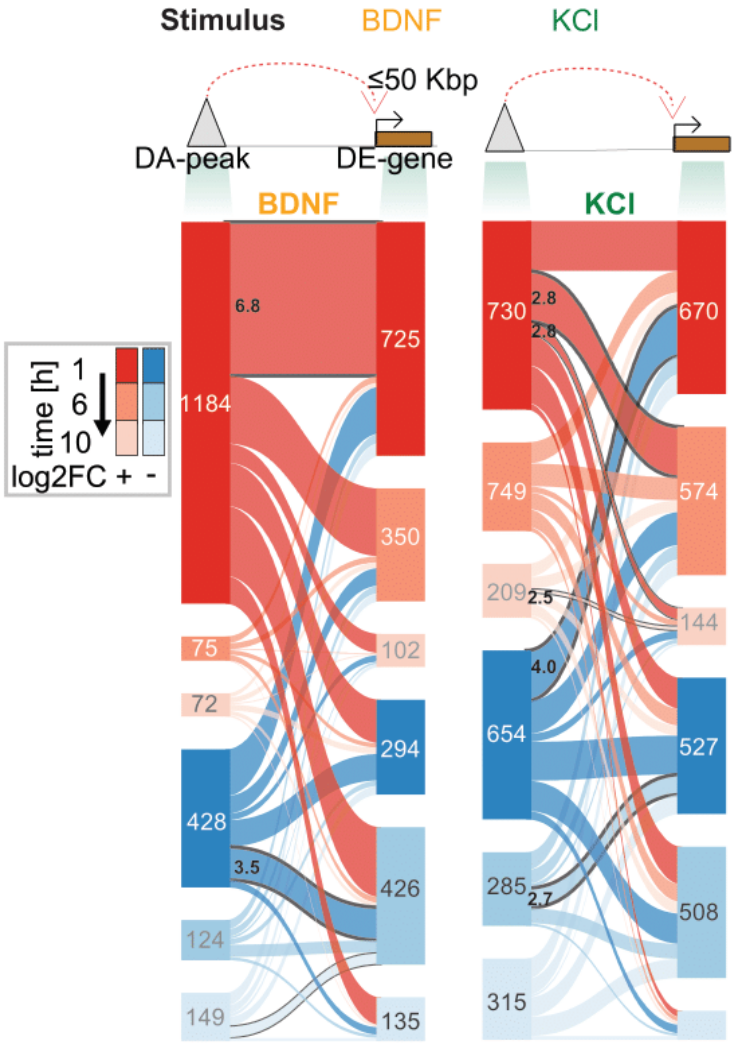

Appendix Figure 2. Number of associations between the changes in accessibility and the changes in gene expression, at different time points, for BDNF (left) and KCl (right).
Peak-to-gene associations shown in Sankey plot are within 50 kb distance. Only significant associations by Fisher's exact test (adjusted $P < 0.1$) are indicated with numbers (association Z-score values > 2.5) in connecting areas. Association scores were calculated using a permutation approach for significant peaks and associated significant gene changes while maintaining timewise changes. Further methodological description in Ibarra, Ratnu, Gordillo *et al* [210].

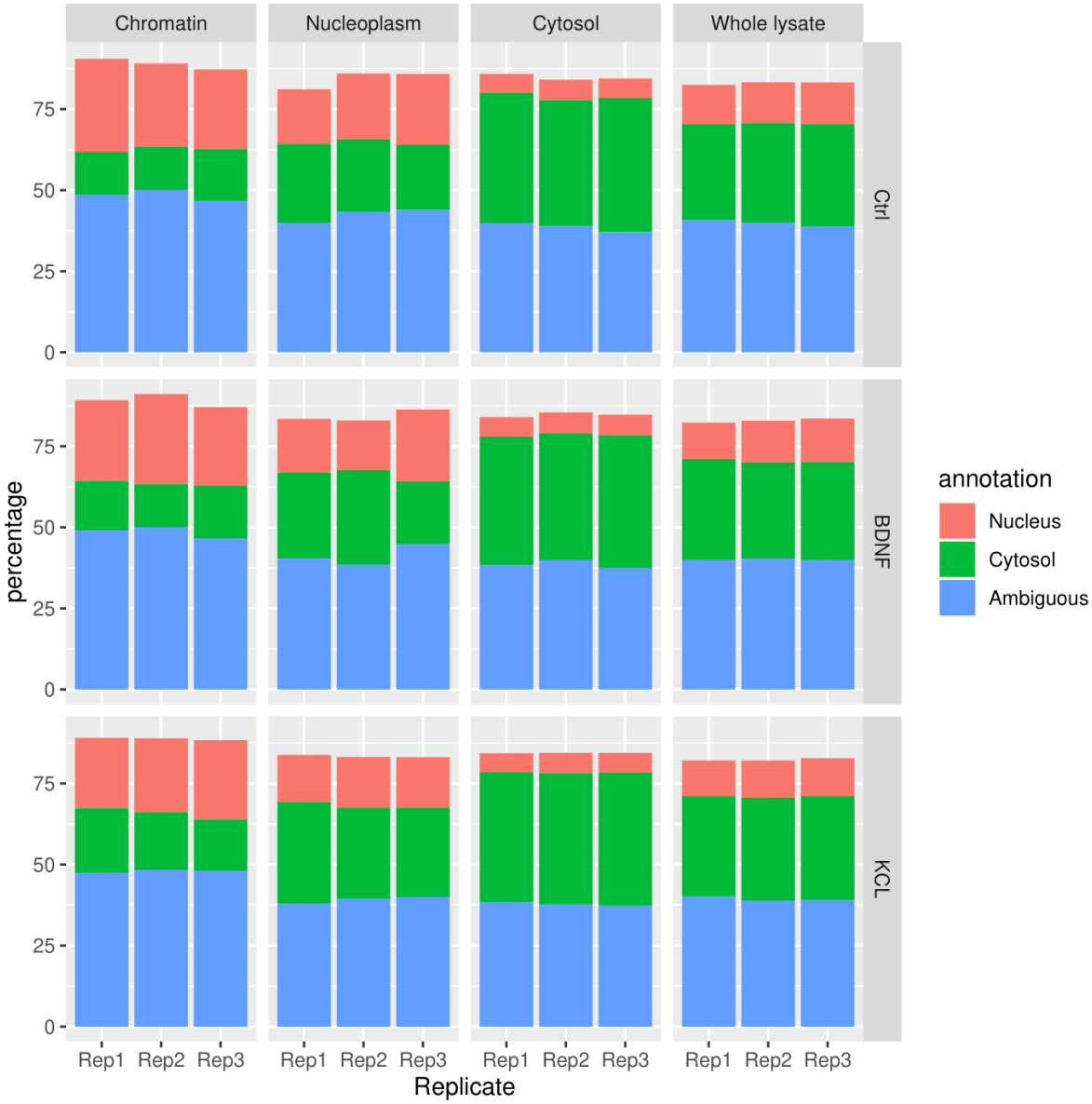

Appendix Figure 3. Enrichment of proteins annotated as nuclear or cytosolic in the subcellular proteomes after 15 minutes of stimulation.
The percentage shown in the bar plots corresponds to the vsn-normalized intensity values for proteins annotated to be nuclear (GO:0005654, GO:0005634, GO:0031965, GO:0044428, GO:0005654, GO:0044451, GO:0005730), cytosolic (GO:0005737, GO:0005829, GO:0044444) or ambiguous (annotated in both categories) with respect to the total intensity of all proteins detected in each replicate per fraction, subcellular compartment and stimulation condition. Stimulations with BDNF and KCl were done for 60 minutes in two biological replicates.

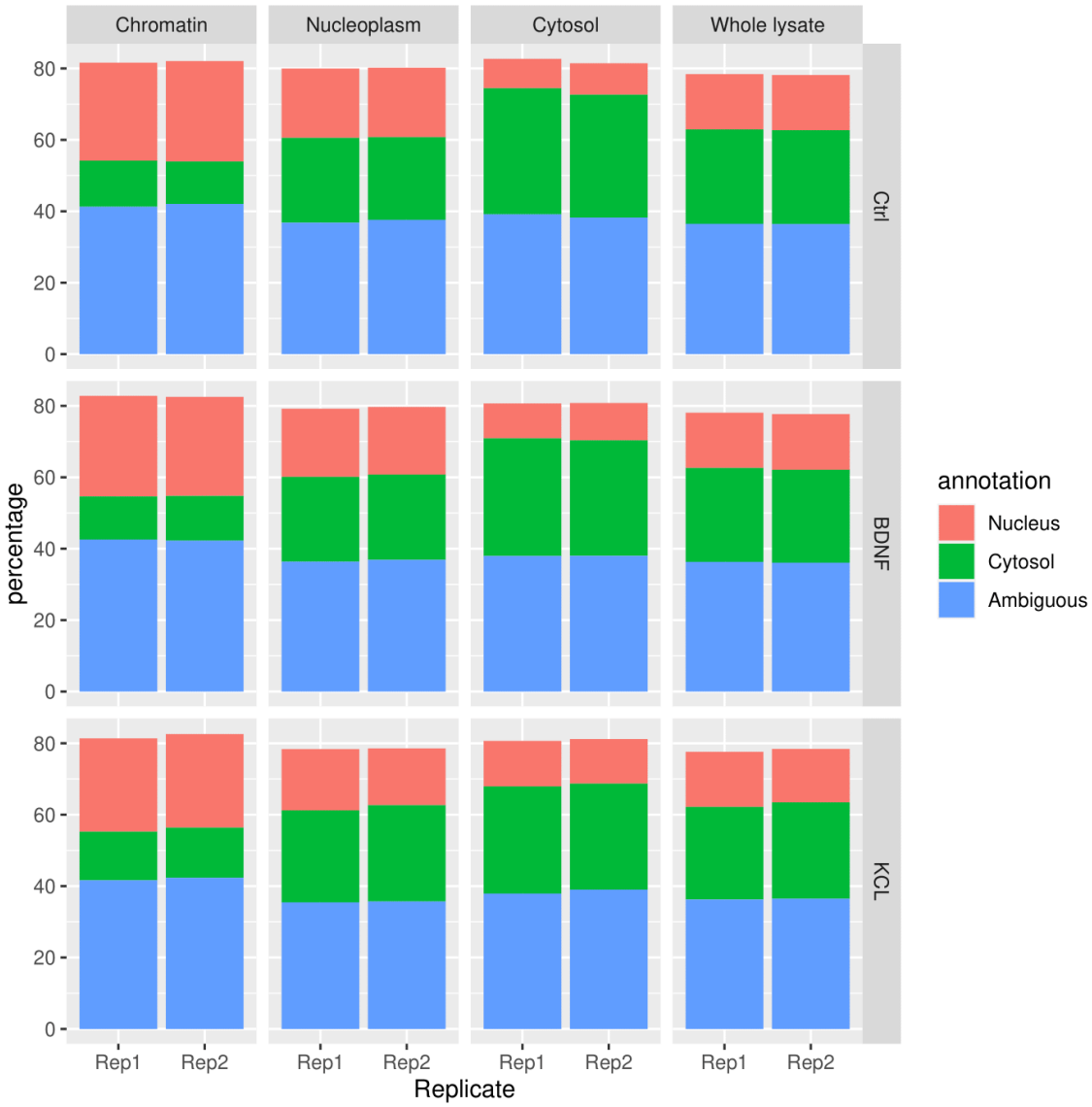

Appendix Figure 4. Enrichment of proteins annotated as nuclear or cytosolic in the subcellular proteomes after 60 minutes of stimulation.
The percentage shown in the bar plots corresponds to the vsn-normalized intensity values for proteins annotated to be nuclear (GO:0005654, GO:0005634, GO:0031a965, GO:0044428, GO:0005654, GO:0044451, GO:0005730), cytosolic (GO:0005737, GO:0005829, GO:0044444) or ambiguous (annotated in both categories) with respect to the total intensity of all proteins detected in each replicate per fraction, subcellular compartment and stimulation condition. Stimulations with BDNF and KCl were done for 15 minutes in 3 biological replicates.

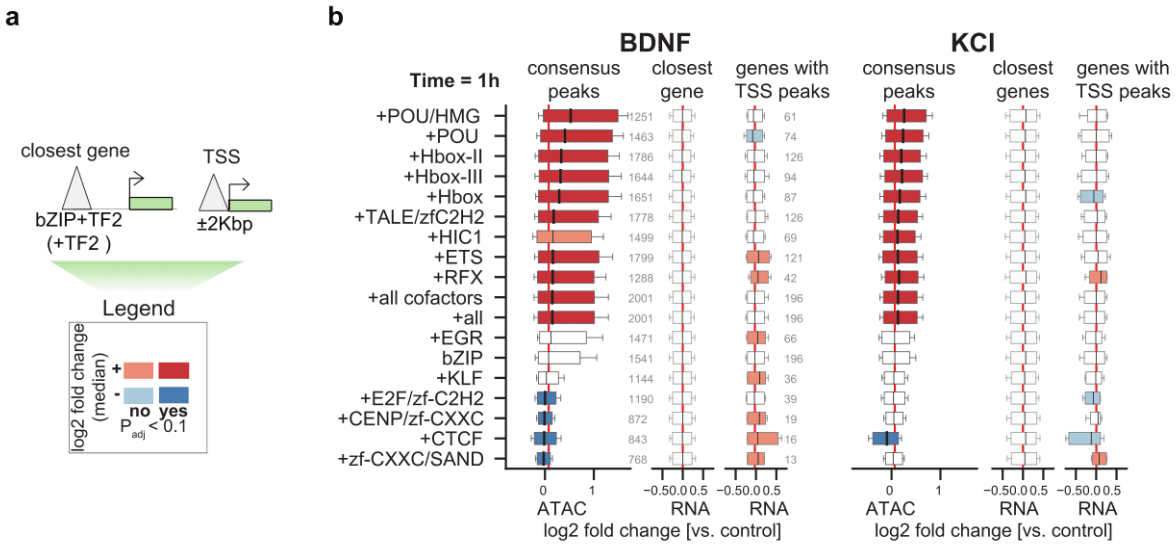

Appendix Figure 5. Accessibility and gene expression changes associated with the presence of Fos (bZIP) motif alone or together with other TFs.

(A) Schematics of the annotation of ATAC peaks based on the presence of the bZIP motif alone or with other TFs. The log2FoldChange median depicts the difference in accessibility or expression between peaks with bZIP together with other TF versus bZIP alone. (B) On the first boxplot, changes in the accessibility of peaks containing bZIP motifs with other TFs in BDNF (left) and KCl (right) versus unstimulated control. The second boxplot shows gene expression changes of the closest genes and (third boxplot) of the closest gene associated when the peak falls on a TSS.

Appendix Table 1. Number of differentially abundant proteins (FDR 10%) in the cytosol, nucleus and chromatin after 15 and 60 minutes of stimulation in mouse primary and mESC-derived neurons, respectively.
Changes are separated per stimulation in both, if both stimuli triggered it, BDNF- or KCl-specific. Color code indicates the magnitude of the change with respect to the values.

|logFC|>0 FDR< 0.1		Cytosol	Nucleus	Chromatin
15 min	Both	28	8	1
	BDNF only	97	26	7
	KCl only	32	35	2
	ns	2834	2922	2981
60 min	Both	113	7	12
	BDNF only	7	6	4
	KCl only	3366	1818	536
	ns	2023	3678	4956

Appendix Table 2. Connections between differentially expressed genes and differentially accessible peaks (FDR < 5%) within a 50 kb distance of the gene TSS, represented in Fig.36.

Cluster	Genes in cluster	Genes with peak	Peaks in cluster
1	577	273	449
2	499	207	357
3	958	461	775
4	1046	420	646
5	1296	518	802
6	523	203	314

Bibliography

1. Waddington, C. H. The epigenotype. *Int. J. Epidemiol.* **41**, 10–13 (1942).
2. Cheung, P., Allis, C. D. & Sassone-Corsi, P. Signaling to chromatin through histone modifications. *Cell* **103**, 263–271 (2000).
3. Greer, E. L. *et al.* Transgenerational epigenetic inheritance of longevity in Caenorhabditis elegans. *Nature* **479**, 365–371 (2011).
4. Riethoven, J.-J. M. Regulatory regions in DNA: promoters, enhancers, silencers, and insulators. *Methods Mol. Biol.* **674**, 33–42 (2010).
5. Aibara, S., Schilbach, S. & Cramer, P. Structures of mammalian RNA polymerase II pre-initiation complexes. *Nature* **594**, 124–128 (2021).
6. Hsin, J.-P. & Manley, J. L. The RNA polymerase II CTD coordinates transcription and RNA processing. *Genes Dev.* **26**, 2119–2137 (2012).
7. Weake, V. M. & Workman, J. L. Inducible gene expression: diverse regulatory mechanisms. *Nat. Rev. Genet.* **11**, 426–437 (2010).
8. Kim, C. G., Swendeman, S. L., Barnhart, K. M. & Sheffery, M. Promoter elements and erythroid cell nuclear factors that regulate alpha-globin gene transcription in vitro. *Mol. Cell. Biol.* **10**, 5958–5966 (1990).
9. Klemm, S. L., Shipony, Z. & Greenleaf, W. J. Chromatin accessibility and the regulatory epigenome. *Nat. Rev. Genet.* **20**, 207–220 (2019).
10. Zaret, K. S. Pioneer transcription factors initiating gene network changes. *Annu. Rev. Genet.* **54**, 367–385 (2020).
11. Malik, S. & Roeder, R. G. Dynamic regulation of pol II transcription by the mammalian Mediator complex. *Trends Biochem. Sci.* **30**, 256–263 (2005).
12. Wendt, K. S. *et al.* Cohesin mediates transcriptional insulation by CCCTC-binding factor. *Nature* **451**, 796–801 (2008).
13. Vokes, S. A., Ji, H., Wong, W. H. & McMahon, A. P. A genome-scale analysis of the cis-regulatory circuitry underlying sonic hedgehog-mediated patterning of the mammalian limb. *Genes Dev.* **22**, 2651–2663 (2008).
14. Gaszner, M. & Felsenfeld, G. Insulators: exploiting transcriptional and epigenetic mechanisms. *Nat. Rev. Genet.* **7**, 703–713 (2006).
15. Slattery, M. *et al.* Cofactor binding evokes latent differences in DNA binding specificity between Hox proteins. *Cell* **147**, 1270–1282 (2011).
16. Giorgetti, L. *et al.* Noncooperative interactions between transcription factors and clustered DNA binding sites enable graded transcriptional responses to environmental inputs. *Mol. Cell* **37**, 418–428 (2010).
17. Sönmezer, C. *et al.* Molecular Co-occupancy Identifies Transcription Factor Binding Cooperativity In Vivo. *Mol. Cell* **81**, 255-267.e6 (2021).
18. Ibarra, I. L. *et al.* Mechanistic insights into transcription factor cooperativity and its impact on protein-phenotype interactions. *Nat. Commun.* **11**, 124 (2020).
19. Segal, E., Raveh-Sadka, T., Schroeder, M., Unnerstall, U. & Gaul, U. Predicting expression patterns from regulatory sequence in Drosophila segmentation. *Nature* **451**, 535–540 (2008).
20. Kim, H. K., Jeong, M. G. & Hwang, E. S. Post-Translational Modifications in Transcription Factors that Determine T Helper Cell Differentiation. *Mol. Cells* **44**, 318–327 (2021).
21. Shaywitz, A. J. & Greenberg, M. E. CREB: a stimulus-induced transcription factor

activated by a diverse array of extracellular signals. *Annu. Rev. Biochem.* **68**, 821–861 (1999).
22. Crawley, C. D. *et al.* DNA damage-induced cytotoxicity is mediated by the cooperative interaction of phospho-NF-κB p50 and a single nucleotide in the κB-site. *Nucleic Acids Res.* **41**, 764–774 (2013).
23. Durchschlag, E., Reiter, W., Ammerer, G. & Schüller, C. Nuclear localization destabilizes the stress-regulated transcription factor Msn2. *J. Biol. Chem.* **279**, 55425–55432 (2004).
24. Tsurumi, C. *et al.* Degradation of c-Fos by the 26S proteasome is accelerated by c-Jun and multiple protein kinases. *Mol. Cell. Biol.* **15**, 5682–5687 (1995).
25. Schreiber, S. L. & Bernstein, B. E. Signaling network model of chromatin. *Cell* **111**, 771–778 (2002).
26. Rossetto, D., Avvakumov, N. & Côté, J. Histone phosphorylation: a chromatin modification involved in diverse nuclear events. *Epigenetics* **7**, 1098–1108 (2012).
27. Loenarz, C. & Schofield, C. J. Expanding chemical biology of 2-oxoglutarate oxygenases. *Nat. Chem. Biol.* **4**, 152–156 (2008).
28. Shimazu, T. *et al.* Suppression of oxidative stress by β-hydroxybutyrate, an endogenous histone deacetylase inhibitor. *Science* **339**, 211–214 (2013).
29. Fujiki, R. *et al.* GlcNAcylation of histone H2B facilitates its monoubiquitination. *Nature* **480**, 557–560 (2011).
30. Henikoff, S. & Shilatifard, A. Histone modification: cause or cog? *Trends Genet.* **27**, 389–396 (2011).
31. Heintzman, N. D. *et al.* Distinct and predictive chromatin signatures of transcriptional promoters and enhancers in the human genome. *Nat. Genet.* **39**, 311–318 (2007).
32. Sankar, A. *et al.* Histone editing elucidates the functional roles of H3K27 methylation and acetylation in mammals. *Nat. Genet.* **54**, 754–760 (2022).
33. Peixoto, L. & Abel, T. The role of histone acetylation in memory formation and cognitive impairments. *Neuropsychopharmacology* **38**, 62–76 (2013).
34. Wang, L.-H., Aberin, M. A. E., Wu, S. & Wang, S.-P. The MLL3/4 H3K4 methyltransferase complex in establishing an active enhancer landscape. *Biochem. Soc. Trans.* **49**, 1041–1054 (2021).
35. Ostuni, R. *et al.* Latent enhancers activated by stimulation in differentiated cells. *Cell* **152**, 157–171 (2013).
36. Delcuve, G. P., Khan, D. H. & Davie, J. R. Roles of histone deacetylases in epigenetic regulation: emerging paradigms from studies with inhibitors. *Clin. Epigenetics* **4**, 5 (2012).
37. Cha, T.-L. *et al.* Akt-mediated phosphorylation of EZH2 suppresses methylation of lysine 27 in histone H3. *Science* **310**, 306–310 (2005).
38. Piunti, A. & Shilatifard, A. The roles of Polycomb repressive complexes in mammalian development and cancer. *Nat. Rev. Mol. Cell Biol.* **22**, 326–345 (2021).
39. Nicetto, D. & Zaret, K. S. Role of H3K9me3 heterochromatin in cell identity establishment and maintenance. *Curr. Opin. Genet. Dev.* **55**, 1–10 (2019).
40. Jang, M. K. *et al.* The bromodomain protein Brd4 is a positive regulatory component of P-TEFb and stimulates RNA polymerase II-dependent transcription. *Mol. Cell* **19**, 523–534 (2005).
41. Yun, M., Wu, J., Workman, J. L. & Li, B. Readers of histone modifications. *Cell Res.* **21**, 564–578 (2011).

42. Haddadderafshi, B. *et al.* The Autism Risk Factor CHD8 Is a Chromatin Activator and Functionally Dependent on the ERK-MAPK Pathway Effector ELK1. *BioRxiv* (2020) doi:10.1101/2020.11.10.377010.
43. Moore, L. D., Le, T. & Fan, G. DNA Methylation and Its Basic Function. *Neuropsychopharmacology* **38**, 23–38 (2013).
44. Bird, A. DNA methylation patterns and epigenetic memory. *Genes Dev.* **16**, 6–21 (2002).
45. Holliday, R. & Pugh, J. E. DNA modification mechanisms and gene activity during development. *Science* **187**, 226–232 (1975).
46. Deaton, A. M. & Bird, A. CpG islands and the regulation of transcription. *Genes Dev.* **25**, 1010–1022 (2011).
47. Bell, A. C. & Felsenfeld, G. Methylation of a CTCF-dependent boundary controls imprinted expression of the Igf2 gene. *Nature* **405**, 482–485 (2000).
48. Saluz, H. P., Jiricny, J. & Jost, J. P. Genomic sequencing reveals a positive correlation between the kinetics of strand-specific DNA demethylation of the overlapping estradiol/glucocorticoid-receptor binding sites and the rate of avian vitellogenin mRNA synthesis. *Proc Natl Acad Sci USA* **83**, 7167–7171 (1986).
49. Jones, P. L. *et al.* Methylated DNA and MeCP2 recruit histone deacetylase to repress transcription. *Nat. Genet.* **19**, 187–191 (1998).
50. Rasmussen, K. D. & Helin, K. Role of TET enzymes in DNA methylation, development, and cancer. *Genes Dev.* **30**, 733–750 (2016).
51. Kriaucionis, S. & Heintz, N. The nuclear DNA base 5-hydroxymethylcytosine is present in Purkinje neurons and the brain. *Science* **324**, 929–930 (2009).
52. Mellén, M., Ayata, P., Dewell, S., Kriaucionis, S. & Heintz, N. MeCP2 binds to 5hmC enriched within active genes and accessible chromatin in the nervous system. *Cell* **151**, 1417–1430 (2012).
53. Li, X. *et al.* Neocortical Tet3-mediated accumulation of 5-hydroxymethylcytosine promotes rapid behavioral adaptation. *Proc Natl Acad Sci USA* **111**, 7120–7125 (2014).
54. Lio, C.-W. J. & Rao, A. TET enzymes and 5hmc in adaptive and innate immune systems. *Front. Immunol.* **10**, 210 (2019).
55. Hota, S. K. & Bruneau, B. G. ATP-dependent chromatin remodeling during mammalian development. *Development* **143**, 2882–2897 (2016).
56. Santoro, S. W. & Dulac, C. Histone variants and cellular plasticity. *Trends Genet.* **31**, 516–527 (2015).
57. Gamble, M. J., Frizzell, K. M., Yang, C., Krishnakumar, R. & Kraus, W. L. The histone variant macroH2A1 marks repressed autosomal chromatin, but protects a subset of its target genes from silencing. *Genes Dev.* **24**, 21–32 (2010).
58. Dell'Orso, S. *et al.* The histone variant macroh2a1.2 is necessary for the activation of muscle enhancers and recruitment of the transcription factor pbx1. *Cell Rep.* **14**, 1156–1168 (2016).
59. Kaikkonen, M. U. *et al.* Remodeling of the enhancer landscape during macrophage activation is coupled to enhancer transcription. *Mol. Cell* **51**, 310–325 (2013).
60. Statello, L., Guo, C.-J., Chen, L.-L. & Huarte, M. Gene regulation by long non-coding RNAs and its biological functions. *Nat. Rev. Mol. Cell Biol.* **22**, 96–118 (2021).
61. Loda, A. & Heard, E. Xist RNA in action: Past, present, and future. *PLoS Genet.* **15**, e1008333 (2019).

62. Fanucchi, S. *et al.* Immune genes are primed for robust transcription by proximal long noncoding RNAs located in nuclear compartments. *Nat. Genet.* **51**, 138–150 (2019).
63. Aliperti, V. & Donizetti, A. Long Non-coding RNA in Neurons: New Players in Early Response to BDNF Stimulation. *Front. Mol. Neurosci.* **9**, 15 (2016).
64. O'Carroll, D. & Schaefer, A. General principals of miRNA biogenesis and regulation in the brain. *Neuropsychopharmacology* **38**, 39–54 (2013).
65. Yap, E. L. *et al.* Bidirectional perisomatic inhibitory plasticity of a Fos neuronal network. *Nature* **590**, 115–121 (2020).
66. Josselyn, S. A. & Tonegawa, S. Memory engrams: Recalling the past and imagining the future. *Science* **367**, (2020).
67. Clayton, D. F. The genomic action potential. *Neurobiol. Learn. Mem.* **74**, 185–216 (2000).
68. Yang, Y. *et al.* Selective synaptic remodeling of amygdalocortical connections associated with fear memory. *Nat. Neurosci.* **19**, 1348–1355 (2016).
69. Martin, S. J., Grimwood, P. D. & Morris, R. G. Synaptic plasticity and memory: an evaluation of the hypothesis. *Annu. Rev. Neurosci.* **23**, 649–711 (2000).
70. Salinas, E. & Sejnowski, T. J. Correlated neuronal activity and the flow of neural information. *Nat. Rev. Neurosci.* **2**, 539–550 (2001).
71. Abraham, W. C., Logan, B., Greenwood, J. M. & Dragunow, M. Induction and experience-dependent consolidation of stable long-term potentiation lasting months in the hippocampus. *J. Neurosci.* **22**, 9626–9634 (2002).
72. Amir, R. E. *et al.* Rett syndrome is caused by mutations in X-linked MECP2, encoding methyl-CpG-binding protein 2. *Nat. Genet.* **23**, 185–188 (1999).
73. Santen, G. W. E. *et al.* Mutations in SWI/SNF chromatin remodeling complex gene ARID1B cause Coffin-Siris syndrome. *Nat. Genet.* **44**, 379–380 (2012).
74. Van Houdt, J. K. J. *et al.* Heterozygous missense mutations in SMARCA2 cause Nicolaides-Baraitser syndrome. *Nat. Genet.* **44**, 445–9, S1 (2012).
75. Kleefstra, T. *et al.* Disruption of an EHMT1-associated chromatin-modification module causes intellectual disability. *Am. J. Hum. Genet.* **91**, 73–82 (2012).
76. Berson, A., Nativio, R., Berger, S. L. & Bonini, N. M. Epigenetic regulation in neurodegenerative diseases. *Trends Neurosci.* **41**, 587–598 (2018).
77. Campbell, R. R. & Wood, M. A. How the epigenome integrates information and reshapes the synapse. *Nat. Rev. Neurosci.* **20**, 133–147 (2019).
78. Peleg, S. *et al.* Altered histone acetylation is associated with age-dependent memory impairment in mice. *Science* **328**, 753–756 (2010).
79. von Schimmelmann, M. *et al.* Polycomb repressive complex 2 (PRC2) silences genes responsible for neurodegeneration. *Nat. Neurosci.* **19**, 1321–1330 (2016).
80. Palay, S. L. & Palade, G. E. The fine structure of neurons. *J. Biophys. Biochem. Cytol.* **1**, 69–88 (1955).
81. Grider, M. H., Jessu, R. & Kabir, R. Physiology, Action Potential. in *StatPearls* (StatPearls Publishing, 2022).
82. Chen, I. & Lui, F. Neuroanatomy, neuron action potential. in *StatPearls* (StatPearls Publishing, 2022).
83. Jal, S. & Khora, S. S. An overview on the origin and production of tetrodotoxin, a potent neurotoxin. *J. Appl. Microbiol.* **119**, 907–916 (2015).
84. Andreae, L. C. & Burrone, J. The role of neuronal activity and transmitter release on synapse formation. *Curr. Opin. Neurobiol.* **27**, 47–52 (2014).

85. Colicos, M. A. Activity-Dependent Synaptic Plasticity. in *Encyclopedia of Neuroscience* (eds. Binder, M. D., Hirokawa, N. & Windhorst, U.) 50–52 (Springer Berlin Heidelberg, 2009). doi:10.1007/978-3-540-29678-2_74.
86. Dudek, S. M. & Bear, M. F. Bidirectional long-term modification of synaptic effectiveness in the adult and immature hippocampus. *J. Neurosci.* **13**, 2910–2918 (1993).
87. Bliss, T. V. & Collingridge, G. L. A synaptic model of memory: long-term potentiation in the hippocampus. *Nature* **361**, 31–39 (1993).
88. Collingridge, G. L., Isaac, J. T. R. & Wang, Y. T. Receptor trafficking and synaptic plasticity. *Nat. Rev. Neurosci.* **5**, 952–962 (2004).
89. Dong, Z. *et al.* Long-term potentiation decay and memory loss are mediated by AMPAR endocytosis. *J. Clin. Invest.* **125**, 234–247 (2015).
90. Lynch, G., Larson, J., Kelso, S., Barrionuevo, G. & Schottler, F. Intracellular injections of EGTA block induction of hippocampal long-term potentiation. *Nature* **305**, 719–721 (1983).
91. Igaz, L. M., Vianna, M. R. M., Medina, J. H. & Izquierdo, I. Two time periods of hippocampal mRNA synthesis are required for memory consolidation of fear-motivated learning. *J. Neurosci.* **22**, 6781–6789 (2002).
92. Abraham, W. C. *et al.* Correlations between immediate early gene induction and the persistence of long-term potentiation. *Neuroscience* **56**, 717–727 (1993).
93. Nguyen, P. V., Abel, T. & Kandel, E. R. Requirement of a critical period of transcription for induction of a late phase of LTP. *Science* **265**, 1104–1107 (1994).
94. Greer, P. L. & Greenberg, M. E. From synapse to nucleus: calcium-dependent gene transcription in the control of synapse development and function. *Neuron* **59**, 846–860 (2008).
95. Sheng, M. & Greenberg, M. E. The regulation and function of c-fos and other immediate early genes in the nervous system. *Neuron* **4**, 477–485 (1990).
96. Hunt, S. P., Pini, A. & Evan, G. Induction of c-fos-like protein in spinal cord neurons following sensory stimulation. *Nature* **328**, 632–634 (1987).
97. Greenberg, M. E. & Ziff, E. B. Stimulation of 3T3 cells induces transcription of the c-fos proto-oncogene. *Nature* **311**, 433–438 (1984).
98. Bartel, D. P., Sheng, M., Lester, ~, Lau, F. & Greenberg, M. E. *Growth factors and membrane depolarization activate distinct programs of early response gene expression: dissociation of los and jun induction*. http://genesdev.cshlp.org/content/3/3/304.full.pdf.
99. Lau, L. F. & Nathans, D. Expression of a set of growth-related immediate early genes in BALB/c 3T3 cells: coordinate regulation with c-fos or c-myc. *Proc Natl Acad Sci USA* **84**, 1182–1186 (1987).
100. Saha, R. N. & Dudek, S. M. Splitting hares and tortoises: a classification of neuronal immediate early gene transcription based on poised RNA polymerase II. *Neuroscience* **247**, 175–181 (2013).
101. Saha, R. N. *et al.* Rapid activity-induced transcription of Arc and other IEGs relies on poised RNA polymerase II. *Nat. Neurosci.* **14**, 848–856 (2011).
102. Tyssowski, K. M. *et al.* Different neuronal activity patterns induce different gene expression programs. *Neuron* **98**, 530-546.e11 (2018).
103. Kitazawa, T. *et al.* A unique bipartite Polycomb signature regulates stimulus-response transcription during development. *Nat. Genet.* **53**, 379–391 (2021).
104. Aitken, S. *et al.* Transcriptional dynamics reveal critical roles for non-coding RNAs

in the immediate-early response. *PLoS Comput. Biol.* **11**, e1004217 (2015).
105. Gomard, T. *et al.* Fos family protein degradation by the proteasome. *Biochem. Soc. Trans.* **36**, 858–863 (2008).
106. Sharp, F. R., Sagar, S. M., Hicks, K., Lowenstein, D. & Hisanaga, K. c-fos mRNA, Fos, and Fos-related antigen induction by hypertonic saline and stress. *J. Neurosci.* **11**, 2321–2331 (1991).
107. Healy, S., Khan, P. & Davie, J. R. Immediate early response genes and cell transformation. *Pharmacol. Ther.* **137**, 64–77 (2013).
108. Bahrami, S. & Drabløs, F. Gene regulation in the immediate-early response process. *Adv. Biol. Regul.* **62**, 37–49 (2016).
109. Vacca, A. *et al.* Conserved temporal ordering of promoter activation implicates common mechanisms governing the immediate early response across cell types and stimuli. *Open Biol.* **8**, (2018).
110. Balamotis, M. A. *et al.* Complexity in transcription control at the activation domain-mediator interface. *Sci. Signal.* **2**, ra20 (2009).
111. Joo, J.-Y., Schaukowitch, K., Farbiak, L., Kilaru, G. & Kim, T.-K. Stimulus-specific combinatorial functionality of neuronal c-fos enhancers. *Nat. Neurosci.* **19**, 75–83 (2016).
112. Monje, P., Marinissen, M. J. & Gutkind, J. S. Phosphorylation of the carboxyl-terminal transactivation domain of c-Fos by extracellular signal-regulated kinase mediates the transcriptional activation of AP-1 and cellular transformation induced by platelet-derived growth factor. *Mol. Cell. Biol.* **23**, 7030–7043 (2003).
113. Wilson, T. & Treisman, R. Fos C-terminal mutations block down-regulation of c-fos transcription following serum stimulation. *EMBO J.* **7**, 4193–4202 (1988).
114. Angel, P. & Karin, M. The role of Jun, Fos and the AP-1 complex in cell-proliferation and transformation. *Biochim. Biophys. Acta* **1072**, 129–157 (1991).
115. Bramham, C. R., Worley, P. F., Moore, M. J. & Guzowski, J. F. The immediate early gene arc/arg3.1: regulation, mechanisms, and function. *J. Neurosci.* **28**, 11760–11767 (2008).
116. Kawashima, T. *et al.* Synaptic activity-responsive element in the Arc/Arg3.1 promoter essential for synapse-to-nucleus signaling in activated neurons. *Proc Natl Acad Sci USA* **106**, 316–321 (2009).
117. Steward, O., Wallace, C. S., Lyford, G. L. & Worley, P. F. Synaptic activation causes the mRNA for the IEG Arc to localize selectively near activated postsynaptic sites on dendrites. *Neuron* **21**, 741–751 (1998).
118. Flavell, S. W. & Greenberg, M. E. Signaling mechanisms linking neuronal activity to gene expression and plasticity of the nervous system. *Annu. Rev. Neurosci.* **31**, 563–590 (2008).
119. Guo, S.-L. *et al.* Serum inducible kinase is a positive regulator of cortical dendrite development and is required for BDNF-promoted dendritic arborization. *Cell Res.* **22**, 387–398 (2012).
120. Lewin, G. R. & Barde, Y. A. Physiology of the neurotrophins. *Annu. Rev. Neurosci.* **19**, 289–317 (1996).
121. Patapoutian, A. & Reichardt, L. F. Trk receptors: mediators of neurotrophin action. *Curr. Opin. Neurobiol.* **11**, 272–280 (2001).
122. Parkhurst, C. N. *et al.* Microglia promote learning-dependent synapse formation through brain-derived neurotrophic factor. *Cell* **155**, 1596–1609 (2013).
123. Park, H. & Poo, M. Neurotrophin regulation of neural circuit development and

function. *Nat. Rev. Neurosci.* **14**, 7–23 (2013).
124. Bartkowska, K., Paquin, A., Gauthier, A. S., Kaplan, D. R. & Miller, F. D. Trk signaling regulates neural precursor cell proliferation and differentiation during cortical development. *Development* **134**, 4369–4380 (2007).
125. Cohen-Cory, S., Kidane, A. H., Shirkey, N. J. & Marshak, S. Brain-derived neurotrophic factor and the development of structural neuronal connectivity. *Dev. Neurobiol.* **70**, 271–288 (2010).
126. Lynch, M. A. Long-term potentiation and memory. *Physiol. Rev.* **84**, 87–136 (2004).
127. Edelmann, E., Lessmann, V. & Brigadski, T. Pre- and postsynaptic twists in BDNF secretion and action in synaptic plasticity. *Neuropharmacology* **76 Pt C**, 610–627 (2014).
128. Schinder, A. F., Berninger, B. & Poo, M. Postsynaptic target specificity of neurotrophin-induced presynaptic potentiation. *Neuron* **25**, 151–163 (2000).
129. Kubo, T., Nonomura, T., Enokido, Y. & Hatanaka, H. Brain-derived neurotrophic factor (BDNF) can prevent apoptosis of rat cerebellar granule neurons in culture. *Brain Res. Dev. Brain Res.* **85**, 249–258 (1995).
130. Almeida, R. D. *et al.* Neuroprotection by BDNF against glutamate-induced apoptotic cell death is mediated by ERK and PI3-kinase pathways. *Cell Death Differ.* **12**, 1329–1343 (2005).
131. Fritzsch, B., Silos-Santiago, I., Bianchi, L. M. & Fariñas, I. The role of neurotrophic factors in regulating the development of inner ear innervation. *Trends Neurosci.* **20**, 159–164 (1997).
132. Gorski, J. A., Zeiler, S. R., Tamowski, S. & Jones, K. R. Brain-derived neurotrophic factor is required for the maintenance of cortical dendrites. *J. Neurosci.* **23**, 6856–6865 (2003).
133. Kwon, M., Fernández, J. R., Zegarek, G. F., Lo, S. B. & Firestein, B. L. BDNF-promoted increases in proximal dendrites occur via CREB-dependent transcriptional regulation of cypin. *J. Neurosci.* **31**, 9735–9745 (2011).
134. Orefice, L. L. *et al.* Distinct roles for somatically and dendritically synthesized brain-derived neurotrophic factor in morphogenesis of dendritic spines. *J. Neurosci.* **33**, 11618–11632 (2013).
135. Vicario-Abejón, C., Owens, D., McKay, R. & Segal, M. Role of neurotrophins in central synapse formation and stabilization. *Nat. Rev. Neurosci.* **3**, 965–974 (2002).
136. Vicario-Abejón, C., Collin, C., McKay, R. D. & Segal, M. Neurotrophins induce formation of functional excitatory and inhibitory synapses between cultured hippocampal neurons. *J. Neurosci.* **18**, 7256–7271 (1998).
137. Messaoudi, E., Ying, S.-W., Kanhema, T., Croll, S. D. & Bramham, C. R. Brain-derived neurotrophic factor triggers transcription-dependent, late phase long-term potentiation in vivo. *J. Neurosci.* **22**, 7453–7461 (2002).
138. Suen, P. C. *et al.* Brain-derived neurotrophic factor rapidly enhances phosphorylation of the postsynaptic N-methyl-D-aspartate receptor subunit 1. *Proc Natl Acad Sci USA* **94**, 8191–8195 (1997).
139. Lin, S. Y. *et al.* BDNF acutely increases tyrosine phosphorylation of the NMDA receptor subunit 2B in cortical and hippocampal postsynaptic densities. *Brain Res. Mol. Brain Res.* **55**, 20–27 (1998).
140. Levine, E. S., Crozier, R. A., Black, I. B. & Plummer, M. R. Brain-derived neurotrophic factor modulates hippocampal synaptic transmission by increasing N-methyl-D-aspartic acid receptor activity. *Proc Natl Acad Sci USA* **95**, 10235–10239

(1998).
141. Aakalu, G., Smith, W. B., Nguyen, N., Jiang, C. & Schuman, E. M. Dynamic visualization of local protein synthesis in hippocampal neurons. *Neuron* **30**, 489–502 (2001).
142. Afonso, P. *et al.* BDNF increases synaptic NMDA receptor abundance by enhancing the local translation of Pyk2 in cultured hippocampal neurons. *Sci. Signal.* **12**, (2019).
143. Katoh-Semba, R., Takeuchi, I. K., Semba, R. & Kato, K. Distribution of brain-derived neurotrophic factor in rats and its changes with development in the brain. *J. Neurochem.* **69**, 34–42 (1997).
144. Dolmetsch, R. E., Pajvani, U., Fife, K., Spotts, J. M. & Greenberg, M. E. Signaling to the nucleus by an L-type calcium channel-calmodulin complex through the MAP kinase pathway. *Science* **294**, 333–339 (2001).
145. Takasu, M. A., Dalva, M. B., Zigmond, R. E. & Greenberg, M. E. Modulation of NMDA receptor-dependent calcium influx and gene expression through EphB receptors. *Science* **295**, 491–495 (2002).
146. Lyons, M. R. *et al.* The transcription factor calcium-response factor limits NMDA receptor-dependent transcription in the developing brain. *J. Neurochem.* **137**, 164–176 (2016).
147. Wu, G. Y., Deisseroth, K. & Tsien, R. W. Activity-dependent CREB phosphorylation: convergence of a fast, sensitive calmodulin kinase pathway and a slow, less sensitive mitogen-activated protein kinase pathway. *Proc Natl Acad Sci USA* **98**, 2808–2813 (2001).
148. Tao, X., Finkbeiner, S., Arnold, D. B., Shaywitz, A. J. & Greenberg, M. E. Ca2+ influx regulates BDNF transcription by a CREB family transcription factor-dependent mechanism. *Neuron* **20**, 709–726 (1998).
149. Tao, X., West, A. E., Chen, W. G., Corfas, G. & Greenberg, M. E. A calcium-responsive transcription factor, CaRF, that regulates neuronal activity-dependent expression of BDNF. *Neuron* **33**, 383–395 (2002).
150. Maynard, K. R. *et al.* Functional Role of BDNF Production from Unique Promoters in Aggression and Serotonin Signaling. *Neuropsychopharmacology* **41**, 1943–1955 (2016).
151. Miyasaka, Y. & Yamamoto, N. Neuronal Activity Patterns Regulate Brain-Derived Neurotrophic Factor Expression in Cortical Cells via Neuronal Circuits. *Front. Neurosci.* **15**, 699583 (2021).
152. West, A. E. *et al.* Calcium regulation of neuronal gene expression. *Proc Natl Acad Sci USA* **98**, 11024–11031 (2001).
153. Pruunsild, P., Kazantseva, A., Aid, T., Palm, K. & Timmusk, T. Dissecting the human BDNF locus: bidirectional transcription, complex splicing, and multiple promoters. *Genomics* **90**, 397–406 (2007).
154. Kaneko, M., Xie, Y., An, J. J., Stryker, M. P. & Xu, B. Dendritic BDNF synthesis is required for late-phase spine maturation and recovery of cortical responses following sensory deprivation. *J. Neurosci.* **32**, 4790–4802 (2012).
155. Hu, X. *et al.* BDNF-induced increase of PSD-95 in dendritic spines requires dynamic microtubule invasions. *J. Neurosci.* **31**, 15597–15603 (2011).
156. Chen, W. G. *et al.* Derepression of BDNF transcription involves calcium-dependent phosphorylation of MeCP2. *Science* **302**, 885–889 (2003).
157. Martinowich, K. *et al.* DNA methylation-related chromatin remodeling in activity-

dependent BDNF gene regulation. *Science* **302**, 890–893 (2003).
158. Ma, D. K. *et al.* Neuronal activity-induced Gadd45b promotes epigenetic DNA demethylation and adult neurogenesis. *Science* **323**, 1074–1077 (2009).
159. Modarresi, F. *et al.* Inhibition of natural antisense transcripts in vivo results in gene-specific transcriptional upregulation. *Nat. Biotechnol.* **30**, 453–459 (2012).
160. Aid, T., Kazantseva, A., Piirsoo, M., Palm, K. & Timmusk, T. Mouse and rat BDNF gene structure and expression revisited. *J. Neurosci. Res.* **85**, 525–535 (2007).
161. Ghafouri-Fard, S., Khoshbakht, T., Taheri, M. & Ghanbari, M. A concise review on the role of BDNF-AS in human disorders. *Biomed. Pharmacother.* **142**, 112051 (2021).
162. Tuvikene, J., Pruunsild, P., Orav, E., Esvald, E.-E. & Timmusk, T. AP-1 Transcription Factors Mediate BDNF-Positive Feedback Loop in Cortical Neurons. *J. Neurosci.* **36**, 1290–1305 (2016).
163. Matsumoto, T. *et al.* Biosynthesis and processing of endogenous BDNF: CNS neurons store and secrete BDNF, not pro-BDNF. *Nat. Neurosci.* **11**, 131–133 (2008).
164. Pang, P. T. *et al.* Cleavage of proBDNF by tPA/plasmin is essential for long-term hippocampal plasticity. *Science* **306**, 487–491 (2004).
165. Mizoguchi, H. *et al.* Matrix metalloproteinase-9 contributes to kindled seizure development in pentylenetetrazole-treated mice by converting pro-BDNF to mature BDNF in the hippocampus. *J. Neurosci.* **31**, 12963–12971 (2011).
166. Hwang, J. J., Park, M.-H., Choi, S.-Y. & Koh, J.-Y. Activation of the Trk signaling pathway by extracellular zinc. Role of metalloproteinases. *J. Biol. Chem.* **280**, 11995–12001 (2005).
167. Al-Qudah, M. A. & Al-Dwairi, A. Mechanisms and regulation of neurotrophin synthesis and secretion. *Neurosciences (Riyadh)* **21**, 306–313 (2016).
168. Mowla, S. J. *et al.* Biosynthesis and post-translational processing of the precursor to brain-derived neurotrophic factor. *J. Biol. Chem.* **276**, 12660–12666 (2001).
169. Lessmann, V., Gottmann, K. & Malcangio, M. Neurotrophin secretion: current facts and future prospects. *Prog. Neurobiol.* **69**, 341–374 (2003).
170. Krüttgen, A., Möller, J. C., Heymach, J. V. & Shooter, E. M. Neurotrophins induce release of neurotrophins by the regulated secretory pathway. *Proc Natl Acad Sci USA* **95**, 9614–9619 (1998).
171. Egan, M. F. *et al.* The BDNF val66met polymorphism affects activity-dependent secretion of BDNF and human memory and hippocampal function. *Cell* **112**, 257–269 (2003).
172. Pezawas, L. *et al.* The brain-derived neurotrophic factor val66met polymorphism and variation in human cortical morphology. *J. Neurosci.* **24**, 10099–10102 (2004).
173. Bibel, M. & Barde, Y. A. Neurotrophins: key regulators of cell fate and cell shape in the vertebrate nervous system. *Genes Dev.* **14**, 2919–2937 (2000).
174. Chao, M. V. Neurotrophins and their receptors: a convergence point for many signalling pathways. *Nat. Rev. Neurosci.* **4**, 299–309 (2003).
175. Ji, Y. *et al.* Acute and gradual increases in BDNF concentration elicit distinct signaling and functions in neurons. *Nat. Neurosci.* **13**, 302–309 (2010).
176. Guo, W., Nagappan, G. & Lu, B. Differential effects of transient and sustained activation of BDNF-TrkB signaling. *Dev. Neurobiol.* **78**, 647–659 (2018).
177. Lee, R., Kermani, P., Teng, K. K. & Hempstead, B. L. Regulation of cell survival by secreted proneurotrophins. *Science* **294**, 1945–1948 (2001).

178. Fayard, B., Loeffler, S., Weis, J., Vögelin, E. & Krüttgen, A. The secreted brain-derived neurotrophic factor precursor pro-BDNF binds to TrkB and p75NTR but not to TrkA or TrkC. *J. Neurosci. Res.* **80**, 18–28 (2005).
179. Roux, P. P. & Barker, P. A. Neurotrophin signaling through the p75 neurotrophin receptor. *Prog. Neurobiol.* **67**, 203–233 (2002).
180. Reichardt, L. F. Neurotrophin-regulated signalling pathways. *Philos. Trans. R. Soc. Lond. B Biol. Sci.* **361**, 1545–1564 (2006).
181. Woo, N. H. *et al.* Activation of p75NTR by proBDNF facilitates hippocampal long-term depression. *Nat. Neurosci.* **8**, 1069–1077 (2005).
182. Ma, X. *et al.* Probdnf dependence of LTD and fear extinction learning in the amygdala of adult mice. *Cereb. Cortex* **32**, 1350–1364 (2022).
183. Nimnual, A. S., Yatsula, B. A. & Bar-Sagi, D. Coupling of Ras and Rac guanosine triphosphatases through the Ras exchanger Sos. *Science* **279**, 560–563 (1998).
184. Kumar, V., Zhang, M.-X., Swank, M. W., Kunz, J. & Wu, G.-Y. Regulation of dendritic morphogenesis by Ras-PI3K-Akt-mTOR and Ras-MAPK signaling pathways. *J. Neurosci.* **25**, 11288–11299 (2005).
185. Leal, G., Comprido, D. & Duarte, C. B. BDNF-induced local protein synthesis and synaptic plasticity. *Neuropharmacology* **76 Pt C**, 639–656 (2014).
186. Takei, N. *et al.* Brain-derived neurotrophic factor induces mammalian target of rapamycin-dependent local activation of translation machinery and protein synthesis in neuronal dendrites. *J. Neurosci.* **24**, 9760–9769 (2004).
187. Huang, W.-C. & Chen, C.-C. Akt phosphorylation of p300 at Ser-1834 is essential for its histone acetyltransferase and transcriptional activity. *Mol. Cell. Biol.* **25**, 6592–6602 (2005).
188. English, J. *et al.* New insights into the control of MAP kinase pathways. *Exp. Cell Res.* **253**, 255–270 (1999).
189. Hisata, S. *et al.* Rap1-PDZ-GEF1 interacts with a neurotrophin receptor at late endosomes, leading to sustained activation of Rap1 and ERK and neurite outgrowth. *J. Cell Biol.* **178**, 843–860 (2007).
190. Liu, L. *et al.* ERK5 activation of MEF2-mediated gene expression plays a critical role in BDNF-promoted survival of developing but not mature cortical neurons. *Proc Natl Acad Sci USA* **100**, 8532–8537 (2003).
191. Corbit, K. C., Foster, D. A. & Rosner, M. R. Protein kinase Cdelta mediates neurogenic but not mitogenic activation of mitogen-activated protein kinase in neuronal cells. *Mol. Cell. Biol.* **19**, 4209–4218 (1999).
192. Hofmann, T. *et al.* Direct activation of human TRPC6 and TRPC3 channels by diacylglycerol. *Nature* **397**, 259–263 (1999).
193. Li, H. S., Xu, X. Z. & Montell, C. Activation of a TRPC3-dependent cation current through the neurotrophin BDNF. *Neuron* **24**, 261–273 (1999).
194. Watson, F. L. *et al.* Rapid nuclear responses to target-derived neurotrophins require retrograde transport of ligand-receptor complex. *J. Neurosci.* **19**, 7889–7900 (1999).
195. Cohen, M. S., Bas Orth, C., Kim, H. J., Jeon, N. L. & Jaffrey, S. R. Neurotrophin-mediated dendrite-to-nucleus signaling revealed by microfluidic compartmentalization of dendrites. *Proc Natl Acad Sci USA* **108**, 11246–11251 (2011).
196. Pazyra-Murphy, M. F. *et al.* A retrograde neuronal survival response: target-derived neurotrophins regulate MEF2D and bcl-w. *J. Neurosci.* **29**, 6700–6709 (2009).

197. Finkbeiner, S. *et al.* CREB: a major mediator of neuronal neurotrophin responses. *Neuron* **19**, 1031–1047 (1997).
198. Kikuchi, K. *et al.* Involvement of SRF coactivator MKL2 in BDNF-mediated activation of the synaptic activity-responsive element in the Arc gene. *J. Neurochem.* **148**, 204–218 (2019).
199. Alder, J. *et al.* Brain-derived neurotrophic factor-induced gene expression reveals novel actions of VGF in hippocampal synaptic plasticity. *J. Neurosci.* **23**, 10800–10808 (2003).
200. Phillips, H. S. *et al.* BDNF mRNA is decreased in the hippocampus of individuals with Alzheimer's disease. *Neuron* **7**, 695–702 (1991).
201. Wong, J. *et al.* Promoter specific alterations of brain-derived neurotrophic factor mRNA in schizophrenia. *Neuroscience* **169**, 1071–1084 (2010).
202. Weickert, C. S. *et al.* Reduced brain-derived neurotrophic factor in prefrontal cortex of patients with schizophrenia. *Mol. Psychiatry* **8**, 592–610 (2003).
203. Duman, R. S., Deyama, S. & Fogaça, M. V. Role of BDNF in the pathophysiology and treatment of depression: Activity-dependent effects distinguish rapid-acting antidepressants. *Eur. J. Neurosci.* **53**, 126–139 (2021).
204. Napoli, C. *et al.* Novel epigenetic-based therapies useful in cardiovascular medicine. *World J. Cardiol.* **8**, 211–219 (2016).
205. Coppedè, F. The potential of epigenetic therapies in neurodegenerative diseases. *Front. Genet.* **5**, 220 (2014).
206. Pintchovski, S. A., Peebles, C. L., Kim, H. J., Verdin, E. & Finkbeiner, S. The serum response factor and a putative novel transcription factor regulate expression of the immediate-early gene Arc/Arg3.1 in neurons. *J. Neurosci.* **29**, 1525–1537 (2009).
207. Schmidt, S. F., Larsen, B. D., Loft, A. & Mandrup, S. Cofactor squelching: Artifact or fact? *Bioessays* **38**, 618–626 (2016).
208. Jiang, D., Jarrett, H. W. & Haskins, W. E. Methods for proteomic analysis of transcription factors. *J. Chromatogr. A* **1216**, 6881–6889 (2009).
209. Gillespie, M. A. *et al.* Absolute quantification of transcription factors reveals principles of gene regulation in erythropoiesis. *Mol. Cell* **78**, 960-974.e11 (2020).
210. Ibarra, I. L. *et al.* Comparative chromatin accessibility upon BDNF stimulation delineates neuronal regulatory elements. *Mol. Syst. Biol.* **18**, e10473 (2022).
211. Kim, T.-K. *et al.* Widespread transcription at neuronal activity-regulated enhancers. *Nature* **465**, 182–187 (2010).
212. Aikawa, Y. *et al.* Treatment of arthritis with a selective inhibitor of c-Fos/activator protein-1. *Nat. Biotechnol.* **26**, 817–823 (2008).
213. Bibel, M., Richter, J., Lacroix, E. & Barde, Y.-A. Generation of a defined and uniform population of CNS progenitors and neurons from mouse embryonic stem cells. *Nat. Protoc.* **2**, 1034–1043 (2007).
214. Babraham Bioinformatics - Trim Galore! https://www.bioinformatics.babraham.ac.uk/projects/trim_galore/.
215. Dobin, A. *et al.* STAR: ultrafast universal RNA-seq aligner. *Bioinformatics* **29**, 15–21 (2013).
216. Liao, Y., Smyth, G. K. & Shi, W. featureCounts: an efficient general purpose program for assigning sequence reads to genomic features. *Bioinformatics* **30**, 923–930 (2014).
217. Love, M. I., Huber, W. & Anders, S. Moderated estimation of fold change and dispersion for RNA-seq data with DESeq2. *Genome Biol.* **15**, 550 (2014).

218. Zhu, A., Ibrahim, J. G. & Love, M. I. Heavy-tailed prior distributions for sequence count data: removing the noise and preserving large differences. *Bioinformatics* **35**, 2084–2092 (2019).
219. Huber, W., von Heydebreck, A., Sültmann, H., Poustka, A. & Vingron, M. Variance stabilization applied to microarray data calibration and to the quantification of differential expression. *Bioinformatics* **18 Suppl 1**, S96-104 (2002).
220. clusterProfiler. https://guangchuangyu.github.io/software/clusterProfiler/.
221. Weirauch, M. T. *et al.* Determination and inference of eukaryotic transcription factor sequence specificity. *Cell* **158**, 1431–1443 (2014).
222. Hughes, C. S. *et al.* Ultrasensitive proteome analysis using paramagnetic bead technology. *Mol. Syst. Biol.* **10**, 757 (2014).
223. Franken, H. *et al.* Thermal proteome profiling for unbiased identification of direct and indirect drug targets using multiplexed quantitative mass spectrometry. *Nat. Protoc.* **10**, 1567–1593 (2015).
224. Ritchie, M. E. *et al.* limma powers differential expression analyses for RNA-sequencing and microarray studies. *Nucleic Acids Res.* **43**, e47 (2015).
225. Gehre, M. *et al.* Lysine 4 of histone H3.3 is required for embryonic stem cell differentiation, histone enrichment at regulatory regions and transcription accuracy. *Nat. Genet.* **52**, 273–282 (2020).
226. Callicott, R. J. & Womack, J. E. Real-time PCR assay for measurement of mouse telomeres. *Comp. Med.* **56**, 17–22 (2006).
227. Buenrostro, J. D., Wu, B., Chang, H. Y. & Greenleaf, W. J. ATAC-seq: a method for assaying chromatin accessibility genome-wide. *Curr. Protoc. Mol. Biol.* **109**, 21.29.1-21.29.9 (2015).
228. Langmead, B. & Salzberg, S. L. Fast gapped-read alignment with Bowtie 2. *Nat. Methods* **9**, 357–359 (2012).
229. Zhang, Y. *et al.* Model-based analysis of ChIP-Seq (MACS). *Genome Biol.* **9**, R137 (2008).
230. Ross-Innes, C. S. *et al.* Differential oestrogen receptor binding is associated with clinical outcome in breast cancer. *Nature* **481**, 389–393 (2012).
231. Tseng, Q. *et al.* A new micropatterning method of soft substrates reveals that different tumorigenic signals can promote or reduce cell contraction levels. *Lab Chip* **11**, 2231–2240 (2011).
232. Kim, S., Kim, H. & Um, J. W. Synapse development organized by neuronal activity-regulated immediate-early genes. *Exp. Mol. Med.* **50**, 1–7 (2018).
233. Yap, E.-L. & Greenberg, M. E. Activity-Regulated Transcription: Bridging the Gap between Neural Activity and Behavior. *Neuron* **100**, 330–348 (2018).
234. Hu, S. C., Chrivia, J. & Ghosh, A. Regulation of CBP-mediated transcription by neuronal calcium signaling. *Neuron* **22**, 799–808 (1999).
235. Hipp, L. *et al.* Single-molecule imaging of the transcription factor SRF reveals prolonged chromatin-binding kinetics upon cell stimulation. *Proc Natl Acad Sci USA* **116**, 880–889 (2019).
236. Sando, R. *et al.* HDAC4 governs a transcriptional program essential for synaptic plasticity and memory. *Cell* **151**, 821–834 (2012).
237. Huang, E. J. & Reichardt, L. F. Neurotrophins: roles in neuronal development and function. *Annu. Rev. Neurosci.* **24**, 677–736 (2001).
238. Chawla, S., Hardingham, G. E., Quinn, D. R. & Bading, H. CBP: a signal-regulated transcriptional coactivator controlled by nuclear calcium and CaM kinase IV.

Science **281**, 1505–1509 (1998).
239. Zheng, F., Zhou, X., Moon, C. & Wang, H. Regulation of brain-derived neurotrophic factor expression in neurons. *Int. J. Physiol. Pathophysiol. Pharmacol.* **4**, 188–200 (2012).
240. Cavalcante, R. G. & Sartor, M. A. annotatr: genomic regions in context. *Bioinformatics* **33**, 2381–2383 (2017).
241. Ganapathi, M. *et al.* Comparative analysis of chromatin landscape in regulatory regions of human housekeeping and tissue specific genes. *BMC Bioinformatics* **6**, 126 (2005).
242. Chiarella, A. M., Lu, D. & Hathaway, N. A. Epigenetic control of a local chromatin landscape. *Int. J. Mol. Sci.* **21**, (2020).
243. Calo, E. & Wysocka, J. Modification of enhancer chromatin: what, how, and why? *Mol. Cell* **49**, 825–837 (2013).
244. Madabhushi, R. *et al.* Activity-Induced DNA Breaks Govern the Expression of Neuronal Early-Response Genes. *Cell* **161**, 1592–1605 (2015).
245. Wu, W. *et al.* Neuronal enhancers are hotspots for DNA single-strand break repair. *Nature* **593**, 440–444 (2021).
246. Garcia-Alonso, L., Holland, C. H., Ibrahim, M. M., Turei, D. & Saez-Rodriguez, J. Benchmark and integration of resources for the estimation of human transcription factor activities. *Genome Res.* **29**, 1363–1375 (2019).
247. Mukhtar, T. *et al.* Tead transcription factors differentially regulate cortical development. *Sci. Rep.* **10**, 4625 (2020).
248. Ibarra, I. L. *et al.* Comparative chromatin accessibility upon BDNF-induced neuronal activity delineates neuronal regulatory elements. *BioRxiv* (2021) doi:10.1101/2021.05.28.446128.
249. Vierbuchen, T. *et al.* AP-1 Transcription Factors and the BAF Complex Mediate Signal-Dependent Enhancer Selection. *Mol. Cell* **68**, 1067-1082.e12 (2017).
250. Korb, E. & Finkbeiner, S. Arc in synaptic plasticity: from gene to behavior. *Trends Neurosci.* **34**, 591–598 (2011).
251. D'Urso, A. & Brickner, J. H. Mechanisms of epigenetic memory. *Trends Genet.* **30**, 230–236 (2014).
252. Kim, M. Y., Lee, J. E., Kim, L. K. & Kim, T. Epigenetic memory in gene regulation and immune response. *BMB Rep.* **52**, 127–132 (2019).
253. Light, W. H. *et al.* A conserved role for human Nup98 in altering chromatin structure and promoting epigenetic transcriptional memory. *PLoS Biol.* **11**, e1001524 (2013).
254. Cunningham, F. *et al.* Ensembl 2022. *Nucleic Acids Res.* **50**, D988–D995 (2022).
255. Chen, L. *et al.* Long non-coding RNA Malat1 promotes neurite outgrowth through activation of ERK/MAPK signalling pathway in N2a cells. *J. Cell. Mol. Med.* **20**, 2102–2110 (2016).
256. Bernard, D. *et al.* A long nuclear-retained non-coding RNA regulates synaptogenesis by modulating gene expression. *EMBO J.* **29**, 3082–3093 (2010).
257. Tan, M. C. *et al.* The Activity-Induced Long Non-Coding RNA Meg3 Modulates AMPA Receptor Surface Expression in Primary Cortical Neurons. *Front. Cell. Neurosci.* **11**, 124 (2017).
258. Clark, B. S. & Blackshaw, S. Understanding the Role of lncRNAs in Nervous System Development. *Adv. Exp. Med. Biol.* **1008**, 253–282 (2017).
259. Yan, H. *et al.* Long non-coding RNA MEG3 functions as a competing endogenous RNA to regulate ischemic neuronal death by targeting miR-21/PDCD4 signaling

pathway. *Cell Death Dis.* **8**, 3211 (2017).
260. Balusu, S. *et al.* Long noncoding RNA *MEG3* activates neuronal necroptosis in Alzheimer's disease. *BioRxiv* (2022) doi:10.1101/2022.02.18.480849.
261. Zhang, H., Tao, J., Zhang, S. & Lv, X. Lncrna MEG3 reduces hippocampal neuron apoptosis via the pi3k/akt/mtor pathway in a rat model of temporal lobe epilepsy. *Neuropsychiatr. Dis. Treat.* **16**, 2519–2528 (2020).
262. Pawar, K., Hanisch, C., Palma Vera, S. E., Einspanier, R. & Sharbati, S. Down regulated lncRNA MEG3 eliminates mycobacteria in macrophages via autophagy. *Sci. Rep.* **6**, 19416 (2016).
263. Li, X. *et al.* LncRNA FTX inhibits hippocampal neuron apoptosis by regulating miR-21-5p/SOX7 axis in a rat model of temporal lobe epilepsy. *Biochem. Biophys. Res. Commun.* **512**, 79–86 (2019).
264. Schubert, M. *et al.* Perturbation-response genes reveal signaling footprints in cancer gene expression. *Nat. Commun.* **9**, 20 (2018).
265. Culmsee, C. *et al.* Reciprocal inhibition of p53 and nuclear factor-kappaB transcriptional activities determines cell survival or death in neurons. *J. Neurosci.* **23**, 8586–8595 (2003).
266. Roy, S. K., Srivastava, R. K. & Shankar, S. Inhibition of PI3K/AKT and MAPK/ERK pathways causes activation of FOXO transcription factor, leading to cell cycle arrest and apoptosis in pancreatic cancer. *J. Mol. Signal.* **5**, 10 (2010).
267. Araujo, J. *et al.* FOXO4-dependent upregulation of superoxide dismutase-2 in response to oxidative stress is impaired in spinocerebellar ataxia type 3. *Hum. Mol. Genet.* **20**, 2928–2941 (2011).
268. Chen, A., Xiong, L.-J., Tong, Y. & Mao, M. Neuroprotective effect of brain-derived neurotrophic factor mediated by autophagy through the PI3K/Akt/mTOR pathway. *Mol. Med. Report.* **8**, 1011–1016 (2013).
269. Switon, K., Kotulska, K., Janusz-Kaminska, A., Zmorzynska, J. & Jaworski, J. Molecular neurobiology of mTOR. *Neuroscience* **341**, 112–153 (2017).
270. Gillespie, M. *et al.* The reactome pathway knowledgebase 2022. *Nucleic Acids Res.* **50**, D687–D692 (2022).
271. Bayraktar, G. & Kreutz, M. R. Neuronal DNA Methyltransferases: Epigenetic Mediators between Synaptic Activity and Gene Expression? *Neuroscientist* **24**, 171–185 (2018).
272. Bayraktar, G. *et al.* Synaptic control of DNA-methylation involves activity-dependent degradation of DNMT3a1 in the nucleus. *BioRxiv* (2019) doi:10.1101/602151.
273. Morris, M. J., Adachi, M., Na, E. S. & Monteggia, L. M. Selective role for DNMT3a in learning and memory. *Neurobiol. Learn. Mem.* **115**, 30–37 (2014).
274. Douet, J. *et al.* MacroH2A histone variants maintain nuclear organization and heterochromatin architecture. *J. Cell Sci.* **130**, 1570–1582 (2017).
275. Miranda, M., Morici, J. F., Zanoni, M. B. & Bekinschtein, P. Brain-Derived Neurotrophic Factor: A Key Molecule for Memory in the Healthy and the Pathological Brain. *Front. Cell. Neurosci.* **13**, 363 (2019).
276. Tuszynski, M. H. *et al.* Nerve growth factor gene therapy: activation of neuronal responses in alzheimer disease. *JAMA Neurol.* **72**, 1139–1147 (2015).
277. Kafitz, K. W., Rose, C. R., Thoenen, H. & Konnerth, A. Neurotrophin-evoked rapid excitation through TrkB receptors. *Nature* **401**, 918–921 (1999).
278. Sharpless, S. K. Supersensitivity-like phenomena in the central nervous system. *Fed. Proc.* **34**, 1990–1997 (1975).

279. Swearengen, E. & Chavkin, C. NMDA receptor antagonist D-APV depresses excitatory activity produced by normorphine in rat hippocampal slices. *Neurosci. Lett.* **78**, 80–84 (1987).
280. McAllister, A. K., Katz, L. C. & Lo, D. C. Neurotrophin regulation of cortical dendritic growth requires activity. *Neuron* **17**, 1057–1064 (1996).
281. Sharma, N. *et al.* ARNT2 Tunes Activity-Dependent Gene Expression through NCoR2-Mediated Repression and NPAS4-Mediated Activation. *Neuron* **102**, 390-406.e9 (2019).
282. Malik, A. N. *et al.* Genome-wide identification and characterization of functional neuronal activity-dependent enhancers. *Nat. Neurosci.* **17**, 1330–1339 (2014).
283. Macías, W., Carlson, R., Rajadhyaksha, A., Barczak, A. & Konradi, C. Potassium chloride depolarization mediates CREB phosphorylation in striatal neurons in an NMDA receptor-dependent manner. *Brain Res.* **890**, 222–232 (2001).
284. Gotoh, H., Kajikawa, M., Kato, H. & Suto, K. Intracellular Mg2+ surge follows Ca2+ increase during depolarization in cultured neurons. *Brain Res.* **828**, 163–168 (1999).
285. Grubb, M. S. & Burrone, J. Activity-dependent relocation of the axon initial segment fine-tunes neuronal excitability. *Nature* **465**, 1070–1074 (2010).
286. Collins, F., Schmidt, M. F., Guthrie, P. B. & Kater, S. B. Sustained increase in intracellular calcium promotes neuronal survival. *J. Neurosci.* **11**, 2582–2587 (1991).
287. Bading, H., Ginty, D. D. & Greenberg, M. E. Regulation of gene expression in hippocampal neurons by distinct calcium signaling pathways. *Science* **260**, 181–186 (1993).
288. Bibel, M. *et al.* Differentiation of mouse embryonic stem cells into a defined neuronal lineage. *Nat. Neurosci.* **7**, 1003–1009 (2004).
289. Jones-Villeneuve, E. M., McBurney, M. W., Rogers, K. A. & Kalnins, V. I. Retinoic acid induces embryonal carcinoma cells to differentiate into neurons and glial cells. *J. Cell Biol.* **94**, 253–262 (1982).
290. Biddie, S. C. *et al.* Transcription factor AP1 potentiates chromatin accessibility and glucocorticoid receptor binding. *Mol. Cell* **43**, 145–155 (2011).
291. Schönthal, A. *et al.* The Fos and Jun/AP-1 proteins are involved in the downregulation of Fos transcription. *Oncogene* **4**, 629–636 (1989).
292. Jobst Rahmsdorf, H., Schonthal, A., Angel, P., Litfin, M. & Ruther, U. Volume 15 Number 4 1987 Nucleic Acids Research Posttrnsriptional reglation of c-fos mRNA expression.
293. Chen, R. H., Abate, C. & Blenis, J. Phosphorylation of the c-Fos transrepression domain by mitogen-activated protein kinase and 90-kDa ribosomal S6 kinase. *Proc Natl Acad Sci USA* **90**, 10952–10956 (1993).
294. Gilley, R., March, H. N. & Cook, S. J. ERK1/2, but not ERK5, is necessary and sufficient for phosphorylation and activation of c-Fos. *Cell. Signal.* **21**, 969–977 (2009).
295. Rauscher, F. J., Voulalas, P. J., Franza, B. R. & Curran, T. Fos and Jun bind cooperatively to the AP-1 site: reconstitution in vitro. *Genes Dev.* **2**, 1687–1699 (1988).
296. Rauscher, F. J. *et al.* Fos-associated protein p39 is the product of the jun proto-oncogene. *Science* **240**, 1010–1016 (1988).
297. König, H. *et al.* Autoregulation of fos: the dyad symmetry element as the major

target of repression. *EMBO J.* **8**, 2559–2566 (1989).
298. Foster, S. L., Hargreaves, D. C. & Medzhitov, R. Gene-specific control of inflammation by TLR-induced chromatin modifications. *Nature* **447**, 972–978 (2007).
299. Saeed, S. *et al.* Epigenetic programming of monocyte-to-macrophage differentiation and trained innate immunity. *Science* **345**, 1251086 (2014).
300. Yoshida, K. *et al.* The transcription factor ATF7 mediates lipopolysaccharide-induced epigenetic changes in macrophages involved in innate immunological memory. *Nat. Immunol.* **16**, 1034–1043 (2015).
301. Larsen, S. B. *et al.* Establishment, maintenance, and recall of inflammatory memory. *Cell Stem Cell* **28**, 1758-1774.e8 (2021).
302. de Laval, B. *et al.* C/EBPβ-Dependent Epigenetic Memory Induces Trained Immunity in Hematopoietic Stem Cells. *Cell Stem Cell* **26**, 657-674.e8 (2020).
303. Miller, C. A. & Sweatt, J. D. Covalent modification of DNA regulates memory formation. *Neuron* **53**, 857–869 (2007).
304. Guo, J. U. *et al.* Neuronal activity modifies the DNA methylation landscape in the adult brain. *Nat. Neurosci.* **14**, 1345–1351 (2011).
305. Oliveira, A. M. M. DNA methylation: a permissive mark in memory formation and maintenance. *Learn. Mem.* **23**, 587–593 (2016).
306. Gupta, S. *et al.* Histone methylation regulates memory formation. *J. Neurosci.* **30**, 3589–3599 (2010).
307. Gupta-Agarwal, S. *et al.* G9a/GLP histone lysine dimethyltransferase complex activity in the hippocampus and the entorhinal cortex is required for gene activation and silencing during memory consolidation. *J. Neurosci.* **32**, 5440–5453 (2012).
308. Marco, A. *et al.* Mapping the epigenomic and transcriptomic interplay during memory formation and recall in the hippocampal engram ensemble. *Nat. Neurosci.* **23**, 1606–1617 (2020).
309. Kozlowski, M. *et al.* MacroH2A histone variants limit chromatin plasticity through two distinct mechanisms. *EMBO Rep.* **19**, (2018).
310. Buschbeck, M. *et al.* The histone variant macroH2A is an epigenetic regulator of key developmental genes. *Nat. Struct. Mol. Biol.* **16**, 1074–1079 (2009).
311. Palomer, E., Carretero, J., Benvegnù, S., Dotti, C. G. & Martin, M. G. Neuronal activity controls Bdnf expression via Polycomb de-repression and CREB/CBP/JMJD3 activation in mature neurons. *Nat. Commun.* **7**, 11081 (2016).
312. Qiao, Y., Kang, K., Giannopoulou, E., Fang, C. & Ivashkiv, L. B. IFN-γ Induces Histone 3 Lysine 27 Trimethylation in a Small Subset of Promoters to Stably Silence Gene Expression in Human Macrophages. *Cell Rep.* **16**, 3121–3129 (2016).
313. Varnaitė, R. & MacNeill, S. A. Meet the neighbors: Mapping local protein interactomes by proximity-dependent labeling with BioID. *Proteomics* **16**, 2503–2518 (2016).
314. Kim, B. R. *et al.* Identification of the SOX2 Interactome by BioID Reveals EP300 as a Mediator of SOX2-dependent Squamous Differentiation and Lung Squamous Cell Carcinoma Growth. *Mol. Cell. Proteomics* **16**, 1864–1888 (2017).
315. Armand, E. J., Li, J., Xie, F., Luo, C. & Mukamel, E. A. Single-Cell Sequencing of Brain Cell Transcriptomes and Epigenomes. *Neuron* **109**, 11–26 (2021).